TRANSPORTATION RESEARCH
RECORD

No. 1490

Maintenance

Management and Maintenance of Bridge Structures

A peer-reviewed publication of the Transportation Research Board

TRANSPORTATION RESEARCH BOARD
NATIONAL RESEARCH COUNCIL

NATIONAL ACADEMY PRESS
WASHINGTON, D.C. 1995

Transportation Research Record 1490
ISSN 0361-1981
ISBN 0-309-06154-7
Price: $26.00

Subscriber Category
IIIC bridges, other structures, and hydraulics and hydrology

Printed in the United States of America

Sponsorship of Transportation Research Record 1490

GROUP 3—OPERATION, SAFETY, AND MAINTENANCE OF TRANSPORTATION FACILITIES
Chairman: Jerome W. Hall, University of New Mexico

Maintenance Section
Chairman: Kenneth A. Brewer, Iowa State University

Committee on Structures Maintenance and Management
Chairman: Larry H. Davis, Florida Department of Transportation
John R. Allen, Bernard R. Appleman, Thomas J. Collins, Ian J. Dussek, Oscar R. George, Ray W. James, Patrick O. McCarthy, Wallace T. McKeel Jr., Daniel S. O'Connor, Ronald L. Purvis, Arunprakash M. Shirole, Robert A. P. Sweeney

Committee on Polymer Concretes, Adhesives, and Sealers
Chairman: Jack J. Fontana, Consultant
Douglas Barnaby, Michael C. Belangie, Gary A. Billiard, Frank J. Constantino, Floyd E. Dimmick, Doran L. Glauz, Stella L. Marusin, Peter Mendis, Rick Montani, Emanuel J. Scarpinato, Raymond J. Schutz, Michael M. Sprinkel, Richard Edwin Weyers

Committee on Corrosion
Chairman: David G. Manning, Ontario Ministry of Transport
Secretary: Yash Paul Virmani, FHWA, U.S. Department of Transportation
John E. (Jack) Bennett, Kenneth J. Boedecker Jr., John P. Broomfield, Gerardo G. Clemena, Carl F. Crumpton, Robert J. Girard, William H. Hartt, Rola L. Idriss, Daniel P. Johnston, J. Alan Kehr, Eric C. Lohrey, Richard L. McReynolds, A. P. Moser, Mohamad Nagi, Theodore L. Neff, Arnold M. Rosenberg, Ali Akbar Sohanghpurwala, David B. Storrar

Transportation Research Board Staff
Robert E. Spicher, Director, Technical Activities
Frank N. Lisle, Engineer of Maintenance
Nancy A. Ackerman, Director, Reports and Editorial Services

Sponsorship is indicated by a footnote at the end of each paper. The organizational units, officers, and members are as of December 31, 1994.

Transportation Research Record 1490

Contents

Foreword

This volume contains 11 papers on the management and maintenance of highway bridge structures. The topics addressed include neural networks in bridge management systems, bridge element deterioration rates, BRIDGIT deterioration models, bridge replacement costs, costs of concrete bridge protection, repair and rehabilitation, polymer crack sealers, service life of concrete sealers, decks and surface coatings, corrosion-inhibited highway deicers, and hydrodemolition to remove deteriorated concrete.

Use of Neural Networks in Bridge Management Systems

HOSNY A. MOHAMED, A. O. ABD EL HALIM, AND A. G. RAZAQPUR

One of the most urgent problems related to highway infrastructure is that the cost of maintaining a network of bridges with an acceptable level of service is more than the available budgeted funds. Low prioritization of the available resources allocated to bridge projects exacerbates the situation. About 42 percent of the 574,000 highway bridges in the United States were reported by FHWA to be structurally deficient or functionally obsolete. Traditional management practices have become inadequate as ways to face this serious problem. Priority-setting schemes for bridge projects range from those done on a subjective basis in which engineering judgment is used to those that use very complex optimization models. However, currently used priority-setting schemes do not have the ability to optimize the system's benefits to obtain optimal solutions. The present objective is to show how artificial neural networks (ANNs) can be used to optimize the system's resources to generate the group of bridge improvements that minimizes the loss of the network benefits. ANNs are algorithms with characteristics that are able to solve certain classes of optimization problems. The advantages of using ANNs include improvements in the speed of operation by parallel implementation either in hardware or in software. It is also possible to implement ANNs by optical devices that operate at higher speeds than traditional electronic chips.

Bridges and pavements represent the major investment in a highway network. In addition, they are in constant need of maintenance, rehabilitation, and replacement. The main problem facing most transportation agencies is that the cost of maintaining the bridge network with an acceptable level of service is more than the available budgeted funds. About one-half of the 574,000 highway bridges in the United States were built before 1940, and 42 percent of them were reported by FHWA to be structurally deficient or functionally obsolete (*1*). This finding forced many states to start developing bridge management systems (BMSs).

BMSs are a relatively new approach developed after the successful application of the systems concept to pavement management. A BMS would organize and carry out the bridge projects to meet the needs of the network. The primary objective of a BMS is to integrate all bridge activities into a comprehensive computerized system such that the most efficient and cost-effective performance is achieved (*2*).

At present the cost of rehabilitation and replacement of bridges consumes most of the funding available for bridge improvements. Setting priorities to carry out these activities represents the most challenging task of the BMS. Priority-setting schemes for bridge projects range from those done on a subjective basis in which engineering judgment is used to those that use very complex optimization models. However, the available schemes can be grouped into four types: sufficiency rating, level-of-service (LOS) deficiency ranking, incremental benefit–cost analysis, and mathematical programming. The first three types calculate a ranking index for each project and then sort all projects in descending order of their indexes. Starting with the project with the highest ranking index, projects will be carried out until the available funds are exhausted. Those techniques could provide good solutions, but not the optimal ones. Mathematical programming techniques can provide better decisions and have been used in BMSs by Pontis and North Carolina. However, it is not the intent of this paper to critique priority-setting schemes for bridge projects. Mohamed (*3*) has provided evaluations and comparisons of the available schemes. The objective of this paper is to show how artificial neural networks (ANNs) can be used to optimize the system's resources to generate the group of bridge improvements that minimize the loss of the network benefits.

Department of Civil and Environmental Engineering, Carleton University, Ottawa, Ontario, Canada K1S 5B6.

ARTIFICIAL NEURAL NETWORKS

An ANN takes after its biological analog through its composition of nodes and the connections among them. The first attempt to simulate neural networks was made in 1943 by McCulloch and Pitts (*4*). The basic idea of ANNs is to construct a network of cells that are called artificial neurons, nodes, units, or processing elements (PEs). The synapses of biological networks are simulated by weighted connection. Figure 1 shows the structure of a single PE in a network. The ith PE receives input (X_j) from the jth PE. The arrows in Figure 1 represent the input connection from other PEs. The weight of each connection (T_{ij}) is analogous to the strength of the synaptic connection between neurons. The PE has only a single output that can be input into many other PEs. The net input into the ith PE can be written as follows (*5*):

$$\text{Input}_i = \sum_j X_j \cdot T_{ij} \tag{1}$$

After estimating the net input, it will be converted to an activation value, $\text{Act}_i(t)$, which is

$$\text{Act}_i(t) = F_i\,[\text{Act}_i(t-1), \text{Input}_i(t)] \tag{2}$$

Equation 2 describes the activation value as a function of the net input, and it may also depend on the previous value of activation, $\text{Act}_i(t-1)$. By applying the output function to the activation value, the output (X_i) of the artificial neuron (i) can be obtained as follows:

$$X_i = f_i\,(\text{Act}_i) \tag{3}$$

Several types of neural networks exist. Each type has a different architecture, activation function, output function, and weighted connections. These characteristics depend on the function of the

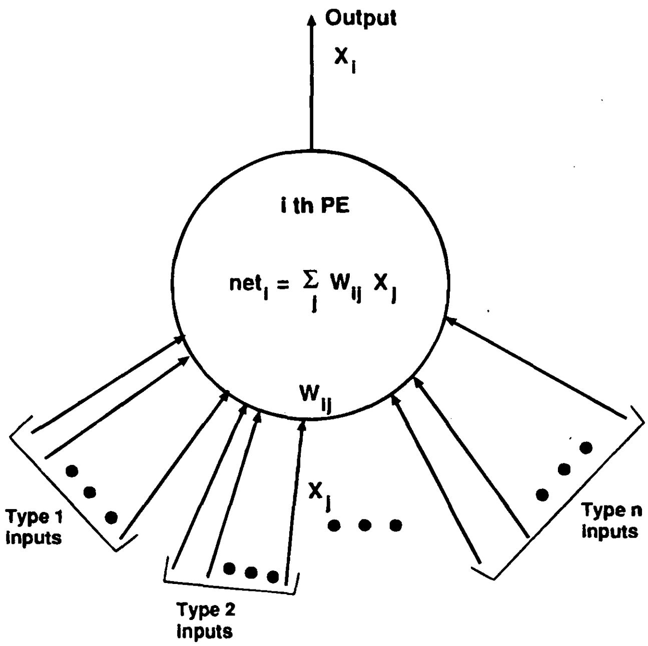

FIGURE 1 Structure of single processing element (*5*).

human brain that the ANN aims to simulate. Such functions include but are not limited to the following (*6*): prediction and estimation, pattern recognition, clustering, and optimization.

Although ANNs have proven to be useful tools in a variety of problem-solving areas, there is relatively little research or practical applications of them in the field of transportation engineering. As a part of a comprehensive research plan to develop a BMS, an ANN was developed to allocate a budget to bridge projects. This paper describes the network that was developed and its application to bridge management.

MODEL FORMULATION

Because the bridge problem has two dimensions (the time dimension and the network dimension) a dynamic programming model has been developed to handle the time dimension. The bridge network is simulated by an ANN. Formulation of the dynamic programming model is beyond the scope of this paper, but Mohamed (*3*) provides details of this model. The objective of the model is to allocate the available budget to bridge projects to minimize the loss of the systems benefits. Budget allocation to bridge projects includes choosing the best improvement alternative for each bridge in the network and determining the optimum timing for carrying it out. The general objective function of the model was formulated as follows:

$$\text{Minimize } Z = \sum_{t=1}^{T} \sum_{B=1}^{N} \sum_{A=0}^{m(t,B)} \mathrm{BL}(t,B,A) \cdot X(t,B,A) \qquad (4)$$

where

z = the total loss of system benefits,
T = analysis period (in years),
N = total number of bridges,
$m(t,B)$ = number of improvement alternatives for bridge B in year t,
$\mathrm{BL}(t,B,A)$ = the amount of loss of system benefits [benefit loss (BL)] if alternative A for bridge B was chosen in year t and
$X(t,B,A)$ = 1 if alternative A for bridge B was chosen in year t and 0 otherwise.

The BL for each alternative can be estimated by the summation of two parts; the first part is the agency BL, and the second part is the increased user cost due to LOS deficiencies (*1*). The input of the model requires information about all possible alternatives for all bridges with the associated life-cycle costs (LCCs) and increased user costs (IUCs) if the alternative were to be implemented in any year of the analysis period. Engineering expertise is needed to determine the possible alternatives to be considered for each bridge in the network. Estimation of life cycle costs and increased user costs for all of the proposed alternatives is required. The BL associated with carrying out any improvement alternative can be estimated from the following formula:

$$\mathrm{BL}\,(t,B,A) = \{[\mathrm{LCC}(t,B,A) - \mathrm{LCC}(t,B,E) + \mathrm{IUC}(t,B,A)]\} \cdot (P/F,\, r,\, t-1) \qquad (5)$$

where

$\mathrm{LCC}(t,B,A)$ = life-cycle cost of alternative A for bridge B if carried out in year t;
$\mathrm{IUC}(t,B,A)$ = increased user costs due to LOS deficiencies associated with alternative t,B,A;
E = the alternative for bridge B in year t that has minimum (LCC + IUC); and
$(P/F, r, t-1)$ = present worth factor for real rate of return r and $(t-1)$ years.

It should be noted that for the do-nothing alternative, BL will be calculated as the present worth of delaying the E alternative for 1 year plus the extra costs of doing nothing, such as posting the bridge. This is because if a bridge was not chosen in year t it will be considered in the optimization of the following year (i.e., (t + 1).

After omitting the time, which is the responsibility of the dynamic programming model, the objective function of the bridge network problem and its constraints can be written as follows:

$$\text{Minimize } Z = \sum_{B=1}^{N} \sum_{A=0}^{m(B)} \mathrm{BL}(B,A) \cdot X(B,A) \qquad (6)$$

subject to

$$\sum_{B=1}^{N} \sum_{A=0}^{m(B)} \mathrm{IC}(B,A) \cdot X(B,A) \leq W \qquad (7)$$

$$\sum_{A=0}^{m(B)} X(B,A) = 1 \text{ for all B} \qquad (8)$$

$$X(B,A) = 1, 0 \qquad (9)$$

where

Z = the benefit loss for any year t,
N = total number of bridges,

$m(B)$ = number of improvement alternatives for bridge B,
$\mathrm{IC}(B,A)$ = initial cost if alternative A was chosen for bridge B,
$\mathrm{BL}(B,A)$ = the loss in system benefits if alternative A was chosen for bridge B,
$X(B,A)$ = 1 if alternative A was chosen for bridge B and 0 otherwise, and
W = the available budget (dollars/year).

To solve the optimization problem associated with the developed dynamic model the neural network technique has been adopted, as discussed in the following section.

DEVELOPED ANN

From the operations researcher's point of view, ANNs are algorithms with certain characteristics that can be used to solve certain optimization tasks. The advantages of using ANNs include improvements in the speed of operation by parallel implementation either in hardware or in software. Therefore, neural networks can do well even on conventional computers. It is also possible to implement ANNs by optical devices, which operate at higher speeds than traditional electronic chips.

The common approach to the construction of optimization neural networks is to formulate the problem in terms of minimizing a cost or energy function. This approach is known as the Hopfield network (*7*). A modified Hopfield network will be used to construct the proposed ANN. Two main steps should be followed in mapping an optimization problem onto a neural network that uses an energy function (*8*): (a) choose a network architecture that decodes neurons' outputs into a solution to the problem, and, (b) formulate an energy function that generates the best solutions at its minima.

Energy functions resemble penalty functions in operation research. The objective function and the problem constraints will be included in the energy function as follows (*9*):

$$E = \sum_i v_i\,(\text{violation of constraint } i) + u\,(\text{cost}) \tag{10}$$

where

E = energy function,
v_i, u = energy function parameters (always > 0), and
cost = an optimization cost function that depends on the problem.

NETWORK STRUCTURE

The ANN developed for the present study is basically a Hopfield network, but with a dynamic penalty parameter. The approach used to map this kind of network was presented by Wang and Chankong (*10*). This network was developed after testing another kind of network with constant penalty parameters. The latter has failed to converge to a stable state, however. Figure 2 shows the network architecture. The network consists of two layers. The first one has two neurons, corresponding to L and ΔL, which will be defined later. The second layer has $n+1$ massively connected neurons, where $n = N \cdot m$, where N is the total number of bridges and m is the number of improvement alternatives for each bridge. It should be noted that the do-nothing alternative is included in the m alternatives.

Each neuron will receive four inputs, and these are feedback input from itself, input from all other neurons, input from neurons representing alternatives for the same bridge, and the benefit loss due to the alternative that the neuron represents. The costs of improvement alternatives will represent the weights of the neuron connections.

The energy function is represented by the following equation:

$$E = Z - L\,[g(x)] \tag{11}$$

where

$$Z = \sum_{i=1}^{n} \mathrm{BL}_i \cdot X_i \tag{12}$$

$$g(x) = \frac{1}{2}\left\{\left(\sum_{i=1}^{n+1} \mathrm{IC}_i \cdot X_i\right) - W\right)^2 + \frac{1}{2}\left[\sum_{j=1}^{N}\left(\sum_{i=m(j-1)+1}^{i=mj} X_i\right) - 1\right]^2\right\} \tag{13}$$

where L is the penalty parameter and $X(B,A)$ is equal to X_i. It should be noted that Z is the original objective function introduced in Equation 6. The first term of the penalty function $g(x)$ represents the budget constraint, whereas the second term represents the constraints of Equation 8, which ensure that for every bridge one and only one alternative should be selected. The form of Equation 13 will ensure that the penalty function $g(x)$ will have its lowest value when all of the constraints are satisfied; otherwise, it will be greater. A slack variable, $X(n+1)$, has been introduced to convert the budget inequality constraint to an equality constraint.

The penalty parameter L will be decreasing by an amount ΔL, which is inversely proportional to the violation of constraints:

$$\Delta L(t) = 1/g[x(t)] \tag{14}$$

$$L(t+1) = L(t) - [\Delta t \cdot \Delta L(t)] \tag{15}$$

where Δt is equal to step size (0.001 to 1.0) and $L(0)$ is the initial penalty parameter (0.0001 to 1.0).

The net input of each neuron will be changed by an amount equal to the change of the energy function due to changing the state of this neuron divided by ΔL. The division by ΔL will change the net input by an amount that is proportional to the violation of constraints. The net input for each neuron will be estimated by the following equation:

$$\mathrm{Input}_i\,(t+1) = \mathrm{Input}_i\,(t) - \Delta t \cdot \left[\frac{\partial E}{\partial X_i} \Big/ \frac{\Delta L(t)}{a}\right] \tag{16}$$

where

$$\frac{\partial E}{\partial X_i} = \mathrm{BL}_i - L\left\{\mathrm{IC}_i \cdot \left[\left(\sum_{j=1}^{n} \mathrm{IC}_j \cdot X_j\right) + X_{n+1} - W\right] + \sum_{j=1}^{n} X_j - N\right\} \text{ for } i = 1 \text{ to } n \tag{17}$$

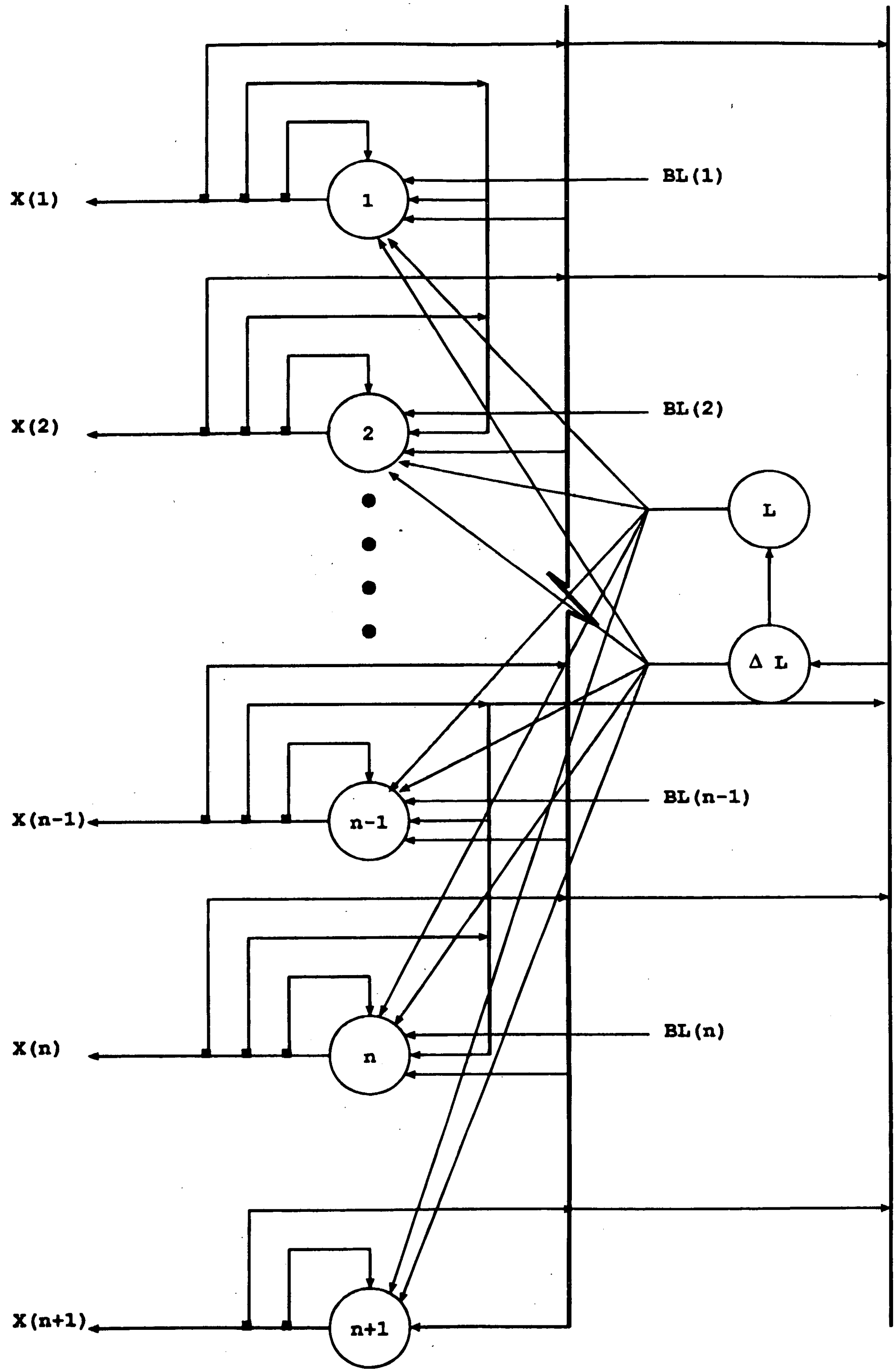

FIGURE 2 Neural network structure.

TABLE 1 Data for Example 1

Bridge	Alternative	Benefit Loss	Initial Costs	Solution
1	1	200,000	600,000	0
	2	500,000	300,000	1
2	1	300,000	500,000	1
	2	700,000	200,000	0

$$\frac{\partial E}{\partial X_{n+1}} = -L\left[\left(\sum_{i=1}^{n+1} \mathrm{IC}_i \cdot X_i\right) - W\right] \tag{18}$$

and where a is an adjusting parameter (10 to 100) and input (0) is the initial state (assumed to be zero).

The activation function $\mathrm{ACT}_i\,(t)$ will be taken as the following deterministic sigmoid function (5):

$$\mathrm{Act}_i\,(t) = \frac{1}{1 + e^{-\mathrm{Input}_i\,(t)/q}} \tag{19}$$

where q is a positive scaling constant.

By applying the output function $X_i\,(t)$ to the activated value, the state or the output of the neuron can be updated as follows:

$$X_i(t) = 0 \qquad \text{if } \mathrm{Act}_i(t) \leq \epsilon \tag{20}$$

$$X_i(t) = 1 \qquad \text{if } \mathrm{Act}_i(t) \geq (1 - \epsilon) \tag{21}$$

$$X_i\,(t) = \mathrm{Act}_i\,(t) \text{ otherwise} \tag{22}$$

where ϵ is the permissible error, which can be set between 0.01 and 0.1.

The initial states of all neurons will be set to zero. The network will be supplied by the BL and the IC of each alternative for all bridges and the available budget (W). Each neuron will begin to send impulses to other neurons through synapses or connections until the network reaches a stable state. A stable state means that each neuron is either on or off; in other words, the output X_i of each neuron is either 1 or zero. When the value of X_i is 1, this alternative will be carried out. On the other hand the value of zero corresponds to canceling this alternative. If a bridge will not receive any improvement the do-nothing alternative will be on.

APPLICATION OF DEVELOPED NETWORK

In this section the application of the developed neural network is demonstrated by using artificial data. A network simulator was constructed by using Turbo Pascal. The code for this program is available on request. Physical implementation of the proposed neural network in a parallel distribution fashion would result in significant computation enhancement. The performance of the simulated network will be demonstrated through two examples.

Example 1

In Example 1 the network was fed data about two bridges, and each bridge had two improvement alternatives. The available budget was \$800,000, and the BLs and ICs were as given in Table 1. Figures 3 and 4 illustrate the convergent patterns of the objective function (Z)

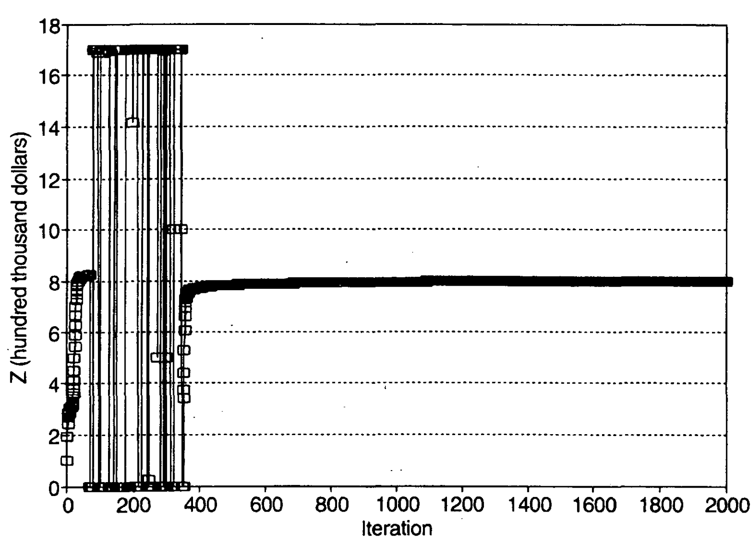

FIGURE 3 Convergent patterns of objective function Z in Example 1.

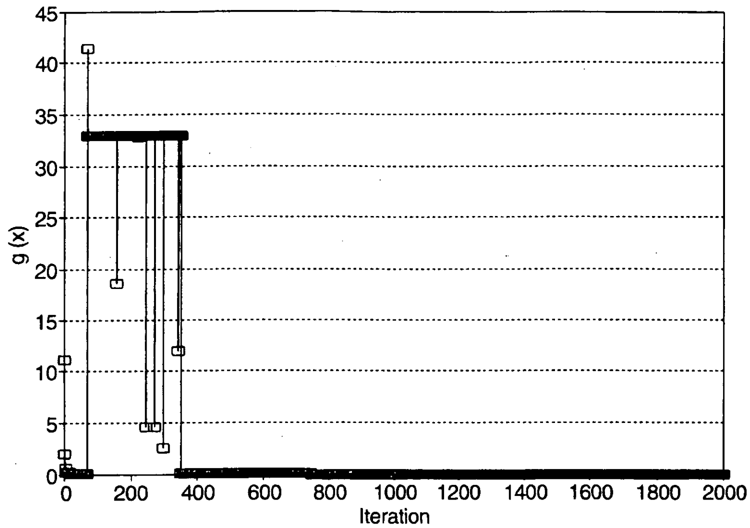

FIGURE 4 Convergent patterns of penalty function $g(x)$ in Example 1.

and the penalty function [$g(x)$], respectively. The optimal solution for this problem is to carry out alternatives 1-2 and 2-1 with a minimum Z of $800,000. It can be seen from Figure 3 that after 100 iterations the network reached the optimum, but it later diverged for about 300 iterations before reaching its stable state. From Figure 4 it can be noticed that between the 100 and the 400 iterations the constraints were violated, because $g(x)$ values were greater than zero. After 400 iterations the network converged and all neurons reached stable states; one for 1-2 and 2-1 and zero for the others. The network selected the best alternatives, which generated the minimum benefit losses, satisfied the budget constraints, and had only one neuron on for each bridge.

Example 2

Example 2 illustrates the ability of the network to find the optimal decision for a network of 10 bridges. Each bridge has two improvement alternatives, and the budget was limited to $3,200,000. A commercial software package for integer programming called DSS was used to find the optimal solution for this problem before running the network simulator. The latter program found the solution in 135 sec, whereas the developed ANN took only 20 sec. The network was able to converge after 6,000 iterations. The network data and the solution are given in Table 2. The objective function at the optima will have a value of 44 hundred thousand. Figure 5 shows

TABLE 2 Data for Example 2

Bridge	Alternative	Benefit Loss	Initial Costs	Solution
1	1	200,000	600,000	0
	2	500,000	300,000	1
2	1	300,000	500,000	1
	2	700,000	200,000	0
3	1	400,000	200,000	1
	2	700,000	200,000	0
4	1	200,000	600,000	0
	2	500,000	300,000	1
5	1	200,000	600,000	0
	2	500,000	300,000	1
6	1	200,000	600,000	0
	2	500,000	300,000	1
7	1	300,000	500,000	1
	2	700,000	200,000	0
8	1	400,000	200,000	1
	2	700,000	200,000	0
9	1	200,000	600,000	0
	2	500,000	300,000	1
10	1	200,000	600,000	0
	2	500,000	300,000	1

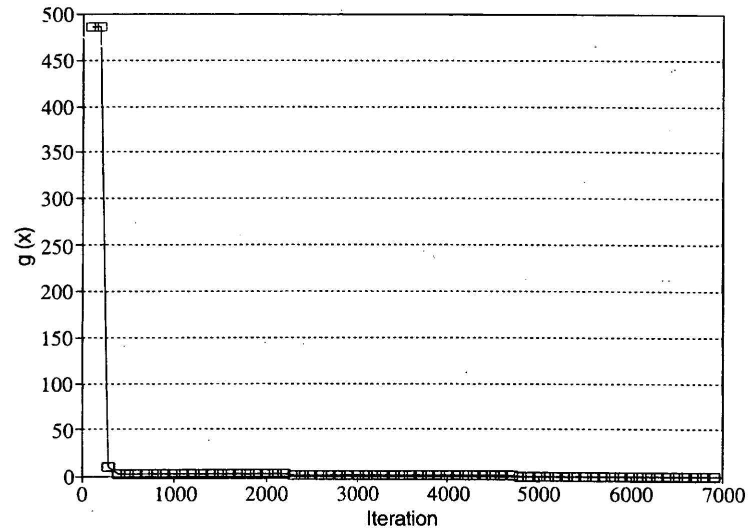

FIGURE 5 Convergent patterns of penalty function $g(x)$ in Example 2.

that the constraints were satisfied after about 500 iterations, and then a search was conducted for the optima until the network converged, as shown in Figure 6.

SUMMARY AND CONCLUSIONS

The low prioritization of budget dollars allocated to bridge activities has led to an imbalance between the needs of a bridge network and fiscal constraints. The cost of rehabilitation and replacement of bridges consumes most of the funding available for bridge improvements. Setting priorities to carry out these activities represents the core of the BMS. Existing priority-setting schemes for bridge projects can provide good solutions but not the optimal decisions for allocating funds to bridge activities. A neural network was developed to allocate a budget to bridge projects in a specific year. The architecture of the developed network reduces the memory storage space required for the computer and improves the speed of operation by parallel implementation either in hardware or in software.

More specifically, the analysis and results presented in this paper lead to the following conclusions:

1. There is an urgent need for an efficient scheme to set priorities for bridge management.
2. The bridge problem has two dimensions. The time dimension can be modeled by dynamic programming, whereas the network dimension can be simulated by a neural network.
3. ANNs can be used to allocate a budget to bridge projects.
4. The ANN that was developed has the potential to be used to allocate funds for large numbers of bridges with unlimited viable alternatives.

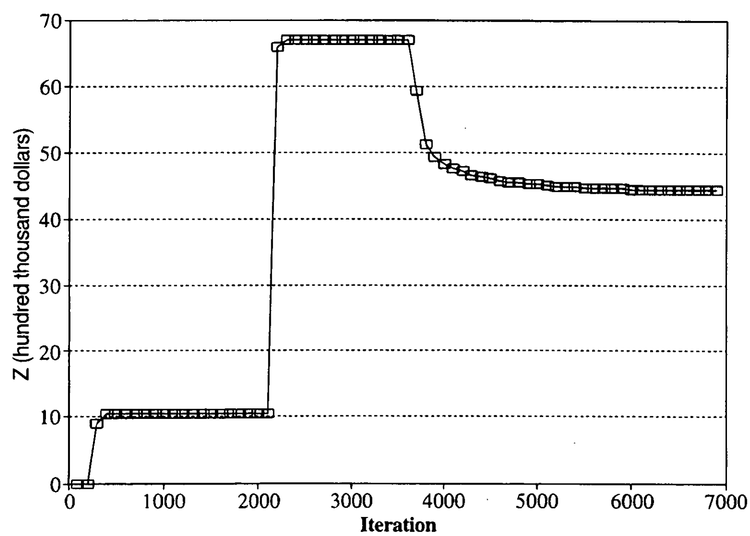

FIGURE 6 Convergent patterns of objective function Z in Example 2.

The network that was developed needs to be tested on real data for a bridge network. The feasibility and performance of the neural network for large bridge networks will be examined when data for such networks are available.

ACKNOWLEDGMENTS

The authors acknowledge the financial assistance provided by the Natural Sciences and Engineering Research Council of Canada (NSERC Scholarships) and the Transportation Association of Canada (TAC Scholarships). The authors also thank the following people for technical advice: George Hibbert of Public Works Canada and R. Hafez of the Department of Systems and Computer Engineering at Carleton University.

REFERENCES

1. *Bridge Management Systems.* Report FHWA DP-71-01R. FHWA, U.S. Department of Transportation, 1989.
2. Mohamed, H. A., A. O. Abd El Halim, and A. G. Razaqpur. Bridge Management Systems: Conceptual Framework. *Proc., Al-Azhar Engineering Third International Conference,* Cairo, Egypt, Dec. 1993.
3. Mohamed, H. A. *Development of Optimal Strategies for Bridge Management systems.* Ph.D. thesis proposal. Department of Civil and Environmental Engineering, Carleton University, Ottawa, Ontario, Canada, 1994.
4. McCulloch, W. S., and W. Pitts. A Logical Calculus of the Ideas Imminent in Nervous Activity. *Bulletin of Mathematical Biophysics,* Vol. 5, 1943, pp. 115–133.
5. Freeman, J. A., and D. M. Skapura. *Neural Networks: Algorithms, Applications, and Programming Techniques.* Addison-Wesley Publishing Company, Inc., Reading, Mass., 1991.
6. Burke, L. I., and J. P. Ignizio. Neural Networks and Operation Research: An Overview. *Computers & Operation Research,* Vol. 19, No. 3/4, 1992.
7. Hopfield, J. J., and D. W. Tank. Neural Computation of Decisions in Optimization Problems. *Biology and Cybernetics,* Vol. 52, 1985, pp. 141–152.
8. Ramanujam, J., and P. Sadayappan. Optimization by Neural Networks. In *Proc., IEEE Second International Conference on Neural Networks,* Vol. II, 1988, pp. 325–332.
9. Looi, C.-K. Neural Network Methods in Combinatorial Optimization. *Computers & Operation Research,* Vol. 19, No. 3/4, 1992.
10. Wang, J., and V. Chankong. Recurrent Neural Network for Linear Programming: Analysis and Design Principles. *Computers & Operation Research,* Vol. 19, No. 3/4, 1992.

Publication of this paper sponsored by Committee on Structures Maintenance and Management.

Bridge Element Deterioration Rates

IMAD J. ABED-AL-RAHIM AND DAVID W. JOHNSTON

Predicting the deterioration rates of bridge elements is an important component of any bridge management system. This is because the prediction of future bridge funding needs is based in part on the existing and future conditions of the bridge element. A methodology for predicting the deterioration rates of bridge elements was developed on the basis of an analysis of historical data from bridge inspections. The methodology is applied to the bridge deck, superstructure, and substructure as example elements. General deterioration curves were developed for the three major bridge elements by material type. More detailed deterioration curves for the bridge elements were also developed for various subgroupings of these elements divided by material and environmental factors.

Deterioration is the process of decline in bridge element condition. It is caused by the environment, traffic, and other spontaneous factors. The prediction of future bridge funding needs is made in part on the basis of the existing and future conditions of the bridge element. It is thus important for the success of any bridge management system to accurately predict the bridge element deterioration rates.

Under current FHWA inspection procedures elements (such as the deck, superstructure, and substructure) are evaluated on a scale of 9 to 0 indicating the degree of deterioration. Unless maintenance or rehabilitation work is performed on the bridge, the element condition rating would be expected either to remain unchanged or to drop in any inspection period. The inspection of bridges is conducted by trained technicians under engineering supervision every 2 years. Bridge-owning agencies keep records of the conditions of the various bridge elements in the Bridge Inventory data file along with other bridge data.

According to the FHWA's *Bridge Management Systems* report (*1*) all studies to date on bridge deterioration rates tend to predict slower declines in bridge condition ratings after 15 years or so. The report also included results from a regression analysis of National Bridge Inventory (NBI) data for deterioration of deck condition and overall structural condition. The results suggest that the national average deck condition rating declines at the rate of 0.104 points per year for approximately the first 10 years and 0.025 points per year for the remaining years. For overall structural condition the values were 0.094 per year for 10 years and 0.025 per year thereafter. This implies that the average conditions never fall below a condition rating of 6 until after 60 years.

However, these results do not fit with the experience encountered in practice, which suggests a much faster decline in condition. The primary difficulty encountered by researchers in developing a reasonable representation of the actual deterioration curves is that the models used to analyze aggregate inventory conditions at a point in time did not take into account the effects of any improvement work done to the bridge elements in the past.

Department of Civil Engineering, North Carolina State University, Raleigh, N.C. 27695.

OBJECTIVE

The objectives of the study were to develop analytical methods for estimating the deterioration rates of the three major bridge elements (deck, superstructure, and substructure) as a function of material types and various environmental factors. The mathematical method developed was to allow periodic reanalysis by using existing (but then current) North Carolina Department of Transportation (NCDOT) bridge data bases.

LITERATURE REVIEW

Several efforts have been made to estimate the deterioration rates of bridge elements. A study conducted at the Transportation Systems Center (TSC) (*2*) used NBI data and regression techniques to develop equations that related the three major bridge element condition ratings to other bridge characteristics found in the NBI. The study included only bridges that were 25 years or younger. Age was found to be the most highly correlated factor, with average daily traffic (ADT) being the next highest. The equations developed were used to predict the change in bridge condition over time. It was suggested on the basis of the equations that were developed that the deck deteriorates slightly faster with age than the superstructure or substructure. The study estimated the average deterioration of decks to be about 1 point in 8 years and that of both the superstructure and substructure to be about 1 point in 10 years.

The FHWA's *Bridge Management Systems* report (*1*) indicated three weaknesses in the TSC study. The first was that the analysis was performed on bridges that were no more than 25 years of age. The second was that the equations developed assumed linear relationships between the bridge element condition ratings and the parameters included in the equations. The third weakness was that the intercept coefficient in the equations was constrained to 9.

In a study by Hyman et al. (*3*) for the Wisconsin Department of Transportation piecewise linear regression was used on numerical condition appraisal data to develop deterioration curves. The study estimated a composite deterioration curve for all bridge types. In addition, deterioration curves were developed for six different bridge types: steel deck girders, other steel structures, reinforced concrete deck girders, concrete slabs, prestressed concrete structures, and culverts.

Chen and Johnston (*4*) conducted a survey of bridge inspectors and maintenance supervisors to determine age to the various levels of condition on the basis of accumulated expert experience by a Delphi approach. A series of trilinear deterioration relationships was developed, largely on the basis of survey results, for major bridge elements and material types.

Jiang and Sinha (*5*) used two approaches for developing deterioration curves. These were (a) regression analysis of condition versus age and (b) Markov chain model techniques.

The Markov chain model technique was used for two kinds of predictions: the condition rating of a bridge at a given age and the service life of a bridge. This technique was based on defining states in terms of a bridge element condition transiting from one condition to another. The zoning technique was used to obtain transition matrices, since the rate of deterioration of bridge conditions varies at different ages, thus making it a nonhomogeneous process. "Bridge age was divided into groups and within each group the Markov chain was assumed to be homogeneous" (*5*). A transition probability matrix was therefore developed for each group.

The Markov chain approach produced unusually slow predictions of element deterioration in comparison with those produced by Chen and Johnston's (*4*) surveys and in comparison with the subjective experience. However, the curve shapes, a flat S curve, were similar to the trilinear shapes developed by Chen and Johnston (*4*).

Saito and Sinha (*6*) also used the Delphi approach to develop deterioration curves for the different bridge elements. This was based on a survey of 14 Indiana Department of Highway employees in charge of bridge inspection and design.

FHWA's *Bridge Management Systems* report (*1*) stated that "All the studies on bridge deterioration to date imply that the rate of deterioration tends to slow down markedly after 15 years or so. In fact, data from many studies—when taken at face value—suggest that the average bridge condition actually improves or heals with age at some point."

This is due to the fact that in most of the studies mentioned earlier no consideration was given to the effect of the work performed on the bridge condition rating. Such effects will mask the actual relationship between the bridge's age and the element's condition rating.

DATA ON BRIDGE ELEMENT CONDITION RATINGS

FHWA requires bridge-owning agencies to keep records of numerous characteristics for every bridge under their jurisdiction. Element condition ratings of the deck, superstructure, and substructure are part of these records. NCDOT has been keeping such records since 1980. These data, which are updated as new inspections occur, are kept in the North Carolina Bridge Inventory (NCBI) data file. A status record of the total file is retained at the end of each fiscal year. Selected fields of these records, including bridge element condition ratings, are stored in the Bridge History files. These files are appended annually to include records of the latest fiscal year.

Unless it is recorded as an *N*, for nonapplicable, the bridge element condition rating can only be an integer from 0 to 9. Thus, when a bridge element changes from one condition rating to another it can only change in integer values such as 1 and 2. Hence, the data for condition rating versus time do not yield a curve when they are plotted (Figure 1).

Bridge elements almost never receive condition ratings 0, 1, or 2 because they are either rehabilitated or replaced before they reach such conditions. Of more than 14,000 bridges in North Carolina, each with three primary elements, only one bridge element had a condition rating of 2 and none had a condition rating of 0 or 1 in 1989. A bridge element only rarely receives a condition rating of 3 since, once again, they are generally either rehabilitated or replaced before reaching this level. Only 185 bridge elements in North Carolina were rated at a condition of 3 in 1989, and the majority of these were timber bridge elements.

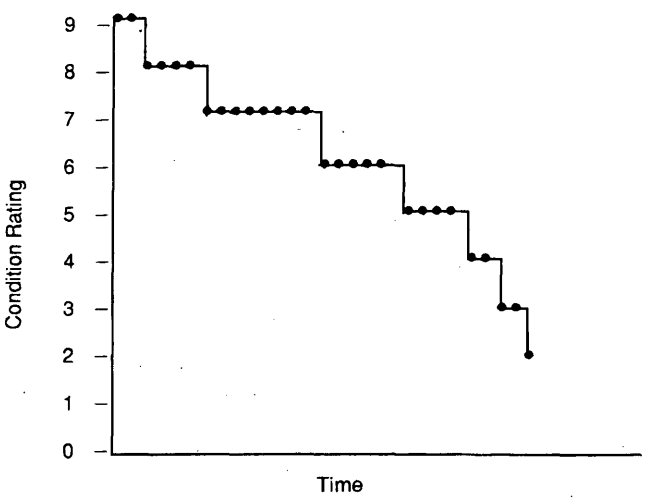

FIGURE 1 Condition rating versus time.

PROBLEMS RELATED TO BRIDGE CONDITION RATINGS

FHWA provided a coding guide (*7*) for evaluating the condition ratings of the various bridge elements. However, it did not provide a detailed reference guide that would explicitly describe the relationship between the deterioration levels of the bridge elements and numeric condition ratings (*6*). Thus, what might be recorded by one inspector as a 6 might be recorded by another inspector as a 5. An actual measure of the effect of this phenomenon on the consistency of the data stored is hard to measure. The states and FHWA have, however, attempted to promote consistency through inspection training.

When work improvement is performed on the bridge, it will increase the condition of the bridge but it will not affect the age, thus distorting the actual relationship between age and condition rating. Although NCDOT keeps records of all of the work performed on the bridges, it is difficult to measure the contributions of various improvement activities toward the condition of the bridge elements. This is caused by the fact that members of a crew performing one type of repair work might go ahead and perform some other minor repairs to other components of the bridge while they are at the site. The condition rating of the other components might thus improve, although the work might incorrectly be recorded only under the primary work item code.

Work improvements performed on bridges will in general either improve the condition rating of the element or increase the stay of the element in its current condition rating. Such work will thus disrupt the actual relationship between the bridge age and condition rating. This is evident in Figure 2, in which the average age of bridges with condition ratings of 4, 5, and 6 are almost equal, whereas the average age of bridges with a condition rating of 3 is less than the average age of the bridges with the previous three ratings. It can also be seen from Figure 2 that there is typically a lot of variation in the data for bridges with the different condition ratings.

These problems are caused by looking at data from only 1 year for bridges with no previous work, bridges with some previous work, and bridges that may have been substantially rehabilitated in the past. Unfortunately, since records only extend back to 1980 for some data and even less for other data, these groups of bridges can-

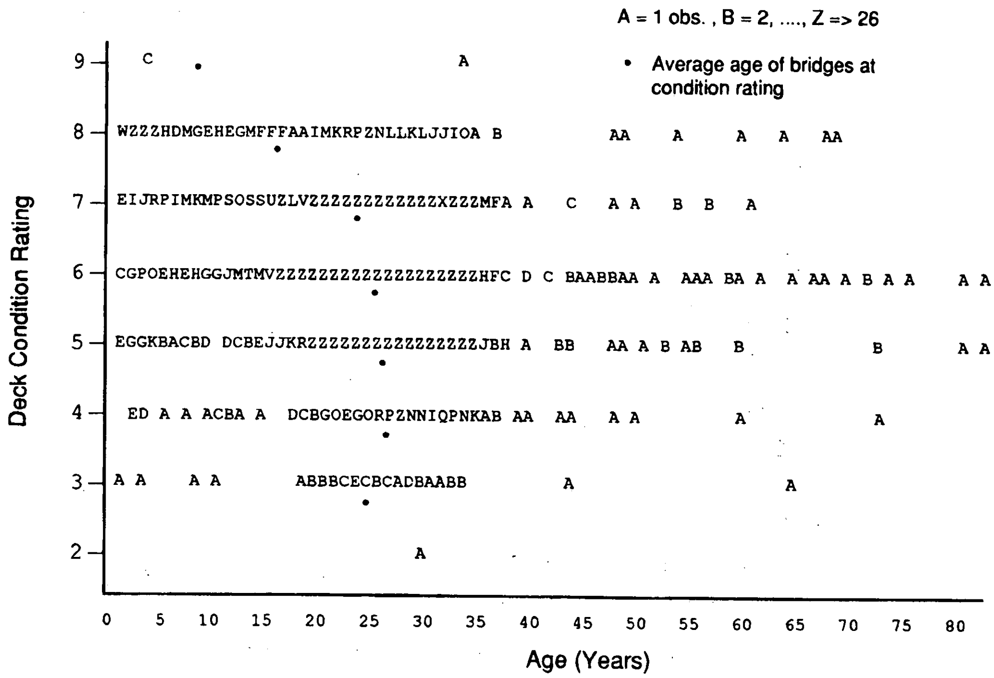

FIGURE 2 North Carolina timber deck condition ratings versus age.

not be separated. A method other than regression on data from a single year must be found.

CHARACTERISTICS OF BRIDGE CONDITION RATING DATA

The actual relationship between a material condition and time should yield a continuous curve when plotted. However, the shape of the "curve" will be affected among many things by the definition of the condition ratings. Take for example a case with two different scales. The definition of a 9 rating might be the same in both scales, but the definition of an 8 rating is very good condition in one scale and average in the other. The time that it takes for a bridge element to drop from a 9 to an 8 will therefore be different for the two scales. Furthermore, the "curve" representing the relationship between the condition rating and time for the two scales will be different. The curves will also be different in the case in which two scales have different ranges. An example of this would be the scale used by FHWA, which has ratings from 0 to 9, versus the one used by Saudi Arabia, which has a range of 0 to 7 (*8*).

As mentioned earlier, according to the FHWA definition of condition ratings, the data will not yield a "curve" when plotted against time (Figure 1). However, a curve can be plotted if the slope of various condition ratings increments can be estimated. A more realistic curve would be one that has a series of linear segments between the successive condition ratings (Figure 3).

The only time measurement related to the condition rating that can be directly used in such analysis is the age of the bridge. However, for traditional techniques such as regression and the Markov chain model, this relationship is usually distorted by previous work improvements performed on the bridge elements. It was therefore necessary to develop a methodology by which the relationship between the bridge element condition rating versus time could be analyzed.

PROPOSED DETERIORATION ANALYSIS METHOD

The approach proposed for finding a solution is to consider each condition rating separately. Once a condition rating (r) is chosen,

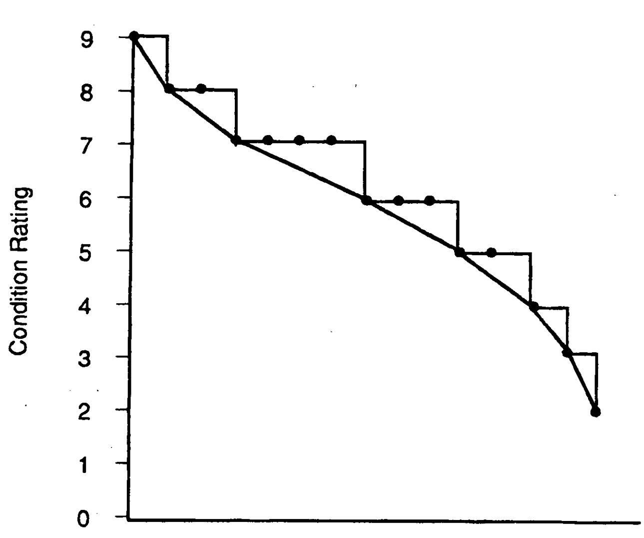

FIGURE 3 Linear segments connecting successive condition ratings.

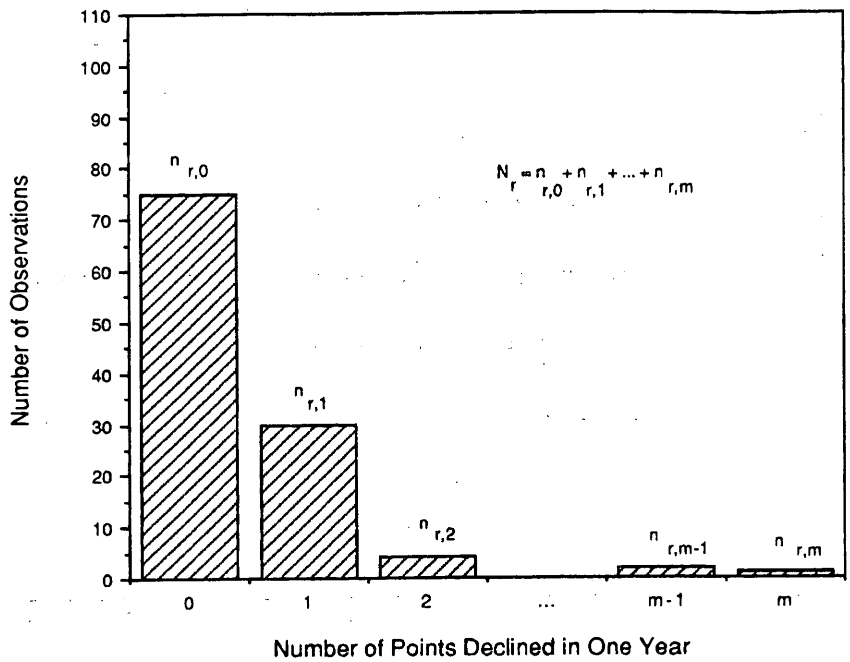

FIGURE 4 Number of observations of condition rating decline.

bridges with that condition rating are identified from the Bridge History file for a selected year, plan t. Records of the element condition rating of the identified bridges for the following year, $t + 1$, are then compared with r. Initially, bridges were considered if the condition rating in the following year, $t + 1$, either did not change or declined to a lower rating. This was to eliminate improved bridges from the study.

The total number of bridges, N_r, having a condition rating of r in year t can be tabulated. For example, Figure 4 shows a distribution of the number of bridges from a particular subset that either changed by 0 points (i.e., did not decline) or declined to a lower condition rating by 1 year later, $t + 1$. The number of bridges for which the condition rating changed by j points from the original r is represented by $n_{r,j}$ with m being the maximum decline possible for r. The summation of $n_{r,j}$ for all possible j's will thus be equal to N_r. The average weighted change within that 1-year period selected will be equal to

$$AVGCHN_r = \frac{\sum_{j=0}^{m} n_{r,j} \times j}{N_r} \tag{1}$$

where

$AVGCHN_r$ = average change from condition rating r within the 1-year period selected (t, $t + 1$);
$n_{r,j}$ = number of bridges changing by j points from condition rating r;
j = r_t − (element condition rating of the same bridge in the following year);
m = maximum number of points the bridge element can drop from r; and
N_r = total number of bridges at r in year t.

The time that it takes to drop by 1 point from r to $r - 1$ can thus be calculated once $AVGCHN_r$ is determined by using similar triangles (Figure 5):

$$\frac{\text{TIME}_r}{(t + 1) - t} = \frac{r - (r - 1)}{AVGCHN_r} \tag{2}$$

where TIME_r is the time that it takes to drop by 1 point from condition level r.

Equation 2 can be reduced to

$$\text{TIME}_r = \frac{1}{AVGCHN_r} \tag{3}$$

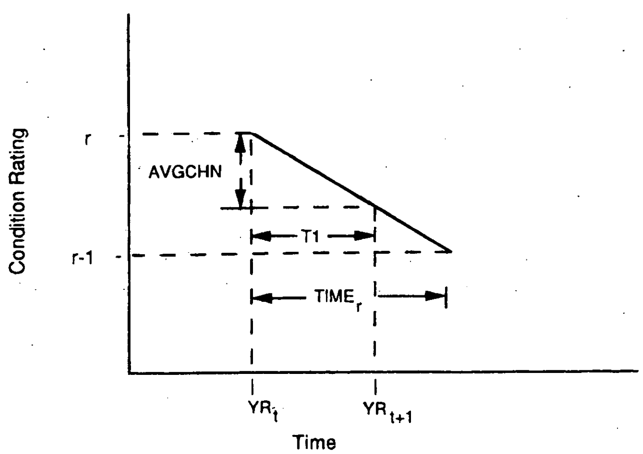

FIGURE 5 Condition rating versus time for selected r.

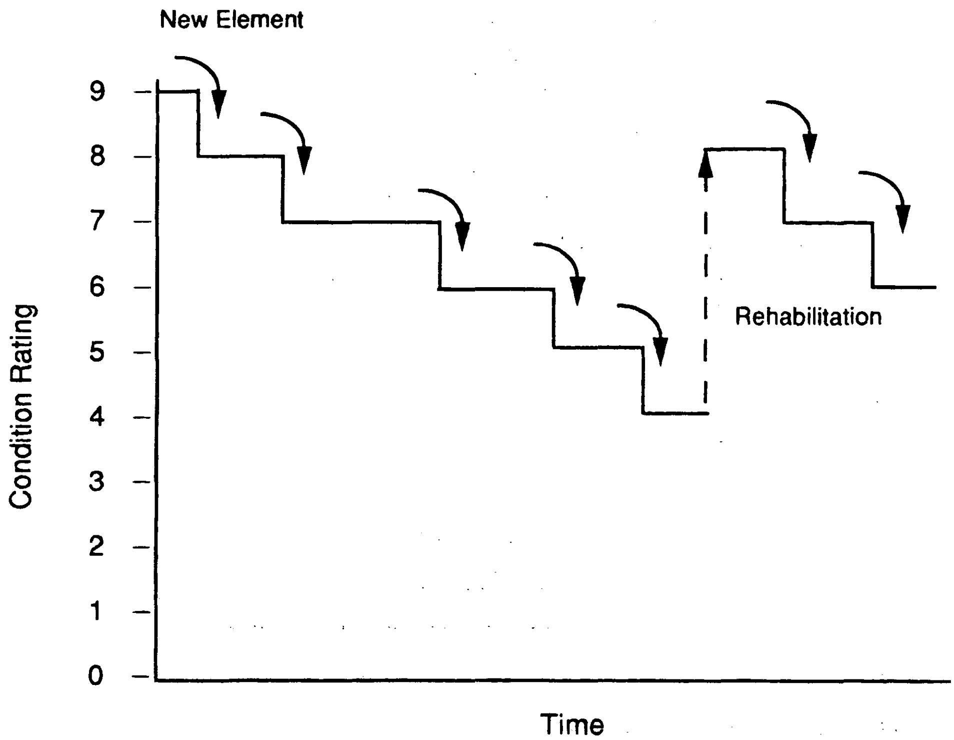

FIGURE 6 Effect of work improvement on bridge element condition rating.

Equation 1 can be modified to the following form for use when data exist for multiple 1-year intervals:

$$AVGCHN_r = \frac{\sum_{t=YR1}^{YRL-1} \sum_{j=1}^{m} n_{(r,t,j)} \times j}{\sum_{t=YR1}^{YRL-1} \sum_{j=0}^{m} n_{(r,t,j)}} \quad (4)$$

where

$YR1$ = first year selected,
YRL = last year selected, and
t = year being considered.

The equation can be applied for each value of condition rating r, calculating the slopes for the linear segments connecting successive condition ratings. Plotting the linear segments for the various condition ratings end-to-end, as in Figure 3, will produce a deterioration curve indicating the relationship between the condition rating and time.

However, two problems are associated with the data and adjustments must be made. First, it was recognized that many bridges are either rehabilitated or replaced as the element condition rating declines to lower levels. Thus, the number of bridges dropping to a lower condition rating becomes small compared with the number improving or remaining unchanged. This can make the numerator of Equation 4 very small compared with the denominator. As a result, the average change calculated would be very small. Hence, the time calculated to decline to a lower condition rating would be overestimated.

The second problem was a significant number of 1-point increases in condition that were not clearly linked to rehabilitation. After consultation with bridge maintenance experts from NCDOT, it was concluded that the improvement of 1 point is sometimes the result of a different conclusion by a subsequent inspector. This upgrading of condition can occur in borderline cases because of the general nature of the condition rating definitions. Another cause for the 1-point improvements was attributed to the effects of very minor work or preventive maintenance.

As a result of the first problem it was determined that considering the observations for improved bridges in the analysis was essential for finding a reasonable solution. A rational method of accounting for the decline before improvement was needed. The bridge element condition rating at r (Figure 6) would have declined to a lower condition rating if the work had not been performed. However, it was not possible to determine how soon this would have occurred. As illustrated in Figure 7, the improvement might occur immediately after a decline to r such as I_0 or at any later time up to just before the time that it would have declined to $r - 1$. Assuming a normal distribution of the improvement timing, a reasonable approximation would be to assume a timing as shown by $I_{0.5}$. This is equivalent to assuming that the rehabilitation is coincident with a decline of one-half point to $r - 0.5$. In reality, a condition rating cannot drop by half of a point. However, the number of observations that had improvement indicated from condition rating r were assumed to decline by $j = 0.5$.

As for problem two, it was determined on the basis of the advice of experts from NCDOT to exclude the data for which there was a

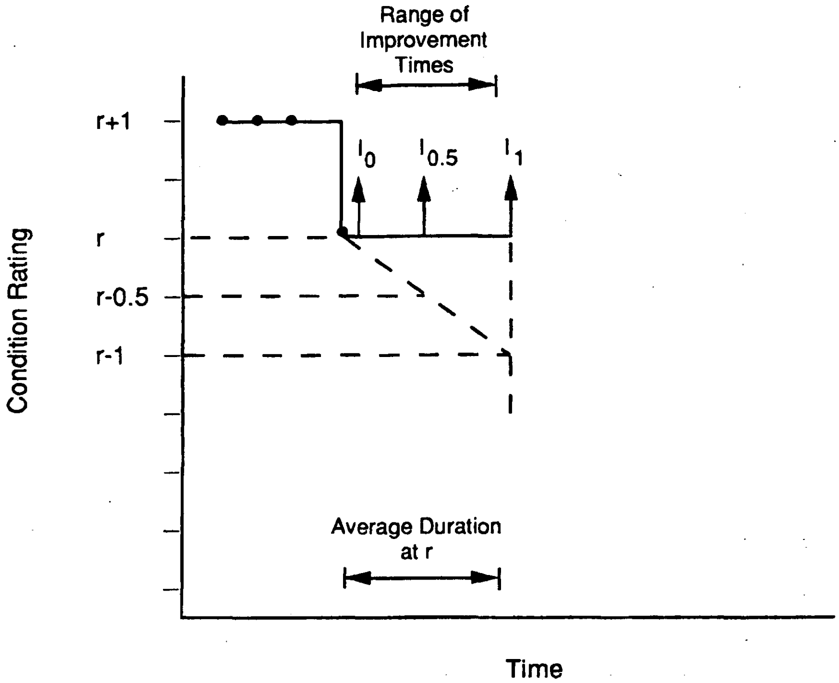

FIGURE 7 Timing of improvements.

1-point improvement. Thus, the number of observations that had an improvement of 1 point was set equal to zero.

Based on this, Equation 4 was reformulated to account for these changes. The general equation can be summarized as

$$AVGCHN_r = \frac{\text{weighted no. of declines} + 1/2 \text{ no. of improving by} > 1 \text{ point}}{\text{total no. of bridges} - \text{no. of bridges improving by 1 point}} \quad (5)$$

The new equation was thus

$$AVGCHN_r = \frac{\sum_{t=YR1}^{YRL-1} \sum_{j=1}^{m} n_{(r,t,j)} \times j + \sum_{t=YR1}^{YRL-1} \sum_{j=-2}^{z} (n_{(r,t,j)} \times 0.5)}{\sum_{t=YR1}^{YRL-1} \sum_{j=z}^{m} n_{(r,t,j)} - \sum_{t=YR1}^{YRL-1} n_{(r,t,-1)}} \quad (6)$$

where z is the maximum number of points the bridge element can improve from r (i.e., $9 - r$).

This methodology was used to develop deterioration curves for the three major bridge elements. Data on bridge condition ratings for the deck, superstructure, and substructure and other bridge characteristics were extracted from the Bridge History file for the years 1980 through 1989. Each bridge element was also initially subdivided by the element material type. The results generated are illustrated elsewhere (*9*). Further subgroupings were then considered for each element.

Deck Groupings for Deterioration Analysis

One of the main causes of deck deterioration is reinforcement corrosion induced by deicing salt. It was therefore desired to include the effects of deicing salts on the deterioration rates of the deck bridge element. However, bridges on which salt is used are not specifically defined in the NCBI. An alternate approach was used on the basis of input received from NCDOT engineers indicating that salt use is roughly limited to federal aid bridges in NCDOT geographic Divisions 5 and 7 through 14 [Table 1 (*a*)]. These divisions are located in the Piedmont and western parts of the state (Figure 8), where ice and snow are more frequent than in the eastern region. All other bridges were defined as nonsalted bridges.

A second variation of this grouping was based on dividing the salt region into two parts, the far west part of the state, which included Divisions 11, 13, and 14, as Salt Region 1, and Divisions 5, 12, and 7 through 10 as Salt Region 2. Salt Region 1 was thus located in the coldest part of the state. Both salt regions included only federal aid bridges. All other bridges in these divisions and all bridges in Divisions 1 through 4 and 6 were categorized as nonsalt bridges. The results indicated that the differences between Salt Regions 1 and 2 were not very significant. However, the effect of the combined salt regions was very obvious compared with that of the nonsalt regions. The grouping with one salt region of federal aid bridges versus all other bridges as nonsalt was therefore selected.

The effect of ADT on bridge deterioration was then considered. This was done by dividing the ADT ranges into six subgroups as shown in Table 1 (*a*). Although some of the results generated for some of the subgroupings were reasonable, the overall pattern did not fit the experience encountered in practice. The majority of those that did not fit the pattern were based on a very limited number of observations, in particular for the upper and lower ranges of ADT.

Bridges on different highway classifications are sometimes built to different standards. Therefore, the effect of highway functional classification on the deterioration rates of bridge decks was also investigated. Another advantage of using the highway functional classification as a way of subgrouping the bridges is that in general

TABLE 1 Deck Groupings for Deterioration Analysis

(a) Preliminary

Trial Groupings	Categories within Group
Salt Region Classification	I. Define Federal Aid bridges in Divisions 5 and 7-14 as salted bridges, vs other bridges and divisions as non salted; or II. Divide Bridges into 3 subgroupings: a) Divisions 11, 13, 14 (Federal Aid salted vs. others non-salted) b) Divisions 5, 7, 8, 9, 10, 12 (Federal Aid salted vs. others non-salted) c) Divisions 1, 2, 3, 4, 6 (all non-salted)
Deck Material Type	a) Reinforced concrete b) Cored slab and precast concrete c) Timber and laminated timber d) Steel plank
Functional Classification	a) Interstate, Principal Arterial, and Minor Arterial b) Major Collector c) Minor Collector d) Local
Average Daily Traffic (ADT)	0 - 200 201 - 800 801 - 2000 2001 - 4000 4001 - 8000 ADT => 8001

(b) Final

Final Groupings	Categories within Group
Salt Region Classification	Define Federal Aid bridges in Divisions 5 and 7-14 as salted bridges, vs other bridges and divisions as non salted.
Deck Material Type	a) Reinforced concrete b) Cored slab and precast concrete c) Timber and laminated timber d) Steel plank
Functional Classification	a) Interstate, Principal Arterial, Minor Arterial, and Major Collector b) Minor Collector and Local

there is an approximate relationship between the traffic volume and the type of highway. Thus, the effect of ADT on deterioration rates would be roughly accounted for by considering the type of highway classification.

Bridges were divided into four subgroups of highway classifications as indicated in Table 1 (*a*). The results generated were promising. However, certain subgroupings still suffered from the lack of a sufficient number of data points. There were almost no observations for the minor collector and local routes in the salt regions. In addition, very limited data existed for the timber and steel decks on Interstates and arterials.

The data for the nonsalt region were further analyzed by combining the Interstate and arterials subgroup with the major collectors. The minor collector and local routes were also combined into one subgroup. Data in the salt region were analyzed as one group. Table 1 (*b*) shows the final groupings for the deck deterioration analysis.

Superstructure Groupings for Deterioration Analysis

The effect of salt on the bridge superstructure condition rating was considered from two perspectives. The first was deicing salt, similar to the earlier approach for bridge decks. The other was to study the effect of seawater since corrosion-related deterioration can occur in any area that is exposed and within the reach of the seawater spray (*10*).

The effect of the deicing salts was first studied. The superstructure elements in the salt region, especially prestressed and reinforced concrete, tended to deteriorate at a faster rate than those in the nonsalt region. However, the effect was not significant for the steel and timber superstructures.

The effect of the seawater on the superstructure deterioration rates was then studied. Bridges were divided into two groups: those bridges in coastal counties (Figure 8) and over a waterway were classified as marine environment; all other bridges were classified

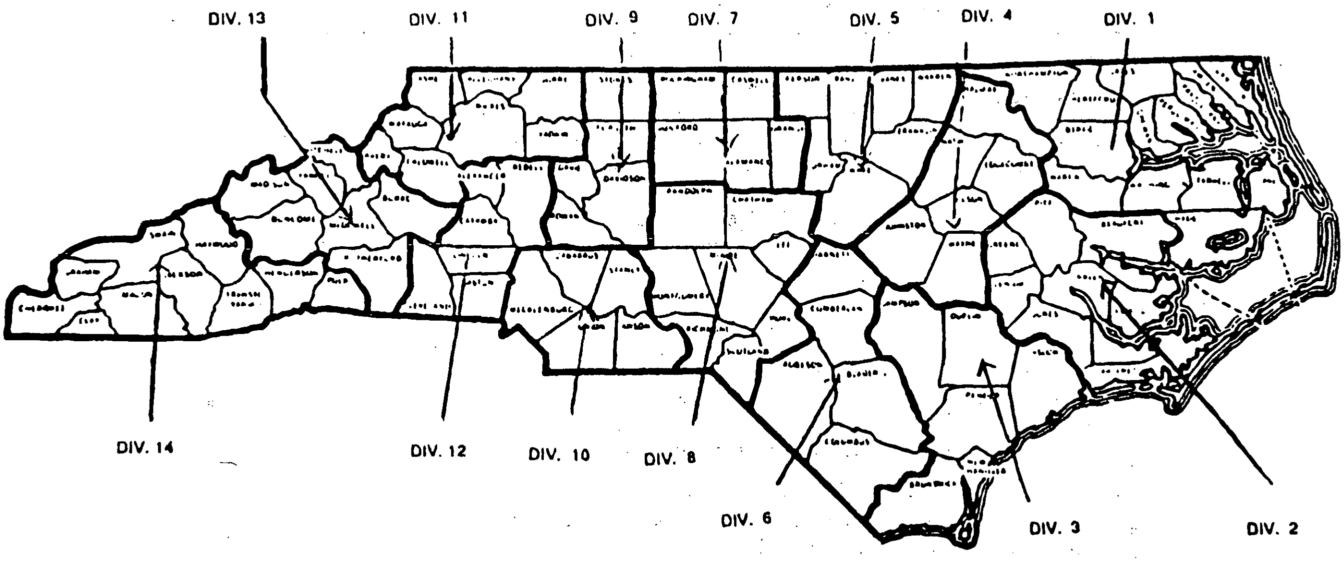

FIGURE 8 Divisions in North Carolina.

as nonmarine environment. The deterioration rates for the marine environment were greater than those for the nonmarine environment. It was also evident that the effect of the seawater was more significant than the effect of the deicing salts. Thus, the effect of the seawater was selected for further analysis.

Bridges were then subgrouped by functional classification, similar to the approach used for bridge decks. The superstructure type was another parameter thought to influence the deterioration rates of the bridge superstructure. Reinforced concrete and steel structures were therefore divided into two subgroups each, as shown in Table 2 (*a*). The steel truss subgroup did not contain sufficient numbers of observations when it was subdivided by highway classification and marine versus nonmarine environment. Thus, all steel trusses were analyzed as one group. The difference in the deterioration rates for the concrete structure types was very small. The subgroups were therefore combined together under reinforced concrete. However, steel trusses tended to deteriorate at a faster rate than the other types of steel structures. The final groupings for the superstructure deterioration analysis are given in Table 2 (*b*).

Substructure Groupings for Deterioration Analysis

The effect of seawater on the deterioration rates of substructure elements was first studied. Bridges were thus divided into groups of marine and nonmarine environments similar to the approach used for the superstructure analysis. However, the nonmarine environment group was further divided into waterway and grade separation. This was done so that the effect of freshwater on the bridge substructure could be evaluated. Bridges were also subgrouped by material type.

DETAILED DETERIORATION RESULTS

Detailed deterioration curves for bridge decks are plotted in Figure 9. From these curves it is apparent that the deicing salt accelerates the deterioration of bridge decks. The effect of the deicing salt was most significant on the prestressed concrete decks; this was followed by the reinforced concrete. The effect of the deicing salt on the steel (asphalt-filled steel pan) and timber decks was very small, as might be expected. It can be noted that the prestressed concrete generally has higher condition ratings at early ages, but once problems occur the condition ratings decline rapidly. This is probably due to recognition by inspectors that evidence of a problem in prestressed members can be a major concern since the small area of steel is sensitive to corrosion or other forms of deterioration. Bridge decks located on minor collector and local routes tended to deteriorate at a slower rate than those located on Interstate, arterial, and major collector routes. This could be attributed to the higher volume of traffic and the higher percentage of trucks that use the latter types of highways. Prestressed concrete was the only exception to this trend, possibly because of variations in the design of prestressed concrete decks.

As for the deterioration rates of the bridge superstructure element, it was evident that the salt from the sea air or water splash increased the deterioration rates of the element. It was also evident that bridges on Interstate, arterial, and major collector routes deteriorated at a faster rate than those on minor collector and local routes. However, the difference in the deterioration rates of the superstructure rates between the two types of highway groupings was not as significant as the difference in the deterioration rates of bridge decks. This could be attributed to the fact that the impact of traffic on the superstructure is not as severe as that on decks. The deterioration curves generated for superstructure elements, subdivided by material and other groupings, can be found elsewhere (*9*).

Bridge substructures located in a marine environment were found to deteriorate at a much faster rate than those located in a nonmarine environment. In addition, those bridges that were over a waterway tended to deteriorate at a faster rate than bridges at a grade separation but at a slower rate than the bridges in a marine environment. The deterioration curves generated for substructure elements, subdivided by material and other groupings, can be found in elsewhere (*9*).

TABLE 2 Superstructure Groupings for Deterioration Analysis

(a) Preliminary

Trial Groupings	Categories within Group
Marine Environment Classification	a) Marine Environment: In a coastal county shown in Figure 8 and over a waterway b) Non-marine Environment: All other bridges not included in the marine environment category
Salt Region Classification	Define Federal Aid bridges in Divisions 5 and 7-14 as salted bridges, vs other bridges and divisions as non salted.
Material and Structure Type	a) Prestressed Concrete b) Reinforced Concrete i) Slab and M-beam ii) T-beam, Girder Floor Beam, Box Beam (Multiple and Single) c) Steel i) Truss (Thru and Deck) ii) All other Types d) Timber
Functional Classification	a) Interstate, Principal Arterial, and Minor Arterial b) Major Collector c) Minor Collector d) Local

(b) Final

Final Groupings	Categories within Group
Marine Environment Classification	a) Marine Environment: In a coastal county shown in Figure 8 and over a waterway b) Non-marine Environment: All other bridges not included in the marine environment category
Material and Structure Type	a) Prestressed Concrete b) Reinforced Concrete c) Steel i) Truss (Thru and Deck) ii) All other Types d) Timber
Functional Classification	a) Interstate, Principal Arterial, Minor Arterial, and Major Collector b) Minor Collector and Local

Overall, the analysis produced a set of results that is consistent with a rational comparative consideration of the material, environment, and other factors.

SUMMARY AND CONCLUSIONS

A methodology was developed for predicting the deterioration rates of the bridge deck, superstructure, and substructure elements as measured by FHWA bridge inspection condition ratings. A set of deterioration curves was developed for the three major bridge elements by material type. Another set of deterioration curves was developed for various subgroupings of the bridge elements on the basis of environment and functional classifications.

1. For decks deicing salts were found to cause the deterioration rates to increase, in particular for prestressed and reinforced concrete decks. The effect of the deicing salts on the timber decks was not very significant. The highway classification was significant in relation to the deterioration rates of the bridge decks. Bridge decks on minor collector and local routes tended to deteriorate at a slower rate than those on Interstate, arterial, and major collector routes. This was attributed to the higher traffic volumes and the higher percentage of trucks that use the latter type of highways.

2. Deterioration rates for the superstructure tended to be higher for those bridges exposed to the splashing of saltwater than those that are not exposed to saltwater. Bridge superstructures on Interstate, arterial, and major collector routes were found to deteriorate at a faster rate than those on minor collector and local routes.

3. The effect of saltwater was found to cause a rapid increase in the deterioration of the bridge substructure. Although freshwater was also found to increase the deterioration rate of the substructure, the impact was not as significant as that of saltwater. Substructure deterioration rates at grade separation were comparatively low.

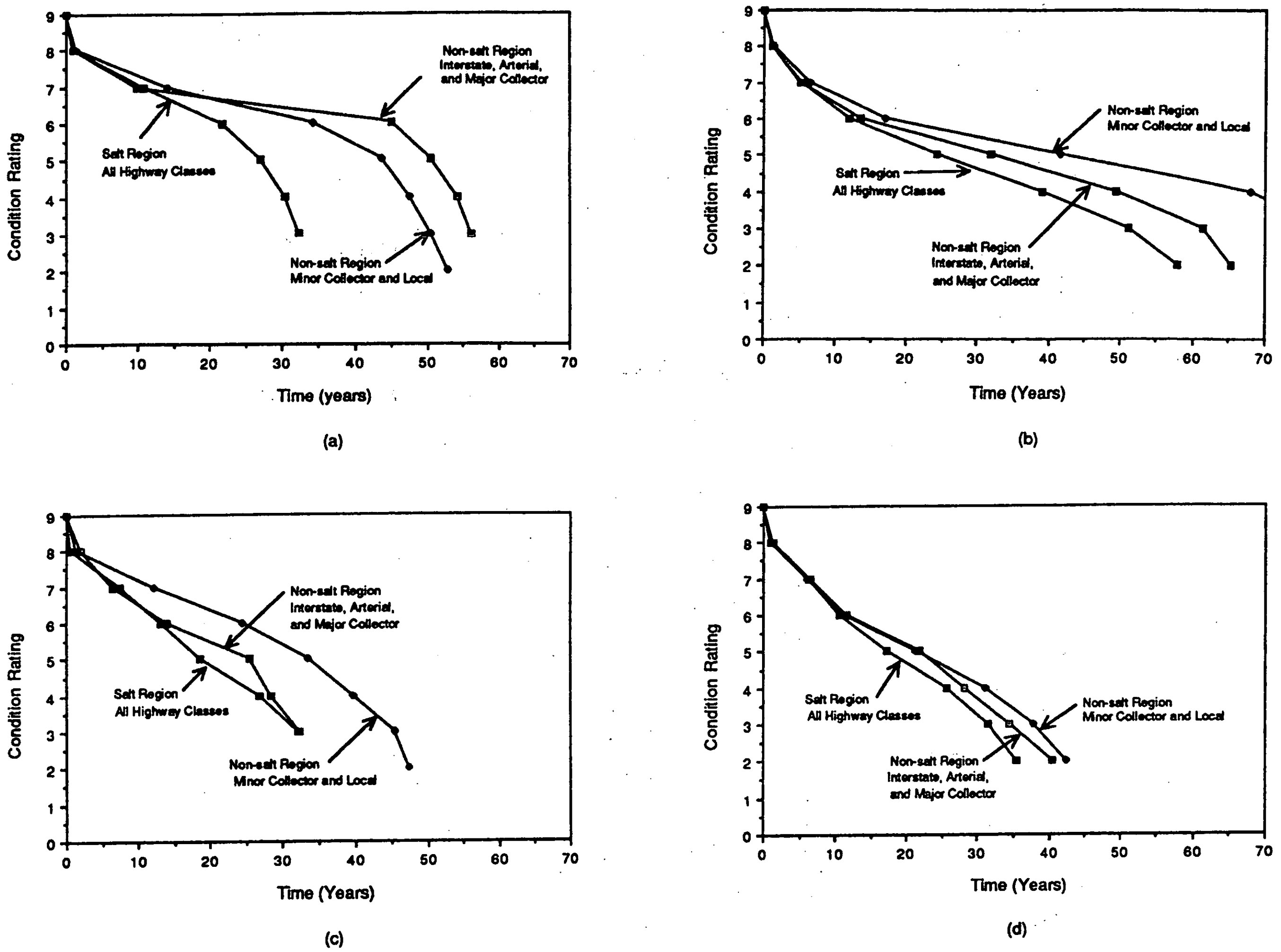

FIGURE 9 Deck condition rating versus time: (*a*) prestressed concrete, (*b*) reinforced concrete, (*c*) steel, and (*d*) timber.

ACKNOWLEDGMENTS

The research described herein was conducted at North Carolina State University with the support of NCDOT. The writers gratefully acknowledge the support provided by NCDOT and the assistance provided by Jimmy D. Lee, State Bridge Maintenance Engineer.

REFERENCES

1. O'Connor, D. S., and W. A. Hyman. *Bridge Management Systems.* Report FHWA-DP-71-01R. FHWA, U.S. Department of Transportation, Oct. 1989.
2. Busa, G., M. Cassella, W. Gazda, and R. Horn. *A National Bridge Deterioration Model.* Report SS-42-U5-26. Transportation Systems Center, U.S. Department of Transportation, Cambridge, Mass., 1985.
3. Hyman, W., D. Hughes, and T. Dobson. *The Least Cost Mix of Bridge Replacement and Repair Work on Wisconsin's State Highways Over Time—A Computer Simulation.* Draft Technical Report. Wisconsin Department of Transportation, Madison, 1983.
4. Chen, C. J., and D. W. Johnston. *Bridge Management Under a Level of Service Concept Providing Optimum Improvement Action, Time, and Budget Prediction.* Report FHWA/NC/88-004; Research Project 86-2. Center for Transportation Studies, Department of Civil Engineering, North Carolina State University, Raleigh, 1987.
5. Jiang, Y., and K. C. Sinha. Bridge Service Life Prediction Model Using the Markov Chain. In *Transportation Research Record 1223,* TRB, National Research Council, Washington, D.C., 1989, pp. 24–30.
6. Saito, M., and K. C. Sinha. *A Delphi Study in Bridge Condition Rating and the Effect of Bridge Improvement Alternatives.* Presented at 69th Annual Meeting of the Transportation Research Board, Washington, D.C., 1990.
7. *Recording and Coding Guide for the Structure Inventory and Appraisal of the Nation's Bridges.* FHWA, U.S. Department of Transportation, Dec. 1988.
8. Harper, W. V., A. Al-Salloum, S. Al-Sayyari, S. Al-Theneyan, J. Lam, and C. Helm. Selection of Ideal Maintenance Strategies in a Network-Level Bridge Management System. In *Transportation Research Record 1268,* TRB, National Research Council, Washington, D.C., 1990, pp. 59–67.
9. Abed-Al-Rahim, I. J., and D. W. Johnston. *Analysis of Relationships Affecting Bridge Deterioration and Improvement.* Research Project 90-6. Center for Transportation Engineering Studies, Department of Civil Engineering, North Carolina State University, Raleigh, 1991.
10. Novokshchenoc, V. *Salt Penetration and Corrosion in Prestressed Concrete Members.* Publication FHWA RD-88-268. FHWA, U.S. Department of Transportation, July 1989.

Publication of this paper sponsored by Committee on Structures Maintenance and Management.

BRIDGIT Deterioration Models

HUGH HAWK

Accurate prediction of the future condition of bridge elements is one of the cornerstones of any bridge management system's (BMS's) optimization model. The BRIDGIT BMS software uses condition state quantities to represent the conditions of the various elements that make up a bridge. The use of condition states does not allow for an easy application of classical deterministic deterioration curves. It is necessary to model the transition of element quantities through their various condition states. Predicting the deterioration of an element through time is essential for estimating the timing of future repair and improvement actions and calculating their associated costs. Deterioration of a bridge element can be represented by a Markov chain process. By this approach transitional rates are calculated to project the quantities of a bridge element that will move to lower condition states in a defined time interval. BRIDGIT uses derivatives of Markov chain processes to model unprotected elements, protection systems (such as paint systems or deck overlays), and protected elements in which the protection system modulates the deterioration of the base element. In addition, BRIDGIT considers the effects of environment, traffic volumes, and previous repairs that may accelerate the deterioration of decks, slabs, and overlays.

The principal objective of NCHRP Project 12-28(2)A (*1,2*), which began in January 1992, was to develop, validate, and document a fully operational microcomputer-based bridge management system (BMS) software package that could readily be used by transportation agencies. The system is based on the conceptual design presented in NCHRP Report 300 as well as the recommendations identified in "Guidelines for Bridge Management Systems" that resulted from NCHRP Project 20-7, Task 46.

This paper is restricted to a discussion of the deterioration models used.

BRIDGIT ELEMENT AND PROTECTION SYSTEM MODELS

BRIDGIT uses condition state quantities to identify the nature, severity, and extent of deterioration of bridge elements and protection systems. Up to five condition states may be defined for an element or protection system model. Condition states for an element or protection system are associated with different levels of physical defects as well as functional performance deficiencies.

As part of the inspection process inspectors must record the quantity or percentage of an element in each condition state. Each condition state can be associated with specific repair actions and unit costs. BRIDGIT automatically considers the replacement and do-nothing alternatives for the element as well.

National Engineering Technology Corporation, 133 Wynford Drive, North York, Ontario, Canada M3C 1K1.

PREDICTION OF FUTURE CONDITION

The information defined for each element deterioration model in BRIDGIT is used to calculate the quantity of element that transitions from a particular condition state to the next lower one in any year. This is accomplished by assuming a Markov chain process (*3*) and calculating the transitional rates for each condition state of an element.

In the Markov chain process the probability that an element transitions from condition state i to another condition state j does not depend on how the element arrived at the ith state. That is, the probability of a quantity of an element moving to a future state always considers its current state as if it were a starting point.

The probability that the process moves to state j from state i in 1 year (i.e., in one step) is called the *transition probability* and is generally denoted p_{ij}. In the case of bridge element deterioration it can be assumed that the probability of transitioning from one state to the next is the same from year to year. This assumption makes it possible to define an n-step matrix of the transitioning process, which is simply the one-step transition matrix raised to the nth power.

Development of Equations for Predicting Future Condition State Quantities

The following assumptions are used by BRIDGIT in applying the Markovian chain process to a practical modeling of bridge element deterioration:

1. Elements cannot improve their condition unless some action has been effected.
2. An element quantity can transition to a lower condition by, at most, one state in 1 year. Thus, it is not possible to deteriorate from Condition State 2 to Condition State 4 in 1 year.
3. For a total quantity of element, *TOTQUAN*, the sum of the normalized quantities in each condition state must be equal to unity.

$$\sum_{i=1}^{5} X_i = 1.0 \qquad (1)$$

where X_i is equal to $QUAN_i/TOTQUAN$ and $QUAN_i$ is the quantity of element in state i at the beginning of the current year of the analysis.

4. The sum of the normalized quantities in each condition state in Y years must be equal to unity.

$$\sum_{i=1}^{5} NEWX_i = 1.0 \qquad (2)$$

where $NEWX_i$ is equal to $NEWQUAN_i/TOTQUAN$ and $NEWQUAN_i$ is the quantity of element in state i in Y years.

These assumptions lead to a Markovian transition probability matrix in which all matrix elements are zero except for the diagonal and one line below the diagonal. Thus:

$$[NEWX] = [P]^{y}\,[X]$$

$$\begin{bmatrix} NEWX_1 \\ NEWX_2 \\ NEWX_3 \\ NEWX_4 \\ NEWX_5 \end{bmatrix} = \begin{bmatrix} P_{11} & 0 & 0 & 0 & 0 \\ (1-P_{11}) & P_{22} & 0 & 0 & 0 \\ 0 & (1-P_{22}) & P_{33} & 0 & 0 \\ 0 & 0 & (1-P_{33}) & P_{44} & 0 \\ 0 & 0 & 0 & (1-P_{44}) & 1.0 \end{bmatrix}^{Y} \begin{bmatrix} X_1 \\ X_2 \\ X_3 \\ X_4 \\ X_5 \end{bmatrix} \quad (3)$$

where P_{ii} is the probability of a state i quantity staying in state i after 1 year.

Note that the transition matrix in Equation 3 is raised to the Yth power to reflect Y years of deterioration.

This matrix equation can be solved by standard mathematical procedures involving eigenvalues and eigenvectors. Equation 3 permits BRIDGIT to determine the future quantities in each state after Y years, [NEWX], based on knowing the initial mix of condition state quantities, [X].

Developing Transition Probabilities

In fully implementing the Markovian model it is necessary to determine the transition probabilities P_{11}, P_{22}, P_{33}, and P_{44} used in Equation 3 to predict the future quantities of an element in each condition state. Initially, BRIDGIT is supplied with default deterioration model data that can be altered by each agency if desired. When sufficient historical condition information is available from annual inspections, BRIDGIT can automatically update these model parameters.

For each element deterioration model the following information must be provided by the user for each condition state of the element, as well as for the four possible environments:

1. The average number of years that it takes for a specific percentage of an *unprotected* element quantity to deteriorate from new condition to another condition state *or worse.*
2. The corresponding fractional element quantity.

BRIDGIT requires that the agency determine this information through research, statistical analysis, or field observation.

Using this information BRIDGIT can calculate the transition probabilities for each condition state.

Table 1 shows a sample deterioration model for a concrete deck element. For a moderate environment it shows 25 percent of the total quantity of element in an average bridge to be in Condition State 3 or worse after 20 years.

DETERIORATION OF PROTECTED AND UNPROTECTED ELEMENTS

The following sections describe the application of the Markov process as well as the models used by BRIDGIT to predict the future conditions of elements and protection systems.

Deterioration of Unprotected Elements and Protection Systems

To predict the future conditions of unprotected bridge elements, BRIDGIT directly applies Equation 3 for different years (Y) over the life of the element. The values used for Y are determined during the development of the life-cycle activity profiles produced by BRIDGIT for each bridge in a network. In addition, Y is adjusted to account for the effect of average daily traffic on the rate of deterioration of the element.

This methodology is used for any elements which that do not have an associated protection system and that include elements such as bare decks, unpainted steel girders, joints, and bearings and is also used for protection systems themselves.

Deterioration of Protected Elements

The deterioration of protected elements is more complex. In general terms BRIDGIT assumes that the protection system modulates the deterioration of the protected element. For example, a concrete deck protected by an asphalt overlay may deteriorate at half the rate of a bare deck if the asphalt is in good condition, at 80 percent of the rate of a bare deck if the asphalt is in fair to poor condition, and perhaps even faster than a bare deck if the overlay is in bad condition.

TABLE 1 Element Deterioration Model for Concrete Decks

Condition State	% of Element in this State or Worse	Time in Years to Deteriorate Specified % of Element by Environment			
		Benign	Low	Moderate	Severe
2	35.00	10	10	8	6
3	25.00	30	25	20	11
4	20.00	50	40	25	15

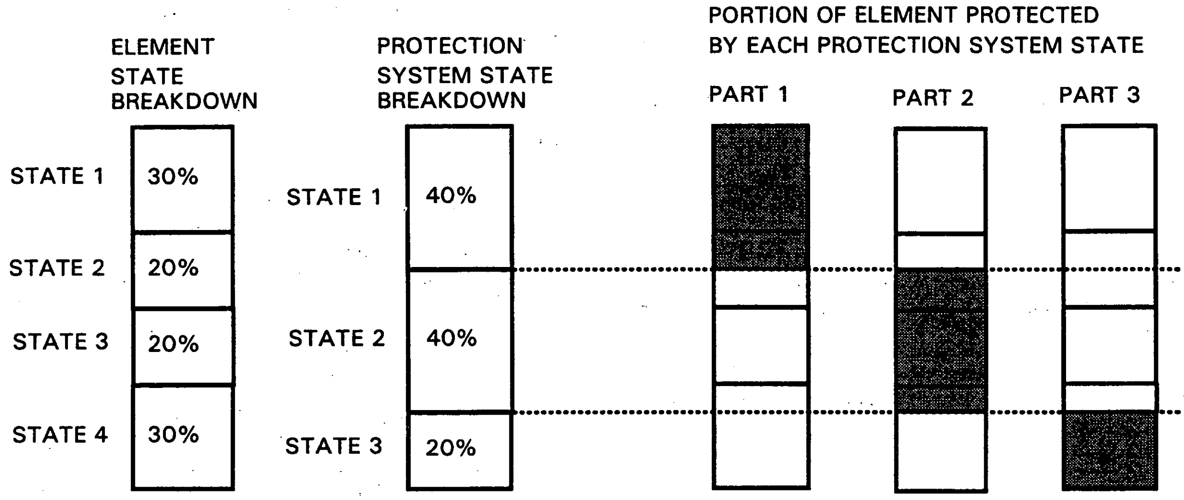

FIGURE 1 Portion of element protected by each protection system state.

BRIDGIT also assumes that element condition and protection system condition are linked (i.e., the locations where the element is in its worst condition are the same as the locations where the protection system is also in its worst condition). For example, steel girder deterioration due to corrosion is assumed to occur where the paint has failed.

As part of the information used to define protection system models, a protection modifier must be specified for each condition state. This represents a factor by which the rate of deterioration of a protected element is decreased. In other words, if the protection modifier for a paint protection system in Condition State 2 is 4 then the rate of deterioration of quantities of element protected by paint in State 2 is one-fourth the rate of deterioration for the unprotected element quantity.

The most difficult part of modeling the deterioration of protected elements is in determining the quantities of base elements that are protected by each associated protection system quantity. BRIDGIT performs the following steps to obtain results for any year of an element's life:

1. Deteriorate the protection system by Y years to calculate the predicted future state quantities $NEWXP_j$ of the protection system.
2. Determine the average protection to the element provided over the Y-year interval. For bridge deterioration modeling averaging is sufficiently accurate provided that the time interval is small compared with the life span of the protection system (i.e., deterioration from state to state is generally linear in the short term).
3. Determine the condition state quantities of the element that are protected by each of the protection system states. Figure 1 illustrates this for an element with four condition states and a protection system with three states. Figure 1 shows, for example, that State 2 of the protection system protects half of State 2 of the base element, all of State 3, and one-third of State 4.
4. BRIDGIT then separates the base element into a series of unprotected elements, one for each condition state of the protection system. These "separated" elements are then deteriorated individually, accounting for the effects of the protection system modifier. This is accomplished by modifying the time interval Y as follows:

$$Y'_j = Y / SUBMOD_j$$

where $SUBMOD_j$ is the protection system modifier for State j of the protection system. Using the transition probabilities already known for the unprotected base element, Equation 3 is used to determine the $[NEWX]$ quantities of the separated elements and for each Y'_j. The final predicted element quantities are then determined by combining the results obtained for the separated elements.

OTHER FACTORS AFFECTING ELEMENT DETERIORATION

Effect of Previous Repairs on Deterioration

For some elements it is appropriate to account for previous repairs in the deterioration rates since repaired elements tend to deteriorate more quickly. This is especially true for concrete decks. This increase in deterioration rate could be due to two factors:

1. Repairs are not of the same quality.
2. Past repairs are indicative of defects that are not detectable by visual inspections. Engineers involved in planning deck repairs always inflate repair quantities in the contract above those indicated by even instrumented inspections because they know that more problems show up during the actual repairs.

BRIDGIT attempts to reflect the effects of these hidden defects by moving a percentage of the State 1 quantity into State 2. This effectively accelerates the deterioration process.

Effects of Average Daily Traffic

It is well understood that the amount of traffic, especially the amount of truck traffic, can influence the deterioration rates of decks, joints, and other elements directly affected by wheel loads. In general, average daily traffic and percent truck traffic are related to the functional classification of the roadway. BRIDGIT makes use of an average daily traffic modifier that is associated with each functional route classification.

BRIDGIT incorporates the effects of the average daily traffic modifier by adjusting the value of Y used in Equation 3. For example, if it is determined that bridge decks on local roads tend to deteriorate at only 70 percent of the rate for the entire bridge population because of low traffic volumes, BRIDGIT uses a value of $Y' = 0.70 \cdot Y$ instead of Y in the equation.

CONCLUSIONS

Markov chain processes are ideally suited to the prediction of future element condition in which each element's condition is defined by a set of condition state quantities.

The deterioration models used in BRIDGIT model elements and protection systems separately and also account for the interplay between the two.

ACKNOWLEDGMENTS

This work formed part of NCHRP Project 12-28(2)A and was sponsored by the AASHTO, in cooperation with the FHWA, and was conducted in NCHRP, which is administered by TRB of the National Research Council.

REFERENCES

1. NET Corp./Delcan Corp. *BRIDGIT User's Manual,* Version 1.0 NCHRP Project 12-28(2)A Report. NCHRP, National Research Council, Washington, D.C., Dec. 1994.
2. NET Corp./Delcan Corp. *BRIDGIT Technical Manual.* NCHRP Project 12-28(2)A Report. NCHRP, National Research Council, Washington, D.C., Dec. 1994.
3. Tsokos, C. P. *Probability Distributions: An Introduction to Probability Theory with Applications.* Duxbury Press, Belmont, Calif., 1972.

Publication of this paper sponsored by Committee on Structures Maintenance and Management.

Bridge Replacement Cost Analysis Procedures

IMAD J. ABED-AL-RAHIM AND DAVID W. JOHNSTON

For some agencies bridge replacement costs are considered to be the highest proportion of funding needs among the three bridge improvement alternatives of maintenance, rehabilitation, and replacement. Estimating the bridge replacement cost is therefore a very important component of any bridge management system implemented in response to the Intermodal Surface Transportation Efficiency Act of 1991. In response to this need analytical procedures were developed for estimating the costs of the bridge structure, roadway improvements, and engineering for budgeting purposes. Methodologies for predicting the new bridge length, width, and maximum span length, which were found to affect the total cost of bridge replacement, on the basis of existing bridge and roadway data characteristics, were also developed.

The Intermodal Surface Transportation Efficiency Act of 1991 requires states to implement a bridge management system (BMS) that considers the life-cycle costs of alternative improvement options. Bridge replacement, rehabilitation, and maintenance are the three general alternatives for improving a deficient bridge. As proposed by Chen and Johnston (*1*) for BMSs the alternative with the lowest life-cycle cost, considering both agency and user costs, is the optimum selection for improving a deficient bridge when adequate funds are available. Thus, it is important to have good estimates of these types of costs when making a decision on which alternative to implement. For some agencies the backlog of bridge replacements accounts for the highest proportion of funding needs among the three improvement alternatives (*2–4*). Furthermore, total agency and user costs are sensitive to replacement costs, as was evident in the sensitivity analysis conducted by Abed-Al-Rahim and Johnston (*5*).

The total cost for replacing a deteriorated or functionally obsolete bridge includes numerous items. Engineering, surveying and inspection services, demolition of the old bridge, construction of a temporary alternate route, new bridge construction, and approach roadway improvements are primary examples. The replacement bridge construction cost will vary with bridge size, site characteristics, and other features. At the forecasting, planning, and budgeting stage of BMS use the detailed design of the bridge is not available. Thus, it is necessary to estimate the replacement cost on a unit-cost basis considering size and other important features. Analytical methods for estimating the planned unit cost of construction can be developed on the basis of the construction costs of previous projects that might have occurred in various years. However, all costs from previous years must be adjusted for inflation, productivity, and technology changes to one common year before such analyses can be conducted.

Predicting some of the characteristics of the bridge being replaced and those that might change with the new bridge is important, since they will affect the total cost of replacement and will therefore influence the decision-making process in a BMS. For example, a new bridge is usually longer than the one it has replaced. This can be attributed to several factors, for example, improving a waterway channel or widening an underpass roadway. Other characteristics that might influence the cost of new bridge construction include bridge width and maximum span length. Although models for predicting such characteristics can be developed, the actual features will not be known until a detailed design is undertaken.

Department of Civil Engineering, North Carolina State University, Raleigh, N.C. 27695–7908.

OBJECTIVE

The objective of the study described here was to develop methodologies and procedures for estimating the unit costs of bridge replacement as a function of various existing bridge and roadway characteristics. Analytical methods for estimating some of the new geometric features for a replacement bridge were also developed. The methods were applied to the bridge inventory and construction cost records of the North Carolina Department of Transportation (NCDOT) as an example.

BACKGROUND

For budgeting purposes, bridge replacement costs are usually estimated on the basis of an average unit cost of the bridge structure. Roadway improvement cost, engineering cost, and other related costs are then added to the bridge structure cost as a percentage of the latter or as a fixed amount. This approach was used by Chen and Johnston (*1*) in the first effort to optimize project selection on a networkwide basis considering both agency and user costs. However, improvements in both the estimation procedure and automated methods of generating the unit costs would be desirable.

Saito and Sinha (*6*) conducted a study of bridge replacement costs for the Indiana Department of Transportation. The cost data used in that study were actual bridge contract costs between the years 1980 and 1985. The data set included 186 bridges that represented various structure, material, and highway types. Two models, the aggregate and component models, for estimating the bridge replacement costs were developed. The aggregate model calculated the total bridge cost by using one equation based on the width and length of the bridge by material type. According to the study the aggregate model tended to give higher predicted values than actual costs in the lower range of bridge size. This could be attributed to combining all of the bridge construction cost components into two variables, the width and length of the bridge. Another difficulty is that the material type of the new bridge is usually not known when doing a network analysis, unless it is assumed that the bridge is being replaced with a bridge of the same material type, which is not always the case. The component model predicted the total cost of the bridge on the basis of the sum of the costs of the superstructure, substructure, approach roadway, and other costs, which were estimated separately on the basis of various parameters. The component model generated more reasonable results than the aggregate model. However, there are difficulties in using such a model as part of a BMS for predicting future funding needs. A number of the factors used in the component model, specifically, the approach length and the amount of earthwork, are difficult to estimate at the system level.

A method for estimating replacement costs for budgeting purposes based on existing bridge characteristics in the National Bridge Inventory is needed. The present study used NCDOT bridge replacement cost data in developing an example model. Since cost data were available from a range of previous years, a methodology was needed for converting the costs from previous years to a common year. Once the costs converted to one common year it was possible to analyze the cost data by breaking the total cost into three components: structure, roadway improvement, and engineering. The significance of various bridge characteristics was analyzed as a measure of importance in predicting replacement cost. Analytical procedures for predicting the new bridge characteristics that influence bridge replacement costs were also developed.

BRIDGE REPLACEMENT COST DATA

NCDOT has recently begun to keep records in the North Carolina Bridge Inventory (NCBI) data file of the total bridge structure cost and other associated costs incurred at the time of construction, in addition to different characteristics of the bridges. Three data fields, in addition to the total bridge project construction cost, are found in the NCBI. These are the bridge structure construction cost, the roadway improvement construction cost, and the engineering cost. The three fields were added in 1991, and the data are accumulating for recently replaced and newly added bridges.

The bridge structure cost includes the costs of such items as removal of the existing bridge, foundation excavation, substructure, superstructure, and deck construction. The roadway improvement cost includes the costs of items related to realigning, raising, widening, and adding lanes to the existing roadway. The engineering cost includes costs related to a preliminary survey of the bridge location, roadway design, structural design, soil analysis, and photogrammetry. Although not recorded as a separate item, the total project cost recorded also includes the costs of other miscellaneous items. Miscellaneous costs include costs for such items as field operation administration, legal costs, pavement markings, and purchase of right-of-way.

NCDOT keeps an Historical File of the annual status of the NCBI. By comparing the "date built" fields in the NCBI files for the first and last years of the selected time period, the bridges replaced in the time period can be identified. If the bridge number exists in both files and the "date built" was different for the same bridge number, then it means that the bridge has been replaced. Furthermore, if cost data for the replacement have been entered the bridge can contribute information for unit-cost analysis.

ADJUSTMENT OF COSTS FOR INFLATION

The expected cost of planned construction work is estimated on the basis of unit costs developed from previous, similar work on bridges constructed in various years. Hence, the previous costs need to be adjusted to the current year (or some future year) by accounting for inflation, changes in productivity, and so forth. Several construction cost indexes that compensate for inflation, productivity, and technology changes have been developed by industry sources for this purpose. Example indexes include the FHWA Price Index, the ENR Index, and the R.S. Means Historical Cost Index.

The FHWA Office of Engineering, Federal-Aid and Design Division publishes various cost indexes on a quarterly basis and by year (7). Some of these indexes, including the Structures Index and the Composite Index, are listed by state. The indexes are based on information submitted for federal-aid construction contracts of more than $500,000. According to the report "the base for each State index is its own particular 'market basket' of quantities and costs during the base period." At the time of the present study the latest index used 1987 as the base year. The FHWA Structures Index for North Carolina was selected since it was based on actual contract construction prices in the state.

Two types of conversions are feasible. First, with the index alone it is possible to convert previous costs (within the years for which the index is tabulated) to the most recent year for which the index is available. Second, if the index is extrapolated into the future, it is possible to convert the cost in the value of the latest year for which the index is available, $COST_{YL}$, or later costs to some year after the cost year for which the index is available. Index data were available for years between 1973 and 1989. The extrapolation model for the FHWA Structures Index was developed by regression techniques.

For the first type of conversion the index is identified corresponding to the initial year of construction, *YC*, and the costs are converted to the dollar value of the latest year, *YL*, for which the index was available as follows:

$$COST_{YL} = COST_{YC} \times \frac{IND_{(YL, YB)}}{IND_{(YC, YB)}} \quad (1)$$

where

$COST_{YC}$ = cost in dollar value of year *YC* of bridge construction;
$COST_{YL}$ = cost in value of latest year for which index is available, with the present being year *YL*;
$IND_{(YC, YB)}$ = cost index for the year *YC* in which the bridge was constructed, with *YB* as the base year; and
$IND_{(YL, YB)}$ = cost index for latest year *YL*, with *YB* as the base year.

As for the second type of conversion, linear regression was tested, and the resulting R^2 value for the FHWA Index was 0.84. This indicated that the model represented the data very well. A quadratic model was also tested to see if a better model could be developed. However, the quadratic component of the model was found to be not significant. Thus, the linear model was selected. The resulting equation for the Structures Cost Index is

$$IND_{(YF, YB)} = 102.21 - 3.9\,(YB - YF) \quad (2)$$

where

$IND_{(YF, YB)}$ = cost index for year *YF* and base year *YB*;
YB = base year for cost index, 1987; and
YF = future year for which the index is being estimated.

The cost in future year YF can then be estimated as

$$COST_{YF} = COST_{YL} \times \frac{IND_{(YF,\ YB)}}{IND_{(YL,\ YB)}} \tag{3}$$

Equation 3 along with Equation 1 or 2 can be used to convert costs to the time value in a desired future year (Figure 1). Equation 2 can be used to predict the indexes for the years since the index was last updated as well as for future years.

STATISTICAL ANALYSIS OF BRIDGE REPLACEMENT COST DATA

Estimating the bridge replacement cost at the system level is done on the basis of the bridge characteristics that could be predicted at such a level. The length and width of the new bridge are some of the parameters that have been commonly used in earlier studies (*1*). Hence, most replacement costs are estimated on a bridge unit-cost basis. However, this does not imply that other parameters could not be included in a model for estimating total bridge replacement costs.

Several approaches can be used to calculate the unit costs for replacement. One approach would be to develop an equation for estimating the unit cost of the bridge structure construction and then add a fixed cost or a percentage cost that accounts for the roadway construction, engineering, and other incidental costs. In the studies by Chen and Johnston (*1*) and Al-Subhi et al. (*2*) through which OPBRIDGE was developed, the cost of a bridge replacement was estimated by the equation

$$TCOST_i = UREPB\ (NBLEN_i \times NBWID_i) \times (1 + EPC) + FIXEDC \tag{4}$$

where

$TCOST_i$ = total cost for replacing bridge i in present value,
$UREPB$ = unit cost for bridge construction per square meter of deck area,
$NBLEN_i$ = predicted length of bridge i (m),
$NBWID_i$ = predicted out-to-out width of bridge i (m),
EPC = engineering cost as a ratio of structural costs, and
$FIXEDC$ = fixed cost for roadway and other incidental costs.

In 1987 dollars the coefficients were estimated to yield the following result:

$$TCOST_i = 495 \times (NBLEN_i \times NBWID_i)\ (1 + 0.12) + 55{,}000 \tag{5}$$

An objective of the present study is to see if a system that would better predict these costs and allow future updating can be put into place. The costs of the bridge structure construction, roadway construction, miscellaneous costs, and engineering cost could each be affected by different factors.

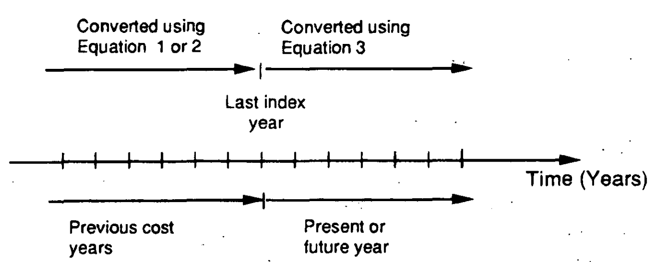

FIGURE 1 Relationship between cost indexes and time.

The results generated from the models developed will be integrated with other programs used to predict future funding needs. A key factor is that the method must realize that the new structure parameters, such as length and width, will be predictable in a BMS such as OPBRIDGE. Roadway improvement parameters, however, will be very limited and more difficult to estimate. Thus, the calculations must build from structure parameters toward a total cost.

Bridge Structure Cost

The significance of several parameters on the unit costs for structure replacement was tested. Only parameters that existed in the NCBI file were considered for this analysis. Some of the parameters considered were bridge deck area, maximum span length, and urban versus rural locations. Although the type of material of the bridge superstructure might be significant and could be considered, it is most probably impractical to include it in the model since the material type is difficult to predict. This is because the type of material is determined on the basis of the most economical design and competition among bidders at a given point in time. Since material economy is partly a function of supply and demand, prices fluctuate and alternate materials may be provided for in some bidding processes. It is therefore not known at the early stages of planning what type of material will be used.

The NCDOT provided cost data for 32 replacement bridges. A unit structure cost was calculated for each bridge by the following equation:

$$UCONST(_{YP,i}) = \frac{CONSCOST(_{YP,i})}{NBLEN_i \times NBWID_i} \tag{6}$$

where

$UCONST(_{YP,i})$ = unit cost of structure construction for bridge i in present dollar value;
$CONSCOST(_{YP,i})$ = structure construction cost for bridge i, converted to present value;
$NBLEN_i$ = total length of new bridge i; and
$NBWID_i$ = out-to-out width of new bridge i.

Unit costs were converted to 1990 dollar values by using Equation 1. The 5th percentile and 95th percentile of the unit cost for the structure was then calculated by using the univariate procedure in SAS. Bridges were eliminated if the unit cost for the structure was lower or higher than the 5th percentile and 95th percentile, respectively. This was to eliminate any recording errors that might produce extreme values.

Table 1(*a*) lists the parameters that were considered in the analysis. These parameters were divided into two groups. The first was for those used to subgroup the bridges. This included highway functional classifications, rural versus urban areas, and waterway versus grade separations. The General Linear Model (GLM) procedure of SAS (*8*) was used to test the significance of the different parameter classes. None of the factors tested were found to be significant.

The second class of parameters was made up of those that could be included as independent variables in the model. Regression analysis is one method that was used to test the significance of the different parameters. In some cases linear regression might be satisfactory, but in other cases it was necessary to test quadratic equa-

TABLE 1 Significance of Variable Parameters Considered on Cost

a) Bridge Structure Construction Cost

	Parameter	Level of Significance
Grouping Parameters	Highway Functional Classification	$P > 5.0\%$
	Rural versus Urban	$P > 5.0\%$
	Water versus Grade Separation	$P > 5.0\%$
Independent Variable Parameters	Width	$P > 5.0\%$
	Length	$P > 5.0\%$
	ADT	$P > 5.0\%$
	Maximum Span Length	$P = 2.6\%$
	Number of Spans	$P > 5.0\%$

b) Roadway Construction Cost and Miscellaneous Costs

Parameter	Roadway Construction Cost	Miscellaneous Costs	Roadway and Miscellaneous Costs Combined
ADT	$P > 5.0\%$	$P > 5.0\%$	$P > 5.0\%$
Old Bridge Width	$P > 5.0\%$	$P = 3.8\%$	$P > 5.0\%$
New Bridge Width	$P < 0.1\%$	$P > 5.0\%$	$P < 0.1\%$
Width Difference (New - Old)	$P > 5.0\%$	$P > 5.0\%$	$P > 5.0\%$
Old Bridge Length	$P > 5.0\%$	$P = 4.1\%$	$P > 5.0\%$
New Bridge Length	$P > 5.0\%$	$P = 0.1\%$	$P = 3.0\%$
Length Difference (New - Old)	$P > 5.0\%$	$P > 5.0\%$	$P > 5.0\%$
Structure Cost	$P > 5.0\%$	$P < 0.1\%$	$P = 3.0\%$
Alignment Rating	$P > 5.0\%$	$P > 5.0\%$	$P > 5.0\%$

tions, multiple regression, or transformation to produce a better representation of the relationships.

The STEPWISE procedure in SAS "performs stepwise regression, which is an attempt to search for the 'best' model by bringing into the regression equation the independent variables one by one" (*9*). The parameters tested by the STEPWISE procedure were width, length, area, maximum span, number of spans, waterway adequacy rating, and average daily traffic (ADT). As indicated in Table 1(*a*) the maximum span length of the new bridge was the only parameter that entered into a model.

A quadratic component of the maximum span length was added to the model. This was found to be significant at the 15 percent level. Higher degrees than the quadratic model were then tested by the GLM procedure, but they were found to be not significant. Logarithmic transformation of the independent and dependent variables was also tested, but it was found to be not significant.

The equation determined for estimating the bridge structure unit cost was

$$UNITSTR = 919 - 40.6(MAXSPAN) + 0.927(MAXSPAN)^2 \quad (7)$$

where *UNITSTR* is the structure unit cost (dollars/m^2 of deck area), and *MAXSPAN* is the maximum span length of the new bridge (m).

Figure 2 shows a plot of the structure unit cost for various maximum spans determined by using Equation 7. It is evident from Figure 2 that the lowest structure unit cost is realized at a maximum span of approximately 23 m (75 ft). As length increases the girder sections increase in proportion to length squared: thus, the increase in cost is reasonable. As length decreases the substructure elements become more numerous and increase the cost.

For estimation purposes the construction cost of a replacement structure could be determined by considering Equation 6 as

$$STRCOST_i = UNITSTR \times NBLEN_i \times NBWID_i \quad (8)$$

Bridge Roadway Improvement Costs and Miscellaneous Costs

The cost of roadway construction is stored separately in NCBI. This field includes costs that are related to any roadway improvements in connection to the replacement of the bridge, such as those related to widening or realignment of the roadway. A measurement was thus needed to calculate the unit cost of roadway construction if this cost item was to be estimated separately. The amount of roadway construction is not generally related to the bridge deck area. Several

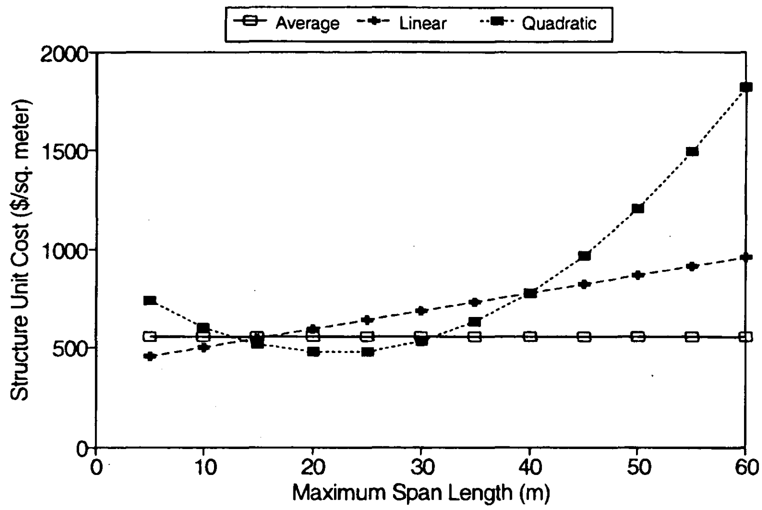

FIGURE 2 Unit structure cost models.

parameters were tested, such as increase in width and length. However, no significant parameter of measure to express the cost as a unit cost that could be related to the data available was identified.

Miscellaneous costs include all other cost items that were not included in the structure, roadway, and engineering costs such as the costs of field administration, right-of-way acquisition, and pavement markers etc. Although it is not stored as a separate item in the NCBI it can easily be calculated as the difference between total cost and the other tabulated costs as follows:

$$MISCCOST = TOTCOST - (STRCOST + ROADCOST + ENGCOST) \quad (9)$$

where

$MISCCOST$ = miscellaneous costs,
$TOTCOST$ = total project cost,
$STRCOST$ = bridge structure cost,
$ROADCOST$ = roadway improvement cost, and
$ENGCOST$ = engineering cost.

Estimating the unit cost of the miscellaneous items independently results in the same problems as those encountered for roadway cost. It was therefore necessary to calculate the roadway cost and miscellaneous cost components on a lump sum basis rather than on a unit-cost basis. This could be done by estimating each item separately or estimating one lump sum value for the two combined.

Preliminary analysis of the data indicated that the average roadway improvement cost and miscellaneous cost were $1.20 million and $0.50 million, respectively. The average ratio of the roadway improvement cost and miscellaneous costs to the structure cost was 2.6 and 1.0, respectively.

Regression models were tested for the two costs independently and in combination. The significance of various subgroupings, including rural versus urban and highway functional classification, was first tested by the GLM procedure. None of the subgroupings were significant in any of the models considered. The STEPWISE procedure was used, since several variables were considered. The variables considered were structures cost and alignment appraisal rating, in addition to the length and width of the new and old bridges.

As indicated in Table 1(*b*) several parameters were found to be significant at the 5 percent significance level. In addition, the R^2 values were greater than 0.5 for all of the models considered.

An attempt was made to develop separate models for small- and large-size projects on the basis of the construction cost of the bridge structure. Bridges were considered small if the structure cost was no greater than $250,000; otherwise, they were considered large. The $250,000 range was selected such that the numbers of observations in each group were almost balanced. Although the R^2 values of the models improved, the results generated were still not acceptable. Different types of transformations, including logarithmic transformations, were attempted, but with no improvement to the results generated.

The model that had the best fit and that generated the best results for roadway construction costs had the following equation:

$$ROADCOST = (177{,}900 \times NBWID) - 1{,}198{,}500 \quad (10)$$

where $ROADCOST$ is the total roadway construction cost (dollars), and $NBWID$ is the new bridge's width (m).

Equation 10 estimates the roadway construction to be less than $0 for a bridge width less than 6.7 m (22.1 ft). However, in reality, even a small two-lane bridge would have a new width of 6.7 m (22.1 ft) or more. Thus, negative values should not be generated in practical situations.

On the other hand, Equation 10 tended to generate high estimates for wider bridges. For example, the cost of roadway construction for a bridge with a width of 15 m (50 ft.) was estimated at $1.5 million. These high estimates might be attributed to the limited number of bridges in the data base. However, consideration should be given to the fact that these high costs are occurring in reality. This indicates that the budget for bridge replacement is being burdened by high costs for approach roadway improvements, which was earlier estimated to average 2.6 times the cost of the structure. If this is typical it is a great burden for the already limited budget for bridge replacement, and consideration should be given to funding the roadway improvements with other funds.

A similar analysis was conducted for the miscellaneous costs. The model that generated the most reasonable results had an R^2 value of 0.7. The equation for the model is

$$MISCCOST = 0.56(STRCOST) + 42{,}500(NBWID) - 364{,}000 \quad (11)$$

where *MISCOST* is the miscellaneous costs (dollars), and *STRCOST* is the total bridge structure construction costs (dollars).

The results generated from Equation 11 had a pattern similar to those for the roadway construction cost. An attempt was also made to develop a model that estimated a value for the total of roadway construction costs and miscellaneous costs. For the combination the following equation generated the best results:

$$ROADMISC = 5.86(STRCOST) - 45{,}200(NBLEN) - 1{,}542{,}800 \quad (12)$$

where *ROADMISC* is the total roadway improvement cost and the miscellaneous costs (dollars), and *NBLEN* is the new bridge's length (m). The R^2 value for Equation 12 was found to be 0.68.

Engineering Costs

Engineering costs include the costs for the design of the roadway and bridge structure, surveying, preliminary site investigations, and testing. The engineering cost is usually estimated on the basis of a percentage of either the bridge structure construction cost or the sum of the latter cost plus the cost for roadway construction and the miscellaneous costs.

Similar to the previous analyses the significances of several parameters were tested. The bridge structure cost was the only parameter significant at the 5 percent level. The model developed had the following equation:

$$ENGCOST = 65{,}384 + 0.136(STRCOST) \quad (13)$$

where *ENGCOST* is the total engineering cost (dollars), and *STRCOST* is the total bridge structure construction cost (dollars). Equation 13 generated an R^2 value of 0.60. Although the magnitude of R^2 is somewhat low, it is considered very reasonable for this type of problem since the costs are affected by many factors that are not related to the bridge parameters in the bridge inventory file.

PROCEDURES FOR PREDICTING NEW BRIDGE CHARACTERISTICS

The different states have historically had somewhat different design practices for bridges. This can be attributed to several factors such as the history of funding available, construction practices, geographic location, climate, navigation needs, and so forth. The different design practices may have influenced many characteristics of bridges, three of which are the total length, width, and maximum span length of the bridge. It was thus desirable to develop prediction procedures for length expansion and width expansion that are based on historical bridge length practices for individual states. The results generated by the bridge total length model can also be compared with the expansion factors developed by FHWA on the basis of nationwide data.

The bridge length expansion factor can be defined as

$$LEF = \frac{NBLEN}{L1} \quad (14)$$

where

LEF = length expansion factor,
$NBLEN$ = new bridge length, and
$L1$ = old length.

The maximum span length of a bridge is the maximum longitudinal distance between two successive sets of piers, columns, or other types of substructure supporting the bridge. The magnitude of this length may influence unit costs of construction and thus may also have an effect on the replacement cost. Hence, it was also desirable to estimate the new maximum span length on the basis of data for the original bridge. The maximum span expansion factor can similarly be defined as

$$MSEF = \frac{MAXSPAN2}{MAXSPAN1} \quad (15)$$

where

$MSEF$ = maximum span expansion factor,
$MAXSPAN2$ = new maximum span length, and
$MAXSPAN1$ = original maximum span length.

Predicting New Bridge Length Based on North Carolina Data

Regression analysis was selected as the method of determining the relation of new length to other factors. The analysis was performed by using the GLM. Both linear and quadratic models were evaluated. By both methods the new length was treated as the dependent variable. Old bridge parameters were investigated as possible independent variables and groupings. Parameters such as old length, waterway adequacy, and underclearance ratings were considered.

The old length was the first independent variable to be considered in a linear regression model. It was found to be significant at the 1 percent significance level. The R^2 value for this model was found to be 0.9854, which was relatively high and meaning in this case that a very good fit was obtained.

The effect of type of service under the bridge was then considered. Bridges were divided into two subgroups: those over a waterway and those at a grade separation. By using GLM it was found that the subgrouping was not significant. This implied that it was not necessary to test the significance of the waterway adequacy rating since this factor only applied to bridges over waterways. The underclearance condition rating was also tested, but it was found to be insignificant. Thus, it was concluded that the old length was the only significant parameter. A quadratic form of the equation that included old length as the independent variable was then tested. However, the quadratic term of the equation was found to be insignificant.

On the basis of this analysis the linear regression model was selected. The equation developed for the new length is

$$NBLEN_{NC} = 8.45 + 1.013 \times L1 \quad (16)$$

where $NBLEN_{NC}$ is the new bridge length based on North Carolina data (m), and $L1$ is the old length (m).

FHWA Expansion Factor for Length of Newly Replaced Bridge

In places where the site-specific data are not available the FHWA Recording and Coding Guide (*10*) provides a graph for the selection of a length-expansion factor to estimate the length of the bridge replacement. These expansion factors are based on nationwide averages of increased bridge lengths as a function of the original lengths.

The graph was developed by plotting the average expansion factors for bridges in various original length ranges. An equation was not developed. Although the graph has provided much insight, an equation relating the model would be helpful for automatic integration into any of the computer programs that have been developed for predicting future bridge funding needs. An equation would also be useful for comparing the newly replaced bridge length prediction graph on the basis of nationwide averages with the North Carolina-based equation.

Development of the equation was accomplished by first determining the expansion factor for various original lengths from the FHWA curve. The new length was then calculated by multiplying the expansion factors by the corresponding original length. These data were then entered into the computer and a linear regression model was tested. The new length was the dependent variable, and the original length was the independent variable. The following equation was generated:

$$NBLEN_{US} = 7.32 + 1.032 \times L1 \qquad (17)$$

where $NBLEN_{US}$ is the new bridge length based on nationwide data (m). It should be stressed that this equation and the resulting R^2 value of 0.99 were based not on the distribution of individual bridge data but only on the averages from the FHWA graph.

A comparison of the results generated from the models for predicting the new length on the basis of North Carolina data and those obtained on the basis of the FHWA model is shown in Figure 3. The results are similar at longer original lengths but show more variation at short lengths. It can also be seen that the expansion factor increases rapidly as the original length becomes shorter in the range of $L1$ less than 30 m (100 ft). For $L1$ greater than 30 m (100 ft) the expansion factor gradually decreases until it almost levels off. At 300 m (1,000 ft) the expansion factor is about 1.04, or a 4 percent increase in length.

Predicting New Bridge Out-to-Out Width

Since bridge replacement cost was to be calculated on a unit-cost basis, it was necessary to predict the out-to-out width of the new bridge, in addition to bridge length. This dimension was estimated in an earlier study by Al-Subhi et al. (2) by the following equation:

$$NBWID_i = NBCDW_i + (WIDTH_i - CDW_i) \qquad (18)$$

where

$NBWID_i$ = predicted out-to-out width of new bridge i,
$NBCDW_i$ = predicted clear deck width of new bridge i based on level-of-service goals and predicted future ADT (*2*),
$WIDTH_i$ = out-to-out width of bridge i that is to be replaced, and
CDW_i = clear deck width of bridge i that is to be replaced.

The purpose of the term ($WIDTH_i - CDW_i$) is to account for site-specific traffic and pedestrian needs. Some bridges have sidewalks and traffic medians, particularly in urban areas. Use of the width difference accounted for such features to be repeated in the new bridge. However, a potential lower limit to this difference was not recognized. Some of the old bridges had the clear deck width virtually equal to the out-to-out width. Although most bridges in rural areas do not feature any closed median or sidewalks, a minimum allowance should be made for the width of the guardrails.

The correction developed was to use the same approach used earlier, but to set a lower limit that is greater than zero for the difference between $WIDTH_i$ and CDW_i. The minimum width differ-

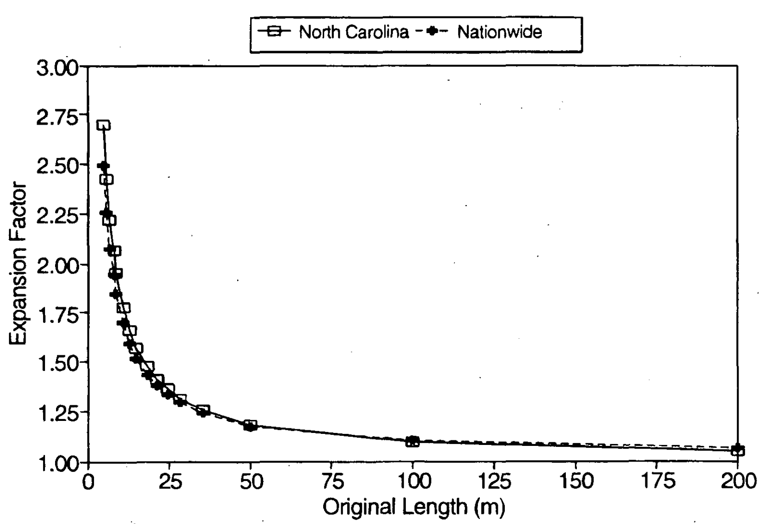

FIGURE 3 Length expansion factor.

ence was determined by analyzing bridges constructed since 1980. The average minimum width difference was estimated to be 0.98 m (3.2 ft), which is somewhat wider than the thickness of the two guardrails.

Predicting New Maximum Span Length

The ability to predict the new maximum span length of a bridge that is to be replaced was found to be significant in estimating the bridge replacement costs. Several factors might influence the new maximum span length. Original maximum span length, original total length, waterway adequacy rating, and number of spans are some of these factors.

Statistical analysis of the NCBI data base was used to develop equations for determining the new maximum span length as a function of various factors. The new maximum span length was the dependent variable in each analysis, and the other factors were the independent variables.

Two different linear regression models were first tested, with one having the original maximum span length and the other the original total length as the independent variables. Although both variables were found to be significant in their respective models, the R^2 values were relatively low (0.4 and 0.2, respectively). A model that considered both variables at the same time generated an R^2 value of 0.47. The assumptions required for regression analyses (the normality of residual distribution and the constancy of variance along the regression lines) were then tested. However, neither assumption was fulfilled, and thus the model was not adequate.

The type of service under the bridge was believed to have an effect on the maximum span length of the new bridge. To assess this effect the GLM procedure was used by dividing the bridges into two subgroups: waterway crossings and grade separations. A total of 442 bridges were constructed for waterway crossings and 39 were constructed for grade separations. Based on the analysis it was found that such a subgrouping was significant at the 1 percent significance level.

Thus, a separate model was tested for each subgroup beginning with bridges over a waterway. Old maximum span length and old length were initially considered to be the two independent variables. Both were found to be significant; however, the two assumptions for regression were not met. The significance of the waterway adequacy rating and the number of spans of the old bridge was then tested for the same subgroup, but they were found to be insignificant.

Thus, a regression model with the old length and maximum span as the independent variables was the most appropriate. Some type of transformation was required before using such a model, since the two assumptions for regression were not met. Several different types of transformations were considered. The best transformation for this set of data was found to be logarithmic. The data were transformed by taking the natural log of both the dependent and the independent variables and then performing the GLM, univariate, and plot procedures.

A model with an R^2 value of 0.56 resulted when this type of transformation was performed on the data. The equation of the model was

$$MAXSPAN2_{WATER} = 4.72 \times MAXSPAN1^{0.16} \times L1^{0.21} \tag{19}$$

Bridges at grade separations were then analyzed separately. The significance of the old length, old maximum span length, underclearance condition rating, and number of spans of the old bridge were tested. It was concluded that a model with old maximum span length as the only independent variable was most appropriate. However, such a model did not meet the two assumptions for regression. A logarithmic transformation of both the independent and the dependent variables was therefore performed.

Further study of the results indicated that the coefficients of the equation developed for the grade separation subgroup had a substantial deviation. This implied that there was not sufficient conclusive evidence that the coefficients of the equations were different for the two subgroups. This could be attributed to the fact that the replaced bridge sample included 442 bridges over waterways versus only 39 bridges at grade separations. For simplicity and because of deficiencies in one of the two models, it was decided to investigate a single model for all bridges.

Thus, the data were further analyzed as one group by testing higher-degree polynomial functions that included old length and old maximum span length as the independent variables. The R^2 values did not improve by much as the degree was increased. The highest degree of polynomial function tested was the fourth degree. The resulting R^2 value was 0.57, but the two assumptions for regression analyses were still not met.

The residual distribution of the first-degree logarithmic transformed model was found to be normal at the 1 percent significance level. The R^2 value for that function was found to be 0.53. Higher-degree polynomial functions of the transformed model were tested, but they were found to be insignificant. Thus, the most appropriate function was

$$MAXSPAN2 = 4.31 \times MAXSPAN1^{0.196} \times L1^{0.216} \tag{20}$$

A graphical representation of Equation 20 for the new maximum span length is presented in Figure 4. The graph shows that the predicted maximum span expansion factor was less than 1 for original maximum spans longer than about 23 m (75 ft). It is most noteworthy that Equation 20 correspondingly reflects the fact that maximum spans for new bridges are shorter if the original span was greater than 23 m (75 ft) and those for new spans are greater if the original span is less than the optimum of 23 m (75 ft). Relating this to Equation 7 it is evident that the designs are seeking the lowest-cost solutions.

SUMMARY AND CONCLUSIONS

The primary objective of the research described here has been to provide analytical methods for estimating the costs of bridge replacement for budgeting purposes in BMSs. Analytical procedures for predicting the length and maximum span length of the new bridge, parameters that were found to be needed for estimating replacement cost, were also developed.

A methodology for estimating the total bridge replacement cost was developed on the basis of an analysis of the costs of previously constructed bridges. A model for estimating the bridge structure cost was developed on the basis of deck area and the maximum span length of the bridge. Models for estimating roadway improvement costs, miscellaneous costs, and engineering cost were also developed. The accumulation of additional data for these last three items would be desirable. The proportion of the total replacement cost devoted to roadway improvements appears to be very significant. The appropriateness of burdening limited bridge improvement

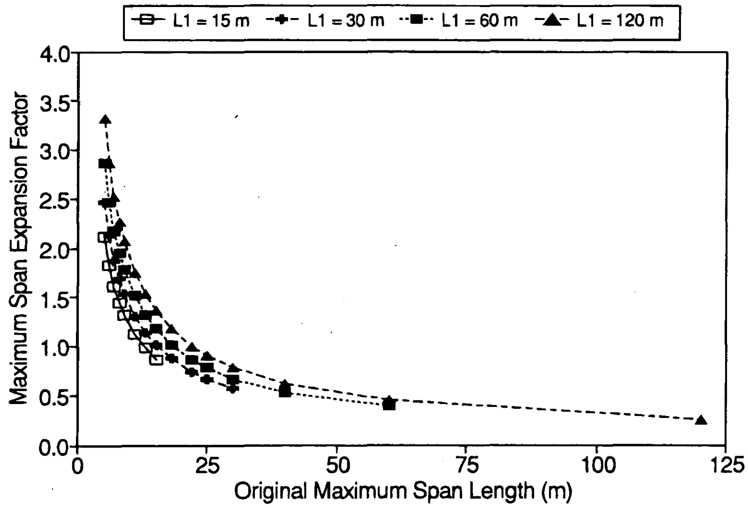

FIGURE 4 Maximum span expansion factor.

funds with significant roadway improvement costs should be evaluated.

ACKNOWLEDGMENTS

The research described herein was conducted at North Carolina State University with the support of NCDOT. The authors gratefully acknowledge the assistance provided by Jimmy D. Lee, State Bridge Maintenance Engineer.

REFERENCES

1. Chen, C.-J., and D. W. Johnston. *Bridge Management Under a Level of Service Concept Providing Optimum Improvement Action, Time, and Budget Prediction.* Report FHWA/NC/88-004. Center for Transportation Studies, Department of Civil Engineering, North Carolina State University, Raleigh, 1987.
2. Al-Subhi, K. M., D. W. Johnston, and F. Farid. *Optimizing System-Level Bridge Maintenance, Rehabilitation, and Replacement Decisions.* Report FHWA/NC/89-001. Center for Transportation Studies, Department of Civil Engineering, North Carolina State University, Raleigh, Jan. 1989.
3. Al-Subhi, K. M., D. W. Johnston, and F. Farid. OPBRIDGE: An Integrated Bridge Budget Forecasting and Allocation Module at the State Level. In *Transportation Research Record 1268,* TRB, National Research Council, Washington, D.C., 1990, pp. 95–109.
4. Al-Subhi, K. M., D. W. Johnston, and F. Farid. Resource-Constrained Capital Budgeting Model for Bridge Maintenance, Rehabilitation, and Replacement. In *Transportation Research Record 1268,* TRB, National Research Council, Washington, D.C., 1990, pp. 110–117.
5. Abed-Al-Rahim, I. J, and D. W. Johnston. *Analysis of Relationships Affecting Bridge Deterioration and Improvement.* Report NC/R&D/93-001. Center for Transportation Studies, Department of Civil Engineering, North Carolina State University, Raleigh, 1993.
6. Saito, M., and K. C. Sinha. *The Development of Optimal Strategies for Maintenance, Rehabilitation and Replacement of Highway Bridges,* Vol. 4. Cost Analysis. Draft Final Report, Research Project C-36-731. Joint Highway Research Project, Engineering Experiment Station, Purdue University, West Lafayette, Ind., 1989.
7. *Price Trends for Federal-Aid Highway Construction, Fourth Quarter, 1990.* Publication FHWA-PD-91-009. Office of Engineering and Design Division, FHWA, U.S. Department of Transportation, 1991.
8. SAS Institute Inc. *SAS User's Guide: Basics, Version 5 Edition.* SAS Institute Inc., Cary, N.C., 1985.
9. Helwig, J. T. *SAS Introductory Guide.* Revised Edition. SAS Institute Inc., Cary, N. C., 1983.
10. *Recording and Coding Guide for the Structure Inventory and Appraisal of the Nation's Bridges.* FHWA, U.S. Department of Transportation, Dec. 1988.

The contents of this paper reflect the views of the authors, who are responsible for the facts and accuracy of the data presented herein. The contents do not necessarily reflect the official views or policies of NCDOT. This paper does not constitute a standard, specification, or regulation.

Publication of this paper sponsored by Committee on Structures Maintenance and Management.

Cost Relationships for Concrete Bridge Protection, Repair, and Rehabilitation

EDWARD J. GANNON, RICHARD E. WEYERS, AND PHILIP D. CADY

Cost information on chemical and physical techniques for concrete bridge protection and rehabilitation is provided. This information constitutes an essential component in determining life-cycle costs for ranking alternative protection and rehabilitation techniques. Most of the cost data were obtained from bid tabulations provided by state highway agencies (SHAs). Fourteen SHAs and two toll road agencies were visited, and 12 of these provided bid tabulation data. The costs obtained from bid tabulations were converted to mid-1991 national average values by using published cost indexes. The national average cost data for each protection and rehabilitation treatment were then subjected to detailed statistical analysis to develop cost models reflecting the effects of four independent variables: work quantity, number of bids, total contract cost, and cost of maintenance and protection of traffic. Eight combinations of these four variables were developed to be the independent variables in the regression analysis. An inverse power model was used. The ultimate choice of factors in each case rested with the regression coefficient (R^2).

The ultimate goal of the Strategic Highway Research Program (SHRP) C100 series of projects is to develop the technology to minimize the life-cycle costs of reinforced concrete bridge components. This implies the development and use of economic models that will be used to evaluate life-cycle costs.

The mechanics of economic models for the evaluation of alternatives based on life-cycle costs are relatively simple and widely understood and accepted. The difficulty is in the identification of suitable alternatives and the input variables for these alternatives. The input variables consist of the costs and service lives of the definable constituents for each alternative.

The purpose of this work is to provide cost information on a number of techniques used to repair or protect bridge components. The data can be used in combination with the respective service lives for determination of life-cycle costs.

The seven systems for which cost information were developed are

- deck patching,
- deck protection systems,
- experimental deck protection systems,
- structural patching,
- structural protection systems,
- "new" deck protection systems, and
- "new" structural patching.

Patching was considered for both decks and structural elements by using portland cement concrete (PCC), quick-set hydraulic cements, and polymer concrete. Protection systems were considered to be applied to the entire deck or structural component. Latex-modified concrete (LMC) overlays, membranes plus asphalt cement concrete overlays, low-slump dense concrete overlays, and sealers were considered for deck systems. Thin polymer overlays, microsilica concrete overlays, and polyester overlays were considered experimental because of limited experience. Structural protection systems included encasement with PCC, sealers, shotcrete, and coatings. New deck protection systems included deep polymer impregnation and posttreatment corrosion inhibitor treatments. New structural patching included corrosion inhibitor treatment systems.

To promote valid comparisons among bridge component patching and protection systems by life-cycle cost analysis it was necessary that the costs be consistent and composed of the appropriate cost components. These included engineering costs, installation costs, user costs, effects on the regional economy, and environmental impact. Not all cost components are applicable in all situations. For a given treatment the applicable cost components will depend on whether the work is accomplished by contract or maintenance force account. It was also evident that some of the cost components would vary widely as functions of additional factors. Examples include maintenance and protection of traffic (MPT), which is primarily dictated by traffic volume, and contractor-related costs, which are heavily influenced by work volume at the site and regional business climate.

Because of the national or broad regional scope of these cost evaluations, cost components that were highly site specific generally were not included in determining costs. Judgment was required to determine if a highly site-specific cost component was a key factor in the cost of a particular alternative. An example might be the ability of one technique to significantly reduce the costs associated with MPT. Since traffic maintenance is a highly site-specific cost component these costs cannot be ignored.

Because of the variations in cost with time due to inflation or deflation it was necessary to include the applicable dates (years) associated with the cost data. This permitted reducing the data to a common base year by using published price indexes. Also, cost data for each applicable cost component should be collected from as wide a population (geographically and chronologically) as possible to establish the variability and dependability for sensitivity analyses.

Two basic approaches can be used to acquire the required cost information. The first involves the use of classical engineering estimating techniques. It is the most rational approach, and it provides an established and a rigorous regimen. The second approach is the empirical procedure involving the systematic examination and evaluation of archival cost data. The major problem associated with the latter approach is that there is usually insufficient documentation of details regarding components of the cost figures. Thus, wide variations often occur between different jurisdictions because the components of the generated cost figures are not totally comparable.

E. J. Gannon and P. D. Cady, The Pennsylvania State University, University Park, Pa. 16802. R. E. Weyers, Department of Civil Engineering, Virginia Polytechnic Institute and State University, Blacksburg, Va. 24061.

Likewise, it is generally not possible to find empirical data that exactly match the sought after cost figure in terms of the desired cost components. However, the empirical approach does have the advantage of inherently incorporating subtle influences on cost figures that generally cannot be accounted for by using straight estimating procedures (e.g., business climate, quantity effects, and productivity). The approach originally proposed was a hybrid of the rational and empirical techniques, attempting to take the maximum advantage of the attributes of each methodology. Unfortunately, this becomes costly, and it was for this reason that the empirical approach was used in the present study.

DATA ACQUISITION

Research Plan

The primary source of these archival cost data was contract bid tabulations from state highway agencies (SHAs). The cost associated with a specific treatment system is reported as a unit cost in a contract document. Unfortunately, for the present research the contractor is only required to reveal the unit cost and not the components of this cost. For example, for an LMC overlay the cost associated with calibrating mixers, engineering any necessary formwork, inspection and testing, and salvage values are not detailed in the bid price. Without this itemized description it is difficult to project historical costs to determine future costs because of the variability associated with these unreported components. Other problems arise when insufficient historical data on which to base a cost estimate are available. Regional variations in costs due to economic conditions and the frequency of applications can also be significant both within a particular SHA and among them. To use historical data as a basis for future costs it is necessary to establish an extensive data base of costs from carefully selected states across the country.

The strategy used to determine which states to visit was based on geographic location, which SHAs used the systems under consideration, and the ability and willingness of the SHA to provide the needed historical data. A total of 15 SHAs were visited.

Several guidelines were developed to aid in the determination of the costs. Road user costs, economic effects, and environmental impact were ignored since these costs are approximately equal for all alternative methods for each system. It was necessary to determine whether the system was more likely to be performed by contract or by departmental forces because the components of cost differ between the two. For contract work the components include preliminary engineering costs, maintenance and protection of traffic costs, inspection, testing and construction engineering costs, and salvage values. For systems applied by maintenance forces the cost components include materials, equipment, labor and supervision, preliminary engineering, inspection, testing, construction engineering, and salvage values.

Contract Work

The information available from the highway agencies for contract work was in the form of bid tabulations, standard specifications, and special provisions.

A total of 829 bid tabulations were obtained from the SHAs. The contracts obtained from the SHAs were for rehabilitation projects involving the treatments and systems previously discussed. Each SHA provided access to historical data. Although all contracts were generally available in an archival form (microfilm or computer tapes), only data for a limited number of years were in readily accessible form (paper copies). The years for which data were available was limited by the available storage space at the SHA and ranged from 1981 to 1991.

Of critical importance to the project was the ability to use the cost information obtained from each SHA to determine a national average cost for the specified repairs. To develop these national trends it is necessary to compare and analyze similar treatments. To ensure that similar materials, methods, and procedures were being compared, standard specifications and contract special provisions were obtained for all of the applicable treatments used by all SHAs. These documents played an important role in allowing comparisons for a given treatment among the different SHAs when the pay quantity or work description for that treatment differed.

Maintenance Force Work

Along with contract work consideration was also being given to analyzing the costs associated with repairs performed by state highway maintenance forces. When the SHAs were visited interviews were conducted with the administrative maintenance engineers and, when time permitted, with district maintenance engineers.

Only eight states that were visited have operational maintenance management systems which can provide detailed data on maintenance force repair costs. These systems provide the maintenance engineer with a good basis for tracking costs and predicting future needs. However, the information generated by these systems is inadequate for use in analyzing costs. The cost centers used are not specific enough or do not contain enough information to provide the required insight into the types of work performed. Thus, it was not possible to obtain accurate costs of maintenance force repairs. Further work on this task was terminated.

Engineering Costs

When developing life-cycle cost models for use in comparing various alternatives for bridge rehabilitation, it is desirable to include the cost of any engineering involved in the alternatives. The methods under consideration are generally accepted as being standard repair techniques. A great deal of effort is being spent on developing these standard repairs, and much time is being spent analyzing methods and materials, but once the standard has been developed, little engineering is required. This is especially true of deck repairs.

This assumption of little engineering cost associated with repairs may not be true for super- or substructure repairs. These types of repairs are usually not as generic as deck repairs and often require additional engineering to design formwork and provide necessary details. A considerable amount of engineering effort is also expended on developing MPT plans.

Because insufficient specific data were available and the costs will generally affect all treatments in about the same fashion, no further consideration was given to engineering costs. The exception to this is the more experimental and new treatment techniques, for which the costs were estimated because of a lack of empirical data.

Salvage Values

The salvage value remaining when the end of the service life is reached is an important factor in life-cycle cost modeling. Salvage value can affect the decision of which method to use. The salvage value is most often thought to be a positive value, such as trade-in allowance or resale; however, in the construction industry the salvage value can be an expense. It may be necessary to dispose of construction materials off-site, in a landfill, and the cost can be high, especially if hazardous materials are salvaged.

After interviewing design engineers, estimators, and construction personnel it was evident that little consideration is given to salvage costs in either contract or maintenance force work. Only in rare cases is salvage material ever considered on bridge rehabilitation work. When salvaging does occur it is usually for readily reusable items, such as guide rail, steel and prestressed beams, and highway lighting fixtures. It is expected that for contractors to remain competitive they will seek the lowest cost for disposal or the highest price for resale. This is then passed on to the SHA in the bid price. For this reason salvage value was not considered.

DATA ANALYSIS

Cost Data Adjustment Factors

On completion of the data acquisition phase, 829 contracts from 13 SHAs from 1981 to 1991 were used for data analysis. To pool information from different geographic regions and different years it was necessary to develop both geographic and inflation factors to adjust the data.

Cost and price indexes are composite costs or prices for given quantities of specified goods or services (*1–8*). They are usually compiled as a function of time and location and are thus indicators of inflation or deflation in a specific area. After a review of available cost indexes related to the present research, the following four were selected for more detailed consideration:

- FHW A Federal-Aid Highway Construction Price Index (*7*),
- FHW A Highway Maintenance and Operating Cost Index (*7*),
- *Engineering News Record* Construction Cost Index (*6*), and
- R.S. Means City Construction Cost Index (*8*).

These four indexes were analyzed for the period covering the past three decades, with 1977 chosen as the base year. Although there were various differences among the indexes, there were also some obvious differences. These are evident in Figure 1, in which the analysis is presented graphically for the period since 1970.

The reason for the divergent behavior of the FHWA Maintenance and Operating Cost Index is not clearly evident. However, it includes traffic service items such as snow and ice control, which not only may account for the behavioral differences but also raises the question of its relevance to the application at hand. Thus, the FHWA Maintenance and Operating Cost Index was judged to be too highly influenced by activities outside the scope of bridge protection, repair, and rehabilitation to warrant further consideration.

The inclination at this point leans heavily toward the FHWA Construction Price Index. This is reinforced by the availability of a geographical breakdown of cost indexes by state, which are published annually by *Engineering News Record* (*6*) in the 2nd

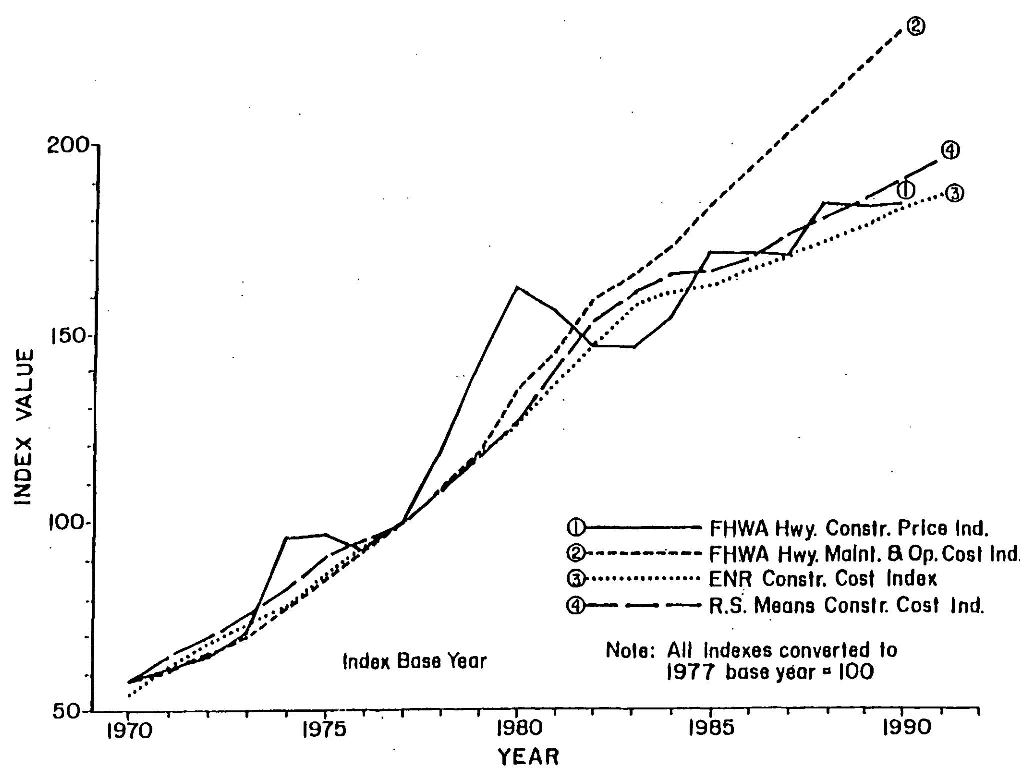

FIGURE 1 Cost indexes as function of time.

"Quarterly Cost Roundup" issues. These are generally published in the fourth weekly issues of the months of March, June, September, and December. However, for many of the states there are large, irrational variations in the index values from year to year that suggest random changes in the index bases or reporting procedures. Since the FHWA Federal-Aid Highway Construction Cost Index has a significant deficiency in this matter, it is prudent to consider using a different index.

It is clear that the R.S. Means City Construction Cost Index is more suitable. First, it is much more comprehensive and detailed than the *Engineering News Record* index. This permits the selection of a more specific subarea index to more nearly match the nature of the construction activities covered by this research. Only one combined index is available with the *Engineering News Record* index. Notice that in this regard the R.S. Means City Construction Cost Index also has the same advantage over the FHWA Federal-Aid Construction Cost Index. Second, it is based on a larger geographical data base than the *Engineering News Record* Construction Cost Index.

Accordingly, the R.S. Means City Construction Cost Index was used to prepare procedures and factors for adjusting archival cost data from SHAs for geographical and time effects. An important extra benefit results from this decision. The R.S. Means City Construction Cost Index is an integral part of the Means cost-estimating system. This naturally leads to procedures that will be used to provide engineering estimates for those activities for which insufficient cost data exist and for experimental and new procedures that have little or no prior history.

Procedures

The R.S. Means City Construction Cost Index was used as the basis for developing a system to convert archival cost data from local jurisdictions into mid-1991 national average values. The purpose is to produce cost figures with defined base to permit valid economic analysis comparisons of alternatives for the protection, repair, and rehabilitation of concrete bridge components. The collateral capability of the developed system to provide estimates of cost for a specific activity at a given geographical location and time by using archival data from a different time and place for the same activity will also be demonstrated.

Functional Relationships

The functional relationships on which the developed system is based are presented in algebraic form below. The general relationship for determining national average cost values is

$$N_n = C_{a,m} \times L_a \times (T_m/T_n) \qquad (1)$$

where

N = national average cost,
C = cost in a particular city (or state),
L = geographical conversion factor for particular city (or state),
T = time conversion factor to convert to mid-1991 value,
a, b = particular cities (or states), and
m, n = particular years.

For the usual case that represents the primary purpose of this effort (converting local archival costs to 1991 national average costs) note that T_n is equal to 1.000 and Equation 1 becomes

$$N = C_{a,m} \times L_a \times T_m \qquad (2)$$

where N is the 1991 national average cost.

If the national average cost for 1991 is known or has been calculated from Equation 2 the present (1991) cost in a particular city (or state), C_a, can be calculated from Equation 3 because T_m is equal to 1.000.

$$C_a = N/L_a \qquad (3)$$

The general equation for estimating the cost in a particular city (or state) in a given year, $C_{a,m}$, from cost data for another city (or state) in a different year, $C_{b,n}$, is

$$C_{a,m} = C_{b,n} \times (L_b/L_a) \times (T_n/T_m) \qquad (4)$$

If the national average cost in 1991, N, is known, the cost in a particular city (or state) in a given year, $C_{a,m}$, can be estimated from

$$C_{a,m} = N/L_a \times T_m \qquad (5)$$

Location and Time Factors

The location and time factors are derived from the R.S. Means City and Historical Cost Indexes, respectively, as presented in the 1992 Means Concrete Cost Data (*8*). The location (L) factors were calculated from the Means Index Values by the following relationship:

$$L = 100/I_c \qquad (6)$$

where I_c is the Means City Index Value. State L values were computed as the arithmetic means of the calculated city L values for each state. Only Division 3 (concrete construction) index values were used. The calculated L values covering the materials, installation, and total aspects of concrete construction can be determined for each city and state.

The time (T) factors were calculated by using the Historical Cost Index from the 1992 Means Concrete Cost Data (*8*) and the following relationship:

$$T = 221.6/I_T \qquad (7)$$

where I_T is the Means Historical Cost Index Value for year T. The resulting time factors can be calculated.

Data Set Development

To better analyze the data to be collected a literature search and interviews with SHA maintenance engineers were performed to develop a more detailed list of work items. The original, very general list of seven repair and protection systems, was expanded to 44 specific work items. These treatment items are listed in Table 1.

Each of the 829 contract bid tabulations obtained from the SHAs was analyzed to obtain information regarding any of the subject treatment items used. Bid tabulations list all work items in the con-

TABLE 1 Specific Treatment Items To Be Costed for Identified Treatment Areas

- 100 Deck Patching
  - 110 Portland Cement Concrete Patches
    - 111 Partial Depth Repairs (square yard)
    - 112 Full Depth Repairs (square yard)
  - 120 Quick-Set Hydraulic Mortar/Concrete Patches
    - 121 Partial Depth Repairs (square yard)
    - 122 Full Depth Repairs (square yard)
  - 130 Polymer Mortar/Concrete Repairs
    - 131 Partial Depth Repairs (square yard)
    - 132 Full Depth Repairs (square yard)
- 200 Deck Protection Systems
  - 210 Latex Modified Concrete Overlay (square yard)
  - 220 Membrane and Asphalt Cement Concrete Overlay (square yard)
  - 230 Low Slump Densified Concrete Overlay (square yard)
  - 240 Sealers
    - 241 Boiled linseed oil (square yard)
    - 242 Silane, Siloxane (square yard)
    - 243 High Molecular Weight Methacrylate Deck Sealer (square yard)
  - 250 Scarification of Concrete Deck Surface
    - 251 Milling or Unspecified Method (square yard)
    - 252 Hydrodemolition (square yard)
  - 260 Removal of Asphalt from Deck Surface (square yard)
- 300 Experimental Deck Protection Systems
  - 310 Thin Polymer Overlay (square yard)
  - 320 Micro-Silica Concrete Overlay (square yard)
  - 330 Polyester Overlay (square yard)
- 400 Structural Patching
  - 410 Portland Cement Concrete Patches
    - 411 Shallow Repairs (square yard)
    - 412 Deep Repairs (square yard)
  - 420 Quick-Set Hydraulic Mortar/Concrete Patches
    - 421 Shallow Repairs (square yard)
    - 422 Deep Repairs (square yard)
  - 430 Polymer Mortar/Concrete Repairs
    - 431 Shallow Repairs (square yard)
    - 432 Deep Repairs (square yard)

tract for each bidder on the project. The number of bidders on any given project ranged from 1 to as many as 15. For each treatment item used in the contract the quantity and each contractor's bid price were recorded. This resulted in a series of data observations for each item. The total number of data observations for all techniques is 10,820. Each observation represents one bid price on a treatment item from one contract by one bidder.

The data obtained from each state were sorted by item numbers and were merged with those for the other states, resulting in individual data bases for each item. Since the items were normalized by modifying the pay units to be consistent and adjusting the unit costs for inflation and location, it was possible to merge all like treatment items. These are the data that were analyzed to produce the cost models.

In statistical modeling it is necessary to have a sufficiently large data set so that the resulting models provide significant estimations. Neter et al. (*9*) suggest that the number of observations should be at least 6 to 10 times the number of the variables in the independent variable pool. There were four independent variables (quantity, number of bidders, contract amount, and MPT amount), with the adjusted national price being the dependent variable. Therefore, the model-building data sets should contain between 24 and 40 observations. This criterion eliminated statistical analysis as a modeling tool for several treatment items. The newly developed treatments along with those with few observations were modeled by using classical estimating techniques. A discussion of the techniques used to determine the cost models for these is not included in this paper. Standard engineering estimation techniques were used and are fully discussed in the SHRP C103 project report (*10*).

Computer Models

In general, the extensive amount of data obtained from the various SHAs provided a sufficient number of observations with which to develop statistical models. Several problems may result from the use of only observational or historical data. The primary concern is

TABLE 1 *(continued)*

500 Structural Protection Systems
- 510 Encase with Portland Cement Concrete (square yard)
- 520 Sealers
  - 521 Boiled Linseed Oil (square yard)
  - 522 Silane, Siloxane (square yard)
- 530 Shotcrete (cubic yard)
- 540 Coatings
  - 541 Epoxy (square yard)
  - 542 Others (square yard)

600 New Deck Protection Systems
- 610 Deep Impregnation, Grooving Technique
  - 611 Monomer, Methyl Methacrylate
  - 612 Corrosion Inhibitor, Postrite
  - 613 Corrosion Inhibitor, Cortec 2020
- 620 Spray-on Corrosion Inhibitor, Inhibitor Modified Overlay System
  - 621 Non-Dried, Postrite
  - 622 Non-Dried, Cortec 2020
  - 623 Non-Dried, Alox 901
  - 624 Dried, Postrite
  - 625 Dried, Cortec 2020
  - 626 Dried, Alox 910

700 New Structural Patching
- 710 Type I Concrete Removal, Patch with Corrosion Inhibitor Concrete
  - 711 DCI
  - 712 Cortec 2000
- 720 Type II Concrete Removal, Spray-On Inhibitor, Patch with Corrosion Inhibitor Concrete
  - 721 Postrite, DCI Concrete
  - 722 Cortec 2020, Cortec 2000 Concrete
  - 723 Alox 901, PCC

that historical data do not result from a controlled experiment. Therefore, the data may not provide adequate information on cause and effect. Without a carefully controlled experiment all of the controlling independent variables may not be observed. Another aspect of this problem is that although an apparent statistical relationship is found to exist, this does not necessarily indicate that there is a causal relationship. If there is a causal relationship at present or in the past, there is no guarantee that this relationship will hold in the future.

After the data were obtained and processed into subsets containing similar work items from each state, model development procedures were instigated. Preliminary work was initiated into determining the possible factors that would affect the model. The only variables available from the bid tabulations that might have an effect on the adjusted national cost were quantity of work, the number of bids, the total contract cost, and the MPT cost. No other factors were available without extensive research of the project contract documents, which was infeasible for the more than 800 contracts used in the study.

With only these four variables used in the model, it was necessary to develop an understanding of how these variables affect the bid price. Cost has two components: fixed cost and variable cost. It is evident that there is a relationship between quantity and cost: as quantity increases, the unit cost decreases.

The state of the economy plays a role in determining the costs of repairs. As the economy worsens, more contractors begin to rely on public projects and the number of bidders on the projects increase. Knowing that competition has increased the contractors must cut costs to a minimum to be competitive. Although simply observing the number of bidders on a specific contract may be a crude indicator, it may provide additional insight and improve the model.

Another factor that has an effect on cost is the difficulty of the work. This difficulty may be the result of poor access to the repair area, remote location of the job site, and so forth. One variable available on the bid tabulations that may provide some information regarding the difficulties on the construction site is the cost of MPT items. Even more is revealed if the ratio of MPT costs to total contract cost is observed. An increase in this ratio indicates that more effort is being expended on job site activities rather than actual rehabilitation work.

The total construction costs should also be considered as a possible factor influencing costs. As the size of a contract increases it allows the contractor to spread overhead and profit over more items and quantities. Although the savings in this case may not be as significant as with other factors, some savings may be realized and this will be considered in the model.

The relationship between the four variables and unit cost can be simplified as follows:

- As quantity increases, cost decreases,
- As the ratio of MPT cost to total contract amount increases, cost increases,
- As the number of bids increases, the cost decreases, and
- As the total contracts amount increases, the cost decreases.

It is desired that these variables be combined into a series of factors that can be modeled to provide cost information. Since the quantity of work is probably the best indicator of cost, it was decided that this variable should be present in all factors. This results in the following eight factors that were used for model development:

Factor 1 = quantity,
Factor 2 = (quantity · contract amount)/MPT amount,
Factor 3 = quantity · contract amount,
Factor 4 = quantity · number of bidders,
Factor 5 = [(quantity) · (contract amount)^2]/MPT amount,
Factor 6 = (quantity · number of bidders · contract amount)/MPT amount,
Factor 7 = quantity · contract amount · number of bidders, and
Factor 8 = (quantity · number of bidders)/MPT amount.

Model Description

It was decided that on the basis of the shapes of the curves produced by plotting each factor with the cost for each item that a nonlinear decay model should be used to fit the data. Four models were proposed:

- an exponential decay model

$$y = b_1x + b_2\exp(-x/b_3) \tag{8}$$

- an inverse power model

$$y = b_1 + b_2x + b_3/x^{b4} \tag{9}$$

- an hyperbolic model

$$y = b_1x + (b_2 + b_3x)/(1 + b_4x) \tag{10}$$

- a logarithmic model

$$y = b_1 + b_2x - b_3\log_{10}(x) \tag{11}$$

These four models are capable of fitting the types of curves produced when each factor is plotted against cost.

The most commonly used measure of a regression model's fit is the coefficient of multiple regression, R^2. It measures the proportionate reduction of total variation in the dependent variable associated with the set of independent variables. The value of R^2 is between 0 and 1 inclusive. The closer that the R^2 value is to 1, the better the model takes into account the variability in the data. Generally, the model is considered a good fit for the data if the R^2 values are greater than 0.80. This type of agreement is usually the result of carefully controlled laboratory experiments in which all causal relationships are known.

It is not expected that the data available for analysis in this task will provide R^2 values in the range of what is normally considered acceptable in controlled laboratory testing. The use of observation data generally produces poor models since all of the causal variables may not be known. This scatter is particularly obvious at the lower ranges of the independent variables. To increase the R^2 value it is necessary to have less scatter and a smoother fit. Although this is desirable, caution must be used so that the true variability is not lost in attempts to improve the model.

In the analysis of the bid tabulations it is obvious that there can be, and very often are, large discrepancies between the bids offered by different contractors for the same item on the same contract. This wild variation can be attributed to several causes, including the following:

- A new contractor may not have the benefit of experience and will not be able to competitively perform certain types of work.
- Some contractors may place a higher profit margin on certain items of work.
- Some items may be subcontracted resulting in higher prices.

SHAs can expect that the price paid for a particular quantity of work will typically be somewhere around the midpoint between the highest and lowest bid for that item. Most states recognize this, and during the interviews with estimators it was revealed that most states keep a running average for use in developing the engineers' estimates. Very few states acknowledge the role that quantity or other factors have on the cost function, however. Most often the SHAs keep track of only the low bidder's cost, but some also track the low bid for the item as well.

Given that the bid price for a particular item may vary widely and that the SHA can expect to pay between the high and the low

TABLE 2 Sensitivity Analysis for Rounding of Factor 1 for Item 111, Partial-Depth PCC Deck Patching

Rounding Level	R^2
none	0.118
5	0.242
10	0.353
15	0.394
20	0.447
25	0
30	0

TABLE 3 Regression Parameters for Item 210, Latex-Modified Concrete Overlay

Factor	Rounding Level	Parameters				R^2
		b_1	b_2	b_3	b_4	
1	100	34.05	0.000147	1682.33	0.8389	0.640
2	10,000	36.21	0	913,880	1.3588	0.697
4	500	32.79	2.6×10^{-5}	2246.05	0.6961	0.807
6	50,000	34.60	2.98×10^{-6}	83,298.0	0.8952	0.727
8	0.01	37.87	-0.00123	0.02809	1.4360	0.899

bids for that item, it is suggested that the median value be used to predict the SHA's cost. The benefit in using the median to describe the data set is that the median is insensitive to a number of extremely small or large datum values. Since it is possible that there will be a large variation in the adjusted national cost for any value of the independent variables, the median of the cost will be used.

To enhance the model further a lumped mass approach will be used. This will be accomplished by taking all observations within a specified area of the plot and applying those observations at the center of this area. The procedure will be to round the independent variables and then find the median cost of all of the resulting observations.

The point that represents the median cost at the rounded value of the independent value will then be weighted by the number of observations. The effect of this approach will be to remove some scatter from the plots, yet weight the statistical analysis in the same manner as the original data.

When using this lumped mass approach to reduce the clutter of data, it is important to carefully select the value to which the independent variable is rounded. If too high a rounded value is used, the trends may be altered. If too small of a value is used, the clutter is not sufficiently removed and the trends may remain hidden.

To obtain the optimum rounding value a sensitivity analysis was performed. This sensitivity analysis was accomplished by starting with no rounding and gradually increasing the amount of rounding. For each rounding level a cost equation was generated and the R^2 value was recorded. The optimum rounding level was determined to be the level that produced the greatest R^2 value. This process is illustrated in Table 2 for Item 111—partial-depth PCC deck patching. As can be seen in Table 2 as the rounding level increases there is an increase in the R^2 value. This is attributed to the lumping and weighting of the data.

By this procedure the outliers are removed from the regression, thus increasing the R^2 value. However, the influence of agglomeration of points is maintained by the weighting. The more data observations that make up a lumped point, the more influence this point has on the regressed model. As mentioned previously if too large a rounded value is used the trend for the data is destroyed. This can be seen in Table 2 for rounding value levels of 25 and 30. When these values are used the trends are destroyed, and a seemingly random pattern of datum points is produced. This is verified by an R^2 value of zero, which indicates no relationship between the independent and dependent variables. For Item 111 this occurred rather quickly between rounding levels of 20 and 25. For most items, however, there was a gradual reduction in the R^2 value before the R^2 value reached zero.

RESULTS AND DISCUSSION OF RESULTS

Detailed descriptions are presented for one item, latex-modified overlays. A generic description of each item is provided so that the cost model can be adapted by any SHA by modifying it for its standard specification. Along with the description is a discussion of the pay quantity for each item. For most items the pay quantity varies from state to state, so this will aid in conversion of the model.

The information tabulated for each item includes the rounding level proposed to lump the data for regression, the values obtained for the four regression parameters (b_1 through b_4), and the R^2 value obtained for the regression. This information is provided for each for the eight factors (independent variables) previously described except when the R^2 value is so low that it indicates that no relationship is exhibited.

Latex-modified concrete overlay (Item 210) consists of all labor, material, and equipment required to furnish and place a latex-modified concrete overlay. The specifications for this work are usually quite lengthy and are very similar for each state. However, there are some differences in the thickness of the overlays. For the purpose of the equation derived here, all LMC overlays were assumed to be 31.8 to 38.1 mm (1.25 to 1.5 in.) in depth. These are the most typical depths specified by SHAs. The pay quantity used for this model is per square yard.

The results of the regression model are given in Table 3. Cost equations were not generated for Factors 3, 5, and 7 because of a lack of fit. All models reported in Table 3 will provide a sufficient accuracy for cost estimation purposes. The best model is based on Factor 8 [(quantity · number of bidders)/MPT amount], which has an R^2 value of 0.899. This value is very high, and it is recommended that it be used as the model for this item.

SUMMARY AND RECOMMENDATIONS

Based on the statistical analyses and engineering estimation described earlier equations were developed to predict the cost of the

TABLE 4 Recommended Price Equations

Item No.	Price Equation
111	$C = 133 + \frac{1{,}382{,}600}{(\text{Factor } 4)^{2.38}}$, \$/SY
112	$C = 214 + 0.01 \cdot (\text{Factor } 4) + \frac{361{,}990}{(\text{Factor } 4)^{2.11}}$, \$/SY
121	$C = 236 - 0.037 \cdot (\text{Factor } 1) + \frac{1408}{(\text{Factor } 1)^{0.50}}$, \$/SY
131	$C = 267 + 0.029 \cdot (\text{Factor } 2) + \frac{83{,}400}{(\text{Factor } 2)^{1.22}}$, \$/SY
210	$C = 38 - 0.0012 \cdot (\text{Factor } 8) + \frac{0.028}{(\text{Factor } 8)^{1.44}}$, \$/SY
220	$C = 9.8 - 0.00017 \cdot (\text{Factor } 1) + \frac{3{,}978{,}400}{(\text{Factor } 1)^{3.10}}$, \$/SY
230	$C = 32 + 8.82 \times 10^{-5} \cdot (\text{Factor } 4) + \frac{22{,}200}{(\text{Factor } 4)^{0.98}}$, \$/SY
241	$C = 1.4 - 3.0 \times 10^{-5} \cdot (\text{Factor } 1) + \frac{10.9}{(\text{Factor } 1)^{1.01}}$, \$/SY
242	$C = 8.7 + 7.04 \times 10^{-5} \cdot (\text{Factor } 1) + \frac{56.1}{(\text{Factor } 1)^{1.24}}$, \$/SY
243	$C = 9 - 2.69 \times 10^{-6} \cdot (\text{Factor } 2)$, \$/SY
251	$C = 7 + 2.38 \times 10^{-5} \cdot (\text{Factor } 1) + \frac{68{,}770}{(\text{Factor } 1)^{1.83}}$, \$/SY
252	use price equation for Item 251
260	$C = 6.4 - 2.5 \times 10^{-5} \cdot (\text{Factor } 4) + \frac{5{,}594}{(\text{Factor } 4)^{1.33}}$, \$/SY

rehabilitation treatments previously listed (Table 4). Although the models are useful in predicting costs, caution should be exercised when using them. Since most equations have an inverse term these models will result in a very high price for very small quantities. For this reason judgment should be used before applying the costs to a life-cycle cost model.

The most commonly used independent variable in the cost models was Factor 1, which represents the quantity of the item. As discussed previously most SHAs base their existing cost models solely on quantity. These cost equations will provide more accurate models while maintaining relative simplicity. The other factors that were used are Factors 2, 4, and 8. These three factors are not as simple as

TABLE 4 (*continued*)

Item No.	Price Equation
310	$C - 56 - 0.00036 \cdot (\text{Factor } 4)$, \$/SY
320	$C - 42 - 8.2 \times 10^{-5} \cdot (\text{Factor } 2) + \dfrac{67{,}470}{(\text{Factor } 2)^{1.01}}$, \$/SY
330	$C - 22 + 0.0012 \cdot (\text{Factor } 1) + \dfrac{42{,}250}{(\text{Factor } 1)^{0.92}}$, \$/SY
411	$C - 487 - 0.367 \cdot (\text{Factor } 1) + \dfrac{291}{(\text{Factor } 1)^{0.81}}$, \$/SY
412	$C - 613 - 0.027 \cdot (\text{Factor } 1) + \dfrac{3{,}328}{(\text{Factor } 1)^{2.92}}$, \$/SY
421	$C - 104 + \dfrac{1{,}485}{(\text{Factor } 1)}$ (see note 1), \$/SY
422	$C - 204 + \dfrac{1{,}435}{(\text{Factor } 1)}$ (see note 1), \$/SY
431	$C - 137 + \dfrac{1{,}476}{(\text{Factor } 1)}$ (see note 1), \$/SY
432	$C - 314 + \dfrac{1{,}468}{(\text{Factor } 1)}$ (see note 3), \$/SY
510	C - \$354/SY (encasing bridge piers)
521	use price equation for Item 241
522	use price equation for Item 242
530	$C - 3{,}610 - 6.11 \cdot (\text{Factor } 1) + \dfrac{18{,}820}{(\text{Factor } 1)^{1.85}}$, \$/CY

(*Continued on next page*)

Factor 1 and require some a priori knowledge about the entire construction project. The additional information required for these factors should be readily available by comparing the project with other similar projects and will provide more accurate models. The degree of accuracy to which this information is estimated may have a significant impact on the resulting cost, and as such a sensitivity analysis should be performed and judgment should be used in deciding on the values for these factors.

ACKNOWLEDGMENTS

This work would not have been possible without the enormous contributions of the bridge, materials, and maintenance engineers of the state departments of transportation. We also thank the SHRP state coordinators, who graciously assisted us by providing the source information contained in this document. Special consideration is extended to SHRP staff, the Expert Task Group for SHRP C103, the

TABLE 4 (*continued*)

Item No.	Price Equation
541	$C = -10 + 7.24 \times 10^{-5} \cdot (\text{Factor 4}) + \dfrac{150}{(\text{Factor 4})^{0.21}}$, \$/SY
542	$C = 18 - 0.0035 \cdot (\text{Factor 1})$, \$/SY

where:

C = price per unit measurement
Factor 1 = quantity
Factor 2 = (quantity * contract amount)/MPT amount
Factor 4 = quantity * number of bidders
Factor 8 = (quantity * number of bidders)/MPT amount

Note 1: For Items 421, 422, 431, and 432 unit prices vary significantly with the locations of the repair. Therefore, for specific bridge members, use the regression coefficients tabulated below for the equation $C = F * Q^{-1} + a$.

Concrete Bridge Member	Treatment #421		Treatment #422		Treatment #431		Treatment #432	
	F	a	F	a	F	a	F	a
Beams	1,226	65	1,226	123	1,226	97	1,415	251
Diaphragms	1,111	175	1,105	238	1,111	207	1,110	371
Piers	1,670	66	1,522	174	1,541	97	1,671	261
Pier Caps	1,398	112	886	263	1,537	97	1,393	308
Backwalls	1,977	65	1,887	174	1,975	98	1,977	261
Abutments	2,016	66	1,886	220	2,018	97	2,017	261
Wingwalls	1,461	65	1,461	123	1,447	102	1,461	261

Note 2: $\$/m^2 = (\$/SY) * 1.196$
$\$/m^3 = (\$/CY) * 1.308$

Advisory Committee, and the Technical Contract Manager, Joseph Lamond.

REFERENCES

1. Jelen, F. C., and J. H. Black. *Cost Optimization and Engineering,* 2nd ed., McGraw-Hill, Inc., New York, 1983.
2. Humphreys, K. K. *Project and Cost Engineers Handbook.* Marcel Dekker, Inc., New York, 1984.
3. Barrie, D. S., and B. C. Paulson. *Professional Construction Management,* 3rd ed. McGraw-Hill, Inc., New York, 1992.
4. Gainsburgh, M. R., and J. Backman. Inflation and the Price Indexes. *Studies in Business Economics, No. 94.* National Industrial Conference Board. U.S. Government Printing Office, Washington, D.C., 1990.
5. Grant, E. L., W. G. Ireson, and R. S. Leavenworth. *Principles of Engineering Economy,* 8th ed. John Wiley and Sons, Inc., New York, 1990.
6. Quarterly Cost Roundup. *Engineering News Record.* McGraw-Hill, Inc., New York, various years.
7. Price Trends for Federal-Aid Highway Construction and Cost Trends—Highway Maintenance and Operations. In *Highway Statistics*—1990. U.S. Government Printing Office, Washington, D.C., 1991.
8. Smit, K. (senior editor). *Means Concrete Cost Data—1992,* 10th Annual Edition. R. S. Means Company, Inc., Kingston, Mass., 1991.
9. Neter, J., W. Wasserman, and M. H. Kutner. *Applied Linear Regression Models,* 2nd ed. Irwin Publishing Company, Boston, Mass., 1989.
10. Gannon, E. J., P. D. Cady, and R. E. Weyers. *Price and Cost Information.* Report SHRP-S-664. Strategic Highway Research Program, National Research Council, Washington, D.C., 1992.

Publication of this paper sponsored by Committee on Corrosion.

Gravity-Fill Polymer Crack Sealers

MICHAEL M. SPRINKEL AND MARY DEMARS

Cracking in bridge deck concrete is a serious problem. Cracks allow the direct infiltration of water and chloride ion and the carbonation of the walls of the crack, causing the reinforcing steel to corrode. Gravity-fill polymer crack sealers consist of two or more low-viscosity liquid monomer or polymer components that can be mixed and poured directly over a cracked surface. The monomer or polymer fills the cracks and hardens into polymer. The laboratory evaluation of three two-component epoxies, a three-component high-molecular-weight methacrylate, and a two-component polyurethane is described. Tests included measurements of the flexural strengths and freeze-thaw durabilities of repaired beams and the gel times and penetration abilities of the sealers. The five sealers were evaluated with respect to the effects of temperature and crack width on the quality of the repair, cost, ease of application, safety, appearance, and odor. The gravity-fill polymer crack sealers completely penetrated 0.2-mm-wide cracks, restored >100 percent of the original flexural strengths of the beams, had satisfactory freeze-thaw durabilities, and had gel times that decreased as the temperature increased. The laboratory tests suggest that all five gravity-fill polymer crack sealers can adequately seal cracks in bridge deck concrete.

Cracking in bridge deck concrete is a serious problem because cracks allow the direct infiltration of water and chloride ion and the carbonation of the walls of the crack. The presence of water and chloride ion and the low pH of carbonated concrete can cause the reinforcing steel to corrode. Gravity-fill polymer crack sealers can be used to fill and seal cracks and thereby extend the life of a bridge deck.

Gravity-fill polymer crack sealers consist of two or more low-viscosity liquid monomer or polymer components that can be mixed and poured directly over a cracked surface. The monomer or polymer fills the cracks and hardens into polymer that seals the cracks, bonds to the crack walls, and restores a percentage of the flexural strength of the original concrete. The repair can be completed within a short time because the only preparation necessary is to blast the crack clean with compressed air and because polymers that cure in minutes or several hours can be selected.

This paper describes the laboratory evaluation of three two-component epoxies (E1, E2, E3), a three-component high-molecular-weight methacrylate (HMWM), and a two-component polyurethane (U) with the properties given in Table 1. Tests included measurements of the flexural strengths and freeze-thaw durabilities of repaired beams and the gel times and the penetration abilities of the sealers. In addition, the five sealers were evaluated with respect to the effects of temperature and crack width on the quality of the repair, cost, ease of application, safety, appearance, and odor (*1*).

FLEXURE TESTS

The objectives of the flexural tests were to determine (a) the effect of crack width on sealer performance, (b) the percentage of the original flexural strength restored by the sealer, and (c) the type of failure (concrete, bond, or polymer). All tests were run at room temperature in a well-ventilated area following the safety precautions outlined by each manufacturer.

Sixty unreinforced portland cement concrete beams 7.6 × 10.2 × 27.9 cm (3 × 4 × 11 in.) (Table 2) approximately 6 months old were tested to failure by using three-point flexural loading (ASTM C78-84), and the ultimate strengths were recorded and are reported as the initial flexural strengths (Table 3). At approximately 2 weeks after the flexural tests the failed beams were prepared for crack sealing as follows.

To maintain cracks of known widths, wire spacers with diameters of 0.2, 0.5, 0.8, and 1 mm were used. The wires were cut into sections of approximately 3.2, 1.9, 1.3 and 1.0 cm (1.25, 0.75, 0.5, and 0.375 in.) in length, respectively. Four pieces of wire were then bent into an L-shape and were attached with duct tape to two outside faces of each cracked beam. Three beams were prepared to receive each product for each crack width. To secure the beams for polymer application the beams were placed in a specially designed jig to hold the sections together under a constant force of a torque screw. The bottoms and sides of the cracked sections were covered with duct tape to prevent leaking.

The polymer was mixed as specified by the material supplier and was poured over the cracks until a pool of polymer remained over the crack. Because of leakage and long penetration times the cracks typically needed to be retreated several times to completely fill the crack.

After 24 hr the beams were removed from the jig. If leaking caused the beams to stick to the jig they were loosened with a hammer and chisel. One week later excess polymer was removed from the exterior of the beams with a wire brush. The repaired beams were stored in the laboratory.

Two weeks after the cracks were sealed the repaired beams were tested again in flexure (ASTM 78-84). The results are reported in Table 3 as final flexural strengths.

Each beam was examined to determine the percentage of the new crack that failed in the concrete, bond, or polymer. Although most beams fail by a combination of failures in the three types the vast majority of the failure area was in the concrete.

The crack sections were sawed perpendicular to the plane of the cracks into three sections, exposing four interior surfaces showing the penetration of the sealers and the failure type inside the beam. Inspection of the sawed sections revealed that all of the polymers penetrated and filled the entire depths of the cracks, including the smallest crack width of 0.2 mm, and that wire spacers maintained constant crack widths.

The results based on the average of flexural tests on three beams are summarized in Table 3. All five polymers performed well by meeting the two desirable criteria of crack sealer materials: sealing the cracks and restoring the flexural strength of the concrete.

Virginia Transportation Research Council, 530 Edgemont Road, Charlottesville, Va. 22903.

TABLE 1 Properties of Crack Sealer Products Tested[a]

Products	Cost $/liter ($/gal.)	Mix Ratios (By Volume)	Viscosity at 23° C, cps [b]	Tensile Strength MPa (psi)	Elonga-tion(%)	Odor
U	18-24 [c] (67-90)	A:1 B:1	A:12 B:16	31 (4500)	<10 (ASTM D412)	Almost none
E1	5 (18)	A:2 B:1	175-250	48 (7000)	1.9 (ASTM D638)	Stinky
E2	21 (80)	A:2 B:1	200-230	22 (3250)	37.5 (ASTM D638)	Mild
E3	9-13 [c] (33-50)	A:3.5, B:1 Weight: A:80% B:20%	300-500	29 (4247)	9.9 (ASTM D638)	Stinky
HMWM	11 (40)	A:1.0 B:0.02 C:0.04-0.08	<100	>10 (>1500)	>30 (ASTM D638)	Extremely pungent

[a] Based on product literature and personal communications with product suppliers.

[b] ASTM D2393.

[c] Lower price represents bulk rates.

Table 3 shows that under controlled laboratory conditions all five polymers on average restored 100 percent or more of the original flexure strength. It is unlikely that such high ratios would be achieved in the field because of carbonation, dirt, debris and other contaminants in the cracks. The higher final flexural strengths can be attributed to the different positions of the beams on the test machine or to the fact that when the initial crack was repaired the next crack developed at a higher flexural strength (*2*). Figure 1, a plot of the ratio of the final (*F*) and the initial (*I*) flexural strength versus crack width, illustrates the trend that as the crack width increases *F/I* decreases for all of the polymers. This trend implies that the polymers act more like adhesives in the narrow cracks and more like low-modulus concretes in the wider cracks.

The majority of the beams recracked in the concrete away from the initial crack site, indicating a strong bond between the polymer and concrete. Figure 2 illustrates the percentage of the new crack resulting from concrete, bond, or polymer failure. Examination of the crack face of the beams repaired with HMWM, E1, and E3 that failed at the initial crack site revealed that the new crack resulted almost entirely from a failure in the concrete. A very small percentage of the new crack was due to failure of the bond, and only a few beams showed an even smaller percentage of failure in the polymer. Several of the beams repaired with U and E2 had significantly higher percentages of bond failure, although E2 achieved one of the high *F/I* values. The majority of beams treated with E2 failed almost completely in the concrete; however, when failure did occur at the bond it comprised a very high percentage of the new crack, increasing the average percent bond failure. A plot of percent bond failure versus crack width showed that crack width has a minimal effect on percent bond failure except with U, in which the relationship seems to be direct.

FREEZE-THAW TESTS

The objective of the freeze-thaw tests was to determine the durability of the polymer crack repairs when they were subjected to ASTM C666 Procedure A.

TABLE 2 Concrete Mixture Proportions

	lb/yd³	kg/m³
Cement Type II Portland	635	375
Coarse Aggregate	1,897	1,119
Granite, specific gravity = 2.83		
Unit weight = 1,646 kg/m³ (103.3 lbs/ft³)		
Fine Aggregate		
Silica sand	1,077	635
Specific gravity = 2.58		
Fineness modulus = 2.70		
Water	286	169
Air = 6.5%	0	0

28-day compressive strength = 39 MPa (5,680 psi)

Fifteen beams that were 7.6 × 10.2 × 40.6 cm (3 × 4 × 16 in.) (Table 2) were prepared and tested in flexure the same way as described for the flexural tests, except only one beam was used for each crack width tested (0.2, 0.5, and 1.0 mm), and no beams with 0.8-mm cracks were prepared. The repaired beams were placed in the freeze-thaw test machine 2 weeks after the repairs were complete. Over a period of 8 weeks the beams were run through 480 rapid cycles of freezing and thawing, following ASTM C666 Procedure A modified by the addition of 2 percent NaCl to the water. Typically, beams are only subjected to 300 cycles, but the beams appeared to be performing so well at 300 cycles that the test was continued for 480 cycles.

Following the 480 cycles of freezing and thawing the beams were tested to failure by using the three-point flexural loading (ASTM C78-84), and the results were recorded and are reported in Table 4, along with the results obtained before repairing the beams.

It is obvious from a comparison of the flexural strength ratios given in Tables 3 and 4 that the freeze-thaw cycling caused significant reductions in the flexural strengths of the repair beams. E1 maintained the highest ratio of flexural strength of 71 percent, whereas U dropped to the lowest ratio of 12 percent as a result of the freeze-thaw testing. A plot of the flexural strength ratio versus crack width showed the same trend as that for beams tested without freeze-thaw cycling: as crack width increases, *F/I* decreases.

It is apparent from a comparison of the failure type results presented in Tables 3 and 4 that although the majority of failures again occurred in the old concrete, the percent bond failure significantly increased as a result of the freeze-thaw testing for U, E1, and E3. For E2 and HMWM the percent bond failure did not increase as a result of freeze-thaw testing. U experienced 100 percent bond failure for all crack widths following freeze-thaw testing.

TEMPERATURE TESTS

The objectives of temperature tests were to observe and measure the behaviors of the polymers at different temperatures. The two properties examined were gel time and penetration. The gel time is an indicator of both the working time and the final cure time of the polymer. Because all polymers completely filled the narrowest crack width, a penetration test was developed to compare the penetration abilities of the crack sealers when poured over four grades of dry filter sand (Table 5).

The tests were run at 7°C, 13°C, 18°C, 24°C, 29°C, and 35°C (45°F, 55°F, 65°F, 75°F, 85°F, and 95°F) at approximately 50 percent relative humidity by using a programmable environmental chamber. All materials were stored in the chamber 24 hr in advance, and specimens were prepared outside the chamber in less than 20 min so that changes in the temperature of the materials were held to a minimum. Approximately 300 ml of the polymer was mixed for 4 min and was used for the three tests (Component A of E3 required additional stirring before mixing).

Gel Time

A cup containing 20 g of the sealer was checked every 10 to 15 min to determine approximate gel time. For this test *gel time* is defined as the time when the polymer first reaches the consistency of Jell-O and no longer moves down the side of the cup when the cup is tipped. The results of the gel time measurements are reported in

TABLE 3 Flexural Test Results

Product	Crack Width (mm)	Flexure Strength Initial MPa	Initial (psi)	Final MPa	Final (psi)	Flexure Strength Ratio (F/I)	Failure Type % Bond	Concrete	Polymer
U	0.2	6.4	930	6.1	872	94%	11%	87%	2%
	0.5	5.6	817	6.4	922	114%	1%	99%	0%
	0.8	6.6	965	5.3	763	79%	49%	51%	0%
	1.0	5.0	725	5.7	833	118%	27%	73%	0%
	Average	6.0	873	5.9	858	100%	20%	80%	0%
E1	0.2	5.9	853	6.5	938	110%	1%	99%	0%
	0.5	5.6	808	6.0	875	114%	0%	100%	0%
	0.8	5.6	815	6.5	937	119%	2%	98%	0%
	1.0	6.3	915	5.5	942	103%	0%	100%	0%
	Average	5.8	848	5.9	923	112%	1%	99%	0%
E2	0.2	5.3	775	5.8	840	115%	17%	83%	0%
	0.5	5.3	770	6.3	913	123%	23%	77%	0%
	0.8	5.8	848	6.1	883	104%	2%	98%	0%
	1.0	5.0	730	5.7	822	114%	27%	72%	1%
	Average	5.4	781	6.0	865	114%	17%	83%	0%
E3	0.2	5.3	762	6.1	880	118%	2%	98%	0%
	0.5	6.0	867	5.5	805	93%	4%	96%	0%
	0.8	6.0	868	5.4	790	95%	2%	97%	1%
	1.0	6.1	890	5.8	845	95%	2%	97%	1%
	Average	5.8	847	5.7	830	100%	2%	97%	1%
HMWM	0.2	4.7	675	6.0	870	131%	2%	98%	0%
	0.5	6.1	890	6.2	905	102%	0%	94%	6%
	0.8	5.3	775	6.6	957	128%	0%	97%	3%
	1.0	5.7	827	6.1	890	108%	0%	100%	0%
	Average	5.5	800	6.3	909	116%	1%	97%	2%

Table 6 and are illustrated in Figure 3. As the temperature increases, the gel time decreases. U gelled the fastest, completely curing in under 2.5 min at 7° C (45°F). El and HMWM marked the next fastest gel times. E3 required a considerably longer time to gel. E2 took the longest time to gel because it has the unique ability to reach an almost-gel state and to maintain that state for hours before completely gelling. Because time constraints made it difficult to monitor the gel sample for E2 for the necessary length of time, values for the gel times at the colder temperatures are estimates.

Penetration Test

To compare the penetration abilities of the polymers, 40 g of polymer (^{Wt}polymer) was poured over 100 g of dry filter sand in 100-ml cups (^{Wt}sand). Two samples of each of three different gradations of sand were used: MX-65 (very fine), MS-45 (fine), and GX-30 (coarse). FX-50 (very coarse) sand was used in the first test only at 13°C (55°F) and was determined to be ineffective in measuring differences in penetration (Table 6). Once the polymer concrete had cured, the cups were peeled away, the excess sand was brushed off, and the hardened mass was weighed (^{Wt}pc). To compare the penetration abilities of the polymer products the following equations were created:

$$\text{Weight of sand lost} = {}^{Wt}\text{sand} + {}^{Wt}\text{polymer} - {}^{Wt}\text{pc}$$

$$\text{Percent penetration} = \left(\frac{{}^{Wt}\text{sand} - {}^{Wt}\text{sand loss}}{{}^{Wt}\text{sand}}\right) \times 100$$

Plots of the percent penetration versus temperature for all three grades of sand (Figures 4 to 6) illustrate the penetration trends for the products. HMWM penetrated 100 percent of all of the sand samples at all temperatures. E2 was a close second, achieving 100 percent penetration at the higher temperatures. The penetration of El also increased as the temperature increased. U performed completely the opposite with respect to temperature; because of its faster cure rate, the U sealer hardened before maximum penetration potential was achieved. E3 was inconsistent, attaining both very high and very low percent penetration values. The order in mixing the components of E3 may have contributed to the scatter; if Component B was added to the thicker Component A, it did not mix as well as when Component A was added to Component B.

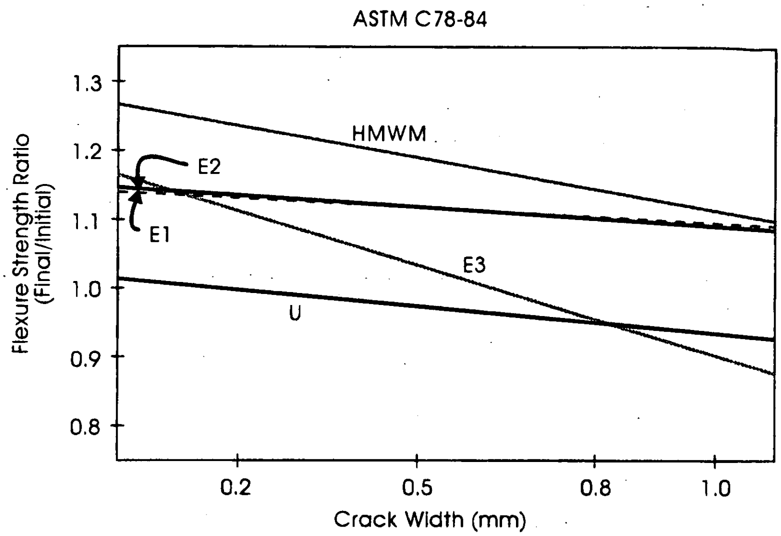

FIGURE 1 Flexure strength ratio versus crack width.

SUMMARY OF RESULTS

Overall Effectiveness of Gravity-Fill Polymer Crack Sealers

The results of the tests described here suggest that gravity-fill polymer crack sealers can more than adequately seal cracks in bridge deck concrete. Under ideal conditions the gravity-fill polymer crack sealers completely penetrated 0.2-mm-wide cracks, restored 100 percent or more of the original flexural strengths, were reasonably durable in freeze-thaw testing, and had gel times that decreased as temperature increased. Therefore, all five gravity-fill polymer crack sealers can be fast, effective, durable, and practical repair materials, although some materials perform better in certain tests.

Effects of Crack Width and Treatment Temperature

Temperature and crack widths influenced performance based on individual products. HMWM is effective under a variety of conditions. E2 also performs well for all crack sizes and temperatures; however, the gel times are extremely long at the colder temperatures. E1, E3, and U all appear to seal narrow cracks better. E1 penetrates better at higher temperatures, no definite effect of tempera-

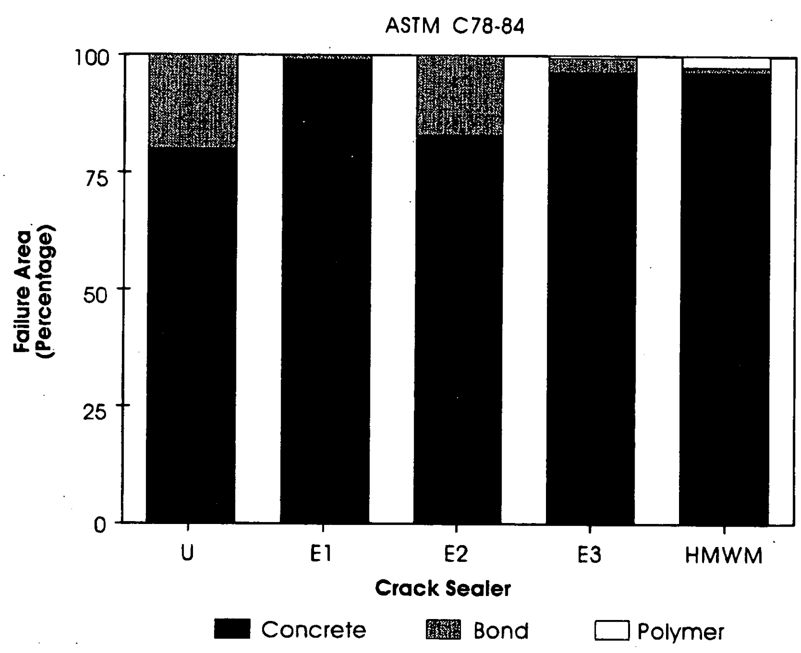

FIGURE 2 Failure mode of new crack.

TABLE 4 Freeze-Thaw Test Results

Product	Crack Width (mm)	Flexure Strength Initial MPa	Initial (psi)	Final MPa	Final (psi)	Flexure Strength Ratio (F/I)	Failure Type % Bond	Concrete	Polymer
U	0.2	4.8	700	1.2	170	24%	100%	0%	0%
	0.5	4.9	710	0.3	45	6%	100%	0%	0%
	1.0	4.1	600	0.3	41	7%	100%	0%	0%
	Average	4.6	670	0.6	85	12%	100%	0%	0%
E1	0.2	4.8	700	3.7	530	76%	0%	100%	0%
	0.5	4.4	635	3.5	515	81%	50%	50%	0%
	1.0	5.1	745	2.8	410	55%	70%	30%	0%
	Average	4.8	693	3.3	485	71%	40%	60%	0%
E2	0.2	4.6	665	3.1	445	67%	15%	85%	0%
	0.5	4.6	670	2.6	380	57%	20%	80%	0%
	1.0	4.1	600	2.7	390	65%	0%	100%	0%
	Average	4.4	645	2.8	405	63%	12%	88%	0%
E3	0.2	4.4	645	2.5	370	57%	30%	70%	0%
	0.5	4.3	630	0.1	11	2%	100%	0%	0%
	1.0	4.5	660	1.0	140	21%	90%	10%	0%
	Average	4.4	645	1.2	174	27%	73%	27%	0%
HMWM	0.2	4.3	620	3.0	440	71%	3%	95%	2%
	0.5	4.4	640	3.3	475	74%	0%	100%	0%
	1.0	4.9	710	2.6	375	53%	0%	100%	0%
	Average	4.5	657	3.0	430	66%	1%	98%	1%

Freeze Thaw: 480 cycles

ture on penetration is evident for E3, and U penetrates the best at lower temperatures.

Critiques of Individual Products

The strengths, weaknesses, and best conditions for use are summarized for each gravity-fill polymer crack sealer product tested.

U

Description U is in a category of its own. It cures incredibly fast, it has almost no odor, and the application procedure is very user friendly. However, its ability to penetrate narrow cracks at high temperatures, seal large cracks effectively, and withstand the stresses of freezing-thawing is somewhat less than those of the other products.

TABLE 5 Sand Grades Used in Penetration Tests

Sand Product[a]	% Passing Sieve Sizes #30	#100	#140
MX-65	99.5%	19.9%	5.4%
MX-45	94.9%	3.5%	1.0%
GX-30	94.5%	2.0%	0.0%
FX-50	29.3%	0.0%	0.0%

[a] donated by Foster Dixiana, P. O. Box 2005, Columbia, South Carolina 29202

TABLE 6 Temperature Test Results

	Temp.		Gel Time			% Penetration in Sand[a]			
Product	°C	°F	(hrs)	(min)	(sec)	MX-65	MX-45	GX-30	FX-50
U	7	45	--	2	30	75	91	95	--
	13	55	--	2	0	63	88	--	100
	18	65	--	1	15	60	89	96	--
	24	75	--	0	45	55	82	84	--
	29	85	--	0	35	58	66	86	--
	35	95	--	0	30	51	57	61	--
E1	7	45	10	--	--	53	81	92	--
	13	55	5	--	--	59	85	--	91
	18	65	2	50	--	73	90	96	--
	24	75	1	45	--	68	82	92	--
	29	85	1	--	--	68	91	94	--
	35	95	--	50	--	74	98	92	--
E2	7	45	19	--	--	87	99	100	--
	13	55	14	30	--	94	94	--	99
	18	65	8	30	--	99	99	100	--
	24	75	6	--	--	99	99	100	--
	29	85	4	--	--	100	100	100	--
	35	95	1	30	--	100	100	100	--
E3	7	45	15	30	--	67	93	84	--
	13	55	11	30	--	55	83	--	96
	18	65	5	--	--	67	95	88	--
	24	75	2	--	--	71	95	81	--
	29	85	2	--	--	79	79	89	--
	35	95	--	50	--	62	72	85	--
HMWM	7	45	10	30	--	100	100	100	--
	13	55	5	30	--	100	100	--	100
	18	65	3	--	--	100	100	100	--
	24	75	1	--	--	100	100	100	--
	29	85	--	40	--	100	100	100	--
	35	95	--	30	--	100	100	100	--

[a] Sands in order of decreasing fineness (left to right).

Application For repairs for which the quickness of repair is critical U is appropriate. It is good for small cracked sections where leaking may be a problem and sealing the underside of the deck is not practical.

E1

Description E1 performed satisfactorily in all tests. Desirable qualities include its low cost, easy mix ratios, low percent bond failure, high freeze-thaw durability, and rapid gel times. However, E1 had a relatively strong odor.

Application E1 can be used for low-budget projects for which the quickness of repair and durability are desirable. E1 works best on small cracks at higher temperatures.

E2

Description E2 is suitable for treating cracks under a variety of conditions. Tests show that E2 has an outstanding capacity to penetrate the full depth of narrow cracks, restore the strength of the concrete, and resist freeze-thaw cycling. Potential drawbacks of the product include extremely long gel times, high cost, and possible

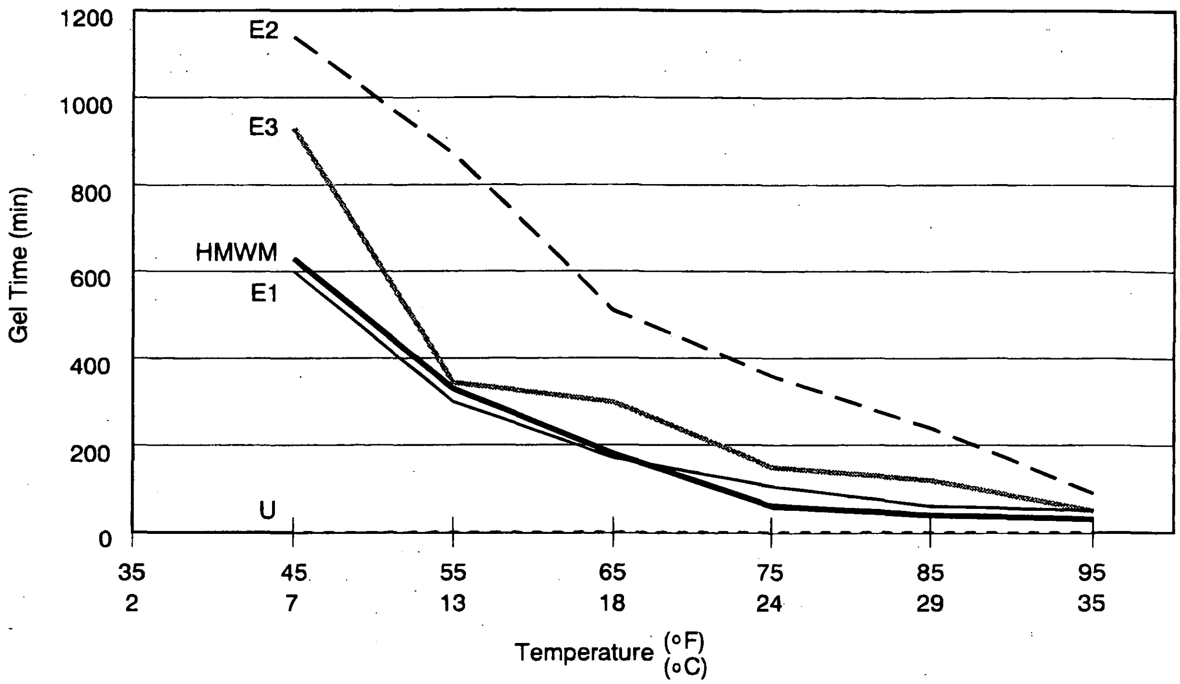

FIGURE 3 Gel time versus temperature for gravity-fill polymer crack sealers.

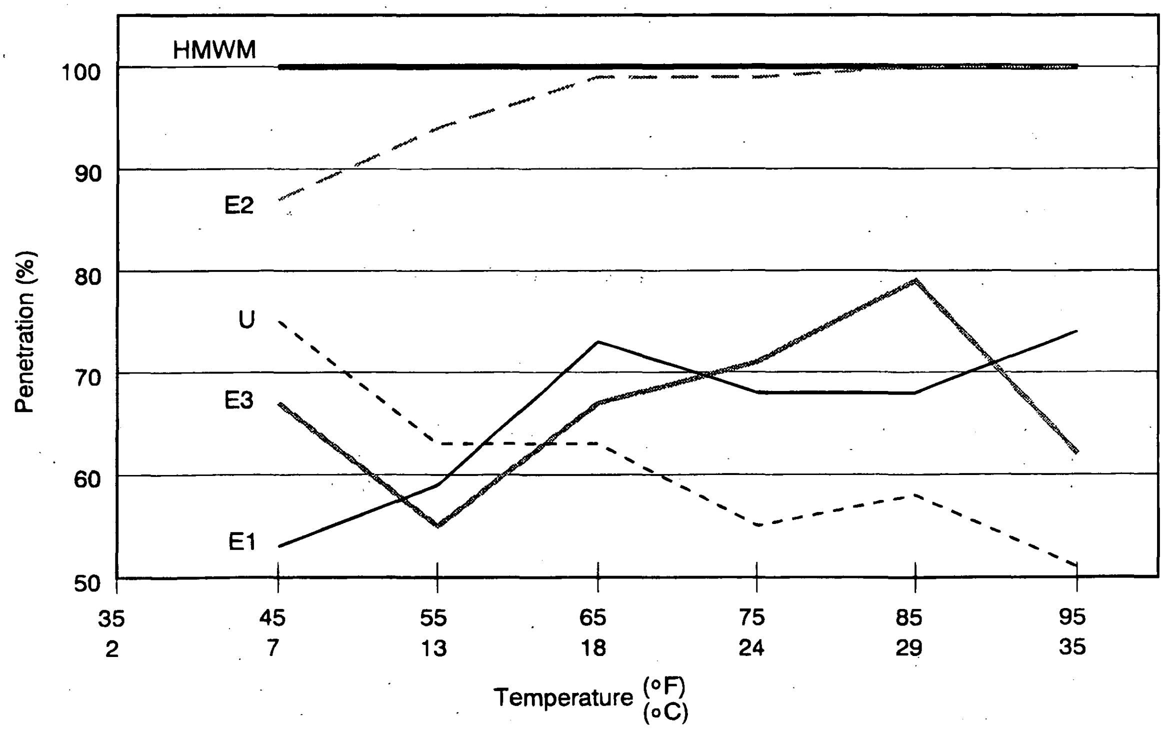

FIGURE 4 Percent penetration versus temperature: MX-65 (very fine).

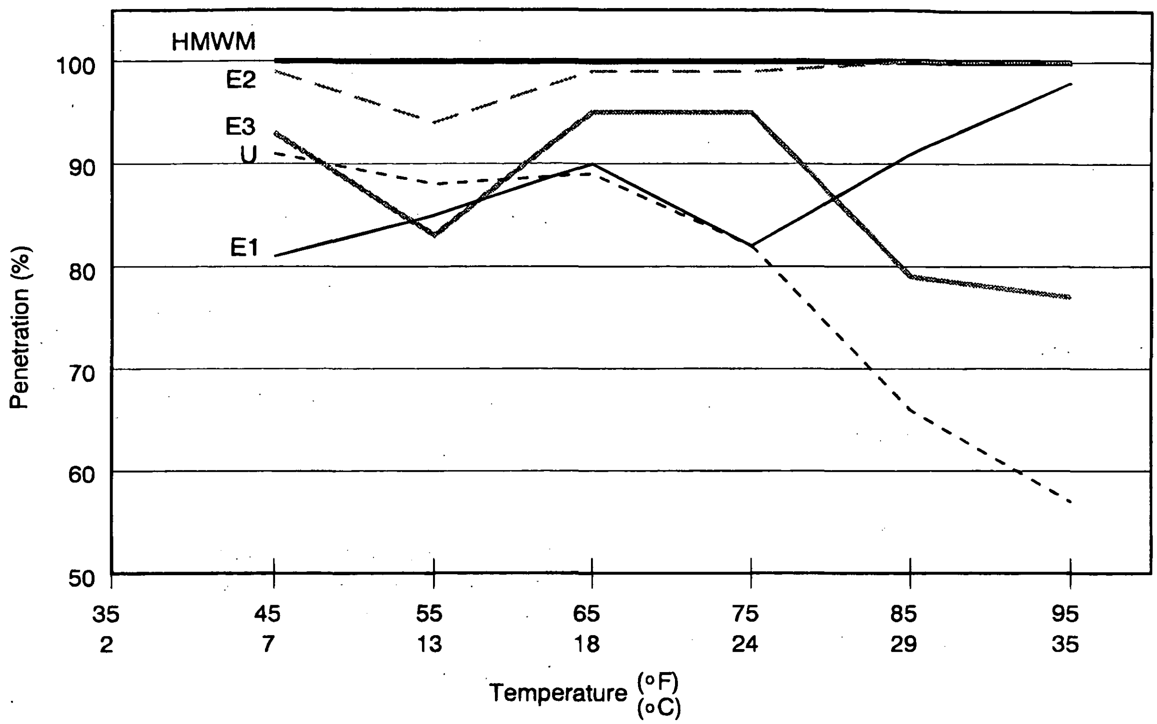

FIGURE 5 Percent penetration versus temperature: MX-45 (fine).

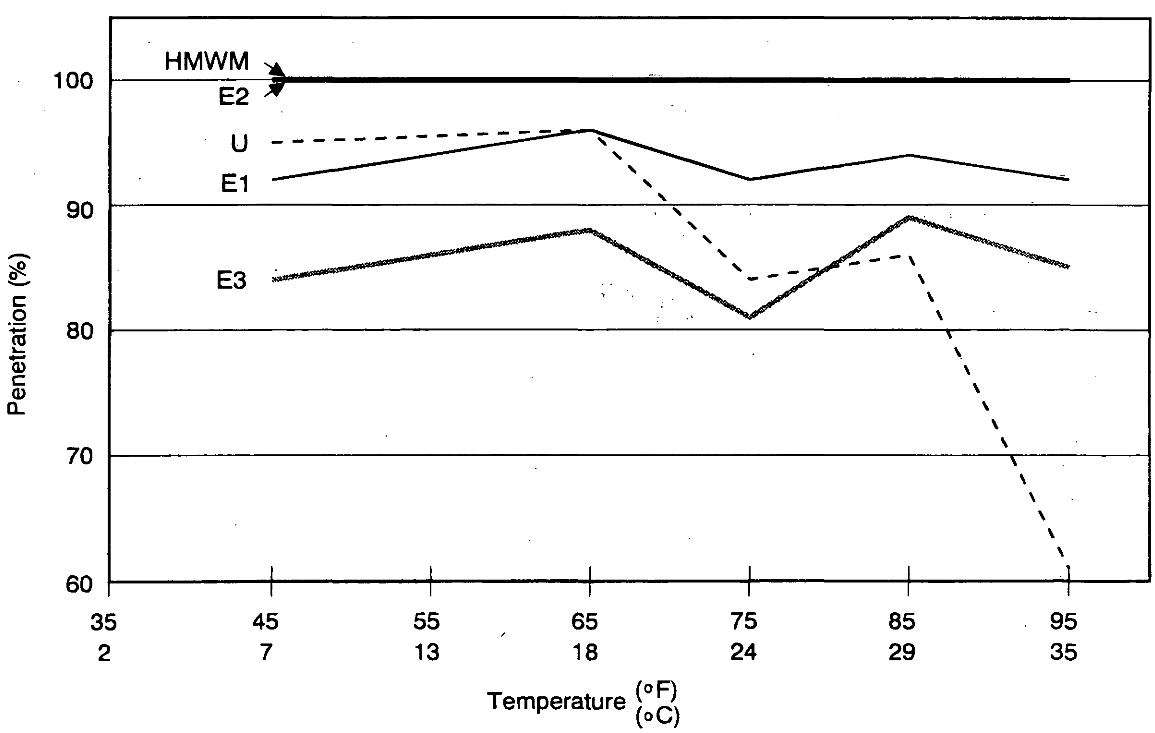

FIGURE 6 Percent penetration versus temperature: GX-30 (coarse).

negative color. However, the components are easy to mix, have a mild odor, and are very safe to use.

Application E2 can be applied to projects for which quality and durability (not quickness of repair) are critical factors. It is excellent for hairline cracks and is ideal for repairs where odor is a concern.

E3

Description E3 performed satisfactorily in most tests. It achieved a low bond failure rate and a good flexural strength ratio and is relatively inexpensive. Because of its long gel times and the wetting additives claimed to be in the product, E3 typically penetrated better at low temperatures, but its performance was scattered. The difficulty in mixing exact proportions is the most probable cause for the variation in results; therefore, further testing is recommended. Its inability to withstand freeze-thaw cycling is a matter of concern.

Application E3 can be used for a low-budget temporary project for which sealing is more critical than fast repair times.

HMWM

Description HMWM outperformed the other products tested. It achieved an outstanding flexural strength ratio and low percent bond failure even after freeze-thaw cycling. It gelled very quickly and penetrated 100 percent of the finest sand at the lowest temperature. Despite these strengths the smell of HMWM is extremely pungent and can explode if the three components are mixed in the wrong order. Also, the mixing ratios are relatively complicated, and its low viscosity may cause problems of leaking to other areas.

Application HMWM is good for all types of projects or for projects for which low budget, time of repair, and durability are all critical factors. It is effective at a temperature range of between 4 and 38°C (40 and 100°F). It is excellent for use on hairline cracks; however, leaking may be a problem. It should be used for projects away from large populations of people in well-ventilated areas.

COMPARISON OF PRODUCTS

A comparative evaluation of the products is provided in Table 7. When equal weight is given to each of the nine properties the total points are similar for the five products and E1, E2, and HMWM are ranked 1, 2, and 3, respectively. When only the performance of the products is considered (last four properties in Table 7) HMWM and E2 are clearly ranked 1 and 2, respectively, E1 is clearly third, and E3 and U are fourth and fifth, respectively.

VIRGINIA DEPARTMENT OF TRANSPORTATION SPECIAL PROVISIONS FOR GRAVITY-FILL CRACK SEALING

I. Description

This work shall consist of preparing concrete cracks and treatment with a polymer crack sealer.

II. Materials

E1, E2, E3, HMWM, U (from approved products list)
Gel time, 50 ml, maximum at 24°C . . . . 6 hr
Tensile strength, minimum at 24°C (ASTM D638) . . . 10MPa (1,500 lb/in.^{2})
Sand penetration, MX-45, minimum at 24°C . . . . 80 percent
A Material Safety Data Sheet (MSDS) shall be furnished with the material to be used on project.

TABLE 7 Comparative Evaluation of Crack Sealers

Product	U	E1	E2	E3	HMWM
Easy to mix	2	1	1	3	5
Odor	1	3	2	3	5
Safety	1	1	1	1	4
Cost	5	1	5	3	3
Cure Time	1	2	5	3	2
Flexural Strength	2	1	1	2	1
Freeze Thaw	5	2	2	4	2
Penetration 7-24°C	4	4	2	4	1
Penetration 24-35°C	5	3	1	3	1
Total Points	26	18	20	26	24
Rank (All Properties)	4	1	2	4	3
Rank (Performance)	5	3	2	4	1

III. Surface Preparation

The concrete surface must be dry! Air blast cracks to remove dust, dirt, and debris with oil-free compressed air.

IV. Application

The concrete surface temperature shall not be less than 13°C (55°F) when the gravity-fill crack sealer is applied. The resin should be applied at the lowest temperature of the day when the cracks are open the most (approximately) 1 a.m. to 9 a.m. Before placing the polymer, dry, no. 50-sieve-size silica sand should be placed in cracks that are wider than 1 mm. The gravity-fill polymer crack sealer should be applied directly to the cracks. Allow a few minutes for the material to seep down into cracks, and then make additional applications until the cracks are filled. Material may be spread over designated cracked area, and material shall be worked into the cracks with a broom. Excess material not worked into cracks should be brushed off the surface before the polymer sets up. Resin shall be applied in a sufficient quantity and number of applications to fill the cracks. An application rate of 124 ml/m or 407 ml/m^2 (1 gal per 100 linear ft or 100 ft^2) is usually adequate. Application of crack sealers shall be done before grooving concrete decks.

V. Limitations of Operations

The Contractor shall plan and prosecute the operations in such a manner as to protect persons and vehicles from injury or damage. Armored joints shall be covered, scuppers shall be plugged, and cracks shall be sealed underneath or other protective measures shall be used in such a manner as to protect traffic, waterways, and bridge components. In the event that material or solvent harms the appearance of bridge components, removal will be required as determined by the Engineer. A sealed surface shall not be opened to traffic until grooving is complete. Grooves shall not be cut until the polymer crack sealer has cured a minimum of 10 times the gel time.

VI. Method of Measurement

When practical as determined by the Engineer crack sealing will be measured in linear meters (feet). Otherwise, crack sealing will be measured in square meters (yards) of cracked surface.

VII. Basis of Payment

Crack sealing will be paid for at the contract unit price bid per linear meter (foot) or square meter (yard), which price shall be full compensation for preparing cracks, furnishing and applying the resin, protection of waterways and traffic, and cleaning up and for all labor, tools, equipment, and incidentals necessary to complete the work.

Payment will be made under the following:

Pay Item	*Pay Unit*
Crack sealing	Linear meter (foot)
Crack sealing	Square meter (yard)

CONCLUSIONS

1. Gravity-fill polymer sealers can seal cracks ranging in width from 0.2 to 1.0 mm.
2. All five products meet current Virginia Department of Transportation specifications.
3. HMWM performed the best, but it has a strong, pungent odor and possible dangerous mixing process.
4. E2 performed almost as well as HMWM but has a long cure time and a high cost.
5. E1 did not perform as well as HMWM or E2 but may be the product of choice when all factors are considered.
6. E3 is ranked fourth because of its low durability and its difficult-to-use mix ratios.
7. U is ranked last, despite the very efficient application method, low odor, and incredibly fast cure times, because it performed the worst in all the tests. Also, it penetrates best at temperatures below 24°C.

RECOMMENDATION

Crack repairs on bridge deck concrete are recommended as follows:

- Preplace sand in cracks with a width greater than 1 mm.
- Place monomers prior to 9:00 a.m. and during colder weather when cracks are widest.
- Cracked concrete surfaces should be dry and sound.
- Air blast or water blast cracks before placing the monomers.
- Broom monomers into the crack until the crack is full.

REFERENCES

1. DeMars, M. *Evaluation of Gravity-Fill Polymer Crack Sealers to Repair Bridge Deck Concrete.* B.S. thesis. University of Virginia, Charlottesville, 1993.
2. Magnum, W. D. *Improved Methods for Sealing Joints and Cracks in Portland Cement Concrete.* M.S.E. thesis. University of Texas at Austin, 1989.

The opinions, findings, and conclusions expressed in this report are those of the authors and not necessarily those of the sponsoring agencies.

Publication of this paper sponsored by Committee on Polymer Concretes, Adhesives, and Sealers.

Service Lives of Concrete Sealers

RICHARD E. WEYERS, JERZY ŻEMAJTIS, AND RICK O. DRUMM

Approximately 16 generic types and more than 450 concrete sealers are used as corrosion protection agents in the United States. However, no standard performance criteria that can be used to determine the cost-effectiveness of the various sealers exist. A study was performed to address the determination of the service lives (reapplication period) of sealers for concrete bridge components in the United States. The environmentally degrading forces of ultraviolet light and abrasion are considered, as is the leakage of the chloride ion through sealed concrete surfaces. A methodology is presented to determine sealer reapplication periods on the basis of the severity of the chloride exposure conditions, bridge site chloride diffusion rates, concrete cover depths, selected corrosion initiation protection period, and chloride leakage factors. The methodology is combined with a laboratory test method to determine sealer leakage factors, and sealer service lives are estimated for a water-based and solvent-based epoxy, a silane, and a siloxane for horizontally and vertically oriented concrete bridge components.

It has been said that steel reinforced concrete is the ideal composite construction material. Concrete is weak in tension but is strong in compression and durable in moist, oxygen-rich environments, whereas steel is strong in tension but is thermodynamically unstable in moist, oxygen-rich environments. The steel provides the tensile strength, and the high pH (pH 12 to 13) of the concrete pore water protects the steel from corroding.

However, certain environmental exposure conditions can disrupt the passive nature of steel in concrete. Carbon dioxide can penetrate porous concrete and through carbonation lower the pH of the concrete to the point at which the steel will spontaneously corrode. Chloride ions can diffuse through the porous concrete and initiate an autogenous corrosion process. Because of the relatively low water-to-cement ratios (less than 0.50) used in the United States carbonation-induced corrosion of the reinforcing steel occurs very infrequently. However, chloride ion-induced corrosion of reinforcing steel is a monumental problem in the United States, particularly for reinforced concrete bridges in the chloride-laden environments of coastal areas and in the northern snowbelt areas where chloride salts are used in winter maintenance activities.

Chloride ion-induced corrosion of reinforced concrete structures is well known. The chloride ion penetrates cracks or diffuses through the porous concrete, reaches a corrosion threshold value, and initiates the corrosion mechanism, and the expanding corrosion products crack and spall the cover concrete. One method that can be used to extend the service lives of steel reinforced concrete structures in chloride-laden environments is to significantly reduce the rate of diffusion of chlorides into the concrete. Concrete sealers, coatings, and membranes have been used extensively to block the ingress of chloride ions into reinforced concrete structures.

Because of their irrelatively low initial cost, concrete sealers offer an attractive solution to the problem of extending the service lives of concrete structures in chloride environments. However, to identify the true cost-effective solution(s) to the maintenance of concrete structures one must determine the minimum life-cycle cost, which is the true definition of cost-effectiveness. To determine the minimum life-cycle cost one must know the initial cost and the service life of the treatment. Thus, the maintenance engineer would know when and how many treatments would be applied over the service life of the structure.

This paper addresses the determination of the service life (reapplication period) of three generic types of concrete sealers applied to steel reinforced concrete bridges in the United States.

BRIDGE ENVIRONMENTS

The service life of a treatment is dependent on the severity of the environment. Decks are exposed to traffic abrasion and long periods of direct sunlight. Superstructure components, beams, and diaphragms are exposed to direct or indirect sunlight and wind abrasion. Substructure components, piers, pier caps, and abutments are exposed to ice, water, or wind abrasion and direct or indirect sunlight. Thus, the service life reduction factors for concrete bridge sealers include abrasion and ultraviolet light in addition to chloride ions. In the snowbelt areas of the United States decks are exposed to the severest conditions: direct exposure to abrasive traffic forces, ultraviolet light, and periodic applications of chloride deicing salts. In the southern coastal areas, however, piers are exposed to the severest conditions: direct exposure to water abrasion, ultraviolet light (part-time daylight exposure), and continuous exposure to chloride ions. Thus, sealer-degrading forces will vary relative to traffic condition: [average annual daily traffic (AADT) and percent trucks], geographical location (average annual snowfall or parts per million of chloride in the water), and latitude, component, and component orientation (period and intensity of ultraviolet light).

Of the range of environmental exposure conditions, traffic conditions result in the highest abrasive forces and a southern exposure may have the longest cumulative hours of ultraviolet light exposure.

EXPERIMENTAL DESIGN

Approximately 16 generic concrete sealer types and more than 450 products are on the market in the United States. However, only two sealing mechanisms are being used: surface agents or pore blockers and penetrating agents or hydrophobic materials. Two sealers each were selected from the two sealing groups: a water-based and a solvent-based epoxy as pore blockers and a silane and siloxane as penetrating sealers.

Since surface finish and exposure orientation influence the performance of a sealer, two specimen types were cast: rough trowel-finished horizontal slabs and a wall surface cast against oiled plywood. A total of 15 horizontal slabs of 91 × 91 × 10 cm were cast. The wall was 30 cm thick, 1.83 m high, and 4.88 m long. Temperature and shrinkage cracking was controlled with a 1.3-cm-diameter steel reinforcing bar with a 5.1-cm cover depth. The wall and slabs

The Charles E. Via Department of Civil Engineering, 200 Patton Hall, Virginia Polytechnic Institute and State University, Blacksburg, Va. 24061-0105.

were cast from the same batch of redi-mix concrete (380 kg of cement, 759 kg of sand, and 1038 kg of stone per cubic meter of concrete), which had a water-to-cement ratio of 0.47. The fresh concrete had a 13-cm slump, 5.4 percent air content, and a unit weight of 2370 kg/m^3. The 28-day compressive strength was 38 MPa.

The 15 slabs were moist cured outdoors for 7 days with wet burlap; this was followed by 24 days of air curing outdoors. The slabs were demolded and placed on concrete blocks to simulate bridge deck exposure conditions. The four sides of the slabs were coated with epoxy, the top surface was lightly grit blasted, and the sealers were applied in the middle to upper middle application range. Three slabs were sealed with each of the four sealer types, and three control slabs were not sealed, but the surfaces were lightly grit blasted.

The wall was cured outdoors in the forms for 7 days; this was followed by 24 days of air curing outdoors. The shaded surface of the wall was lightly grit blasted and was sectioned off into 70-cm-wide vertical strips that were separated by 10-cm-wide stripes spray-painted red. The vertical test sections were sealed with the same sealer types and the same application rates as the horizontal slabs except for the siloxane sealer, whose manufacturer suggested a different coverage range for vertical surfaces. Of five test sections one was sealed with each of the four sealer types and one control section was not sealed but was lightly grit blasted.

In addition, the four sealer types were applied to two existing bridge decks. The sealer test sections were 90 cm wide and were separated by 10-cm-wide unsealed stripes. The sealer test sections were perpendicular to the direction of the traffic and extended from the edge of the 3-m-wide breakdown lane, across the breakdown lane, and across one 3.65-m-wide traffic lane. Before the sealer treatment the test sections were lightly grit blasted. The bridge decks are located near Blacksburg, Virginia. The Pepper's Ferry Bridge, a low-traffic-volume bridge, carries Virginia Route 114, a secondary route, over the New River and had an AADT in 1990 of 12,430. The other bridge, a high-traffic-volume bridge, carries Interstate 81 over Virginia Route 611. It had an AADT of 24,270 in 1990. Table 1 presents the sealer application rates along with the method of application for the horizontal laboratory test slabs, the vertical laboratory wall test sections, and the bridge deck test sections. All sealers were applied in accordance with the manufacturers' recommendations.

The environmental exposure conditions for the slabs, wall, and bridge decks were full direct sunlight and cyclic ponding with sodium chloride solution, partial direct sunlight and cyclic running sodium chloride solution, and full direct sunlight, deicer salt applications, and traffic wear, respectively. The slabs were ponded with 3 percent (by weight) sodium chloride solution continuously for 3 days; this was followed by 4 days of air drying. The average depth of the ponding solution was 8 mm, and the ponding dikes were covered with a white plexiglass sheet during ponding to prevent a greenhouse effect. For the wall test sections a 3 percent sodium chloride solution was pumped from a reservoir up to a distribution pipe that evenly distributed the solution to the test sections. The chloride solution flowed down over the wall, collected in the reservoir, and recirculated.

The wall wetting period was 8 hr for 3 consecutive days; this was followed by 4 days of drying. The flow rate across each test section was about 0.015 L/sec. The outdoor period of exposure to chloride for the slabs, wall, and bridge decks was 30 weeks, extending over a winter, spring, and summer.

PERFORMANCE MEASUREMENTS

To assess the service life performances of the sealers, chloride content, ultraviolet light exposure times, and traffic abrasion rates were measured. The chloride contents of the slabs were measured at three locations and depths (1.3, 2.5, and 3.8 cm) at the end of the 10, 20, and 30 weeks. Since there were three slabs for each treatment, a total of nine chloride contents were measured at each depth for each sealer. The chloride contents of each wall test section were measured at five locations at the same three depths used for the slab sections. The background chloride contents of the slab and wall concrete were determined and subtracted from the measured values to

TABLE 1 Sealer Treatments of Slabs, Wall, and Bridge Deck Test Sections

Slabs and Bridge Deck Test Sections	Treatment	Application Rate m^2/l	Application Method
Water-based epoxy	single	53	slabs - brush deck - roller
Solvent-based epoxy	first second	88 132	slabs & deck - brush
Silane	single	47	slabs & deck - low pressure sprayer
Siloxane	single	39	slabs & deck - flood & brush
Wall Test Sections			
Water-based epoxy	single	53	brush
Solvent-based epoxy	first second	88 132	brush
Silane	single	47	low pressure sprayer
Siloxane	single	53	low pressure sprayer

determine the ingress chloride contents. The chloride contents of the bridge deck test sections were not measured because they had been in service for some time before they were treated, and thus it was not possible to measure the chloride exclusion effectiveness of these sealed sections. The chloride contents were determined in accordance with the ASTM Standard Method [C-114, Section 19, Chloride (Reference Method)].

The number of hours of exposure to sunlight or ultraviolet light were recorded for the slabs and the wall sections. The sunlight exposure hours for the bridge deck would be about the same as those for the slabs because the slabs had the same horizontal orientation as the decks and the decks were within 10 km of the slab locations on the campus of Virginia Polytechnic Institute and State University.

The rate of traffic wear was measured by using a 3-m straightedge extending across the traffic lane, and the wear profile was determined by measuring the depth of wear at 15-cm intervals. The low-traffic deck had been in service for only 2 years, and thus the total wear was too small to be measured at the time that the measurements were taken with a ruler measuring to the nearest 0.01 mm, whereas the high-volume deck had been in service for 27 years and the wear rate was easily determined.

Table 2 presents the chloride contents, sunlight exposure hours, and deck traffic wear rate.

ANALYSIS AND DISCUSSION

As shown in Table 2 the wear rate of a bridge with an AADT of 24,270 is about 0.17 mm/year in the United States. Penetrating sealers have typical penetration depths of 1.5 to 3.0 mm. Thus, the maximum service life of a penetrating sealer on a high-traffic-volume bridge deck (AADT of 20,000 to 30,000) is about 9 to 10 years. On less traveled roadways the maximum service life due to the wear effect may be longer, because more heavily traveled routes may be shorter. Note that the penetration depth is the greatest depth of penetration. Thus, when the wear depth reaches the penetration depth much of the sealer, and therefore its effectiveness, will have been worn away. On the basis of wear a conservative maximum service life of penetrating sealers on bridge decks with AADTs of 20,000 to 30,000 is about 8 years. For components that are subjected to less abrasive forces such as columns, piers, pier caps, beams, and abutments, a maximum service life of 10 years is a reasonably conservative estimate.

For pore-blocking epoxy sealers the maximum service life on abrasion surfaces is 1 year. Visual observations revealed that these sealers wore off both the low- and high-traffic-volume decks in less than 1 year.

TABLE 2 Chloride Contents, Sunlight Exposure Hours, and Traffic Wear Rate for Sealer Performance Tests

Chloride Contents at Depths of 1.3 and 2.5 cm, kg/m^3							
Week	**10**		**20**		**30**		**Sunlight Exposure Hours**
Depth	**1.3**	**2.5**	**1.3**	**2.5**	**1.3**	**2.5**	
Slabs							
Control	1.1	0.1	2.2	0.1	4.1	0.6	950
Water-Epoxy	0.7	0.0	1.6	0.0	3.8	0.5	950
Solvent-Epoxy	1.0	0.1	2.1	0.1	4.1	0.6	950
Silane	0.0	0.0	0.0	0.0	0.1	0.0	950
Siloxane	0.0	0.0	0.0	0.0	0.0	0.0	950
Wall							
Control	1.9	0.2	3.4	0.1	4.5	0.7	190
Water-Epoxy	0.2	0.1	0.4	0.0	1.1	0.0	190
Solvent-Epoxy	0.2	0.0	0.6	0.1	1.6	0.2	190
Silane	0.1	0.0	0.1	0.0	0.2	0.0	190
Siloxane	0.0	0.0	0.1	0.0	0.4	0.0	190
Decks		**Sunlight Exposure Hours**			**Wear Rate mm/Year**		
Low-volume		950			---		
High-volume		950			0.17		

It is well known that ultraviolet light degrades epoxies. Because of the penetrating nature of the silane and siloxane, it is expected that sunlight degradation would be much less. As shown in Table 2 there is little to no difference in the amount of chloride contamination over 30 weeks between the silane- and siloxane-sealed slabs and wall sections that cannot be explained by the higher surface absorption of the wall. Note that if ultraviolet light did degrade these sealers, then the wall should contain less chloride than the slab, because the wall was exposed to only 20 percent of the sunlight to which the slabs were exposed and only one-third the total cumulative hours of exposure to chloride solution.

Relative to the amount of chloride ingress into the two surface types, the ingress of chlorides was much faster for the wall than the slabs (see control chloride contents Table 2). At 30 weeks both control test specimens contained the same amount of chloride when the wall chloride exposure time was one-third that of the slabs (Table 2). However, the rate (chlorides/exposure time) of chloride ingress into the wall and slabs are about the same for the epoxy sealers. Because of the poor sealing characteristics of epoxies, the maximum service life will be less than those for the silane and siloxane tested. The service lives of these epoxies on nonabrasion surfaces would then be based on a chloride leakage factor, as would those for the silane and siloxane tested.

Leakage factor is the amount of chloride that passes through a sealed concrete surface over a period of time. The period of time chosen for the laboratory testing period was 30 weeks. Thirty weeks was chosen because a long time period is needed for the rate of chloride ingress to reach a near steady-state diffusion rate. Also, the magnitude of the chloride content at the 2.5-cm depth must be sufficiently large as to not induce a significant error in the service life estimate through errors in measuring small chloride contents. The logic used to estimate the service lives of sealers is to multiply the laboratory service life determined from field site conditions by the allowable leakage factor to laboratory leakage factor ratio ($LR_{allowable}/LR$). The allowable leakage factor is determined from field site conditions (amount of chloride present, chloride diffusion rate, and cover depth of the reinforcing steel) and the selected corrosion protection period. The corrosion protection period (time to initiate corrosion) generally used in the United States is 50 years. Note that the service lives presented here include the effects of ultraviolet light and other weathering damage on chloride leakage through the sealed surfaces.

The diffusion of chloride ions through porous materials such as chloride is described by Fick's Second Law:

$$C_{(x,t)} = C_0(1 - erf(X/2)\sqrt{D_c t}) \tag{1}$$

where

- $C_{(x,t)}$ = chloride concentration at depth X after time t;
- C_0 = equilibrium chloride concentration; for the case of bridge components the equilibrium chloride concentration is 1.3 cm below the surface;
- erf = error function;
- D_c = chloride diffusion constant;
- t = time; here it was taken as the desired 50 years of protection from corrosion initiation; and
- X = depth at which the chloride content is calculated; depth X for estimating sealer service life is the depth of 2.5 percent of the reinforcing steel, which is dependent on the design cover depth and quality of construction; here, X is 4.1 cm, from an average depth of 5.1 cm with a standard deviation of 0.5 cm.

Note that the solution presented here is an approximate solution because the chloride concentration (C_0) is taken as an average chloride level. With a constant rate of chloride leakage the total allowable chloride concentration ($C_{0-\text{total}}$) is twice the value of C_0.

The five specific steps used in the procedure are as follows:

1. Estimate the average chloride concentration level ($C_{0-\text{ave}}$) that is allowed to build up over 50 years that will keep the chloride concentration at the select rebar depth (in this case 4.1 cm) below the corrosion threshold level of 0.71 kg/m^3 for the various field environmental effective chloride diffusion constants (D_c). The total allowable chloride ($C_{0-\text{total}}$) is (2.0) ($C_{0-\text{ave}}$).
2. Estimate the equivalent field time that corresponds to 30 weeks of ponding of untreated specimens by using the field environmental effective diffusion constants (D_c) and the 30-week C_{0-30} values. The resulting time equivalency is expressed at t_{eq}.
3. By using the time equivalent (t_{eq}) and the total allowable chloride content ($C_{0-\text{total}}$) determine the average 50-year allowable equivalent chloride content (C_{0-eq}).
4. Determine the laboratory leakage factor (in percent) and compare it with the allowable leakage factor (in percent). The laboratory percent leakage (LR) is the 1.3-cm-depth chloride content of the sealed surface divided by the 1.3-cm-depth chloride content of the unsealed (control) surface. The allowable percent leakage ($LR_{allowed}$) is C_{0-eq} divided by the field site chloride exposure concentration (C_0).
5. By using the ratio of the leakage factors ($LR_{allowed}$/LR) and the equivalent time (t_{eq}) determine the estimated service life (reapplication time) for the specific site conditions (t_{sl}).

The following example is presented to assist the reader in following the logic used to estimate the service lives of sealers in various bridge site environments. The bridge site chloride environmental exposure conditions in the United States have been categorized as low (C_0, 0 to 2.4 kg/m^3), moderate (C_0, 2.4 to 4.8 kg/m^3), high (C_0, 4.8 to 5.9 kg/m^3), and severe (C_0, 5.9 to 8.9 kg/m^3) with diffusion constants (D_c) of 0.32, 0.58, and 0.84 cm^2/year present in each of the four categories.

For an effective field D_c of 0.32 cm^2/year, a depth X of 4.1 cm below the surface, and the corrosion chloride initiation concentration of 0.71 kg/m^3, the $C_{0-\text{ave}}$ at 50 years is 1.51 kg/m^3. $C_{0-\text{total}}$ is then 3.02 kg/m^3.

$$C_{(x,t)} = C_{0-\text{ave}}[1 - erf(X/2\sqrt{D_c t})] \tag{2}$$

$$0.71 = C_{0-\text{ave}}[1 - erf(4.1/2\sqrt{(0.32)(50)})]$$

The equivalent field time t_{eq} calculated from the results of the 30-week laboratory test, which has chloride equilibrium concentration (C_{0-30}) at a 1.3-cm depth of 4.1 kg/m^3 and a chloride content ($C_{x,t}$) of 0.6 kg/m^3 at depth X of 2.5 cm with the effective field diffusion constant (D_c) of 0.32 cm^2/year, is 4.8 years.

$$C_{(x,t)} - C_{0-30}[1 - erf(X/2\sqrt{D_c t})] \tag{3}$$

$$0.6 = 4.1[1 - erf(2.54/2\sqrt{0.32 t_{aq}})]$$

TABLE 3 Bridge Component Exposure Matrix for Sealer Life Determination on Horizontal Specimens (in Years)

Environment	Co used (kg/m^3)	Diffusion Constant, D_c (cm^2/yr)		
		$D_c = 0.32$ $t_{eq} = 4.8$	$D_c = 0.58$ $t_{eq} = 2.6$	$D_c = 0.84$ $t_{eq} = 1.8$
Severe (range: 5.9-8.9)	8.9	SIL 6.3 SLX 10	SIL 1.5 SLX 10	SIL 0.7 SLX 10
High (range: 4.8-5.9)	5.9	SIL 9.6 SLX 10	SIL 2.3 SLX 10	SIL 1.0 SLX 10
Moderate (range: 2.4-4.8)	4.8	SIL 10 SLX 10	SIL 2.8 SLX 10	SIL 1.2 SLX 10
Low (range: 0-2.4)	2.4	SIL 10 SLX 10	SIL 5.7 SLX 10	SIL 2.4 SLX 10

NOTE: If the service life t_{sl} exceeded 10 years, then 10 years was recorded as the maximum service life. It is reasoned that the maximum service of all sealer is limited by weathering forces to 10 years. For bridge decks, service life is limited by traffic abrasion to 8 years.

TABLE 4 Bridge Component Exposure Matrix for Sealer Life Determination on Vertical Specimens (in Years)

Environment	Co used (kg/m^3)	Diffusion Constant, D_c (cm^2/yr)		
		$D_c = 0.32$ $t_{eq} = 5.0$	$D_c = 0.58$ $t_{eq} = 2.8$	$D_c = 0.84$ $t_{eq} = 1.9$
Severe (range: 5.9-8.9)	8.9	SIL 3.8 SLX 1.9	SIL 0.9 SLX 0.5	SIL 0.4 SLX 0.2
High (range: 4.8-5.9)	5.9	SIL 5.7 SLX 2.9	SIL 1.4 SLX 0.7	SIL 0.6 SLX 0.3
Moderate (range: 2.4-4.8)	4.8	WBE 1.3 SIL 7.1 SLX 3.5	SIL 1.7 SLX 0.9	SIL 0.7 SLX 0.4
Low (range: 0-2.4)	2.4	SBE 1.8 WBE 2.6 SIL 10 SLX 7.1	SBE 0.4 WBE 0.6 SIL 3.4 SLX 1.7	SIL 1.5 SLX 0.7

NOTE: If the service life t_{sl} exceeded 10 years, then 10 years was recorded as the maximum service life. It is reasoned that the maximum service of all sealer is limited by weathering forces to 10 years.

Continuing the example, $C_{o-total}$ for 50 years is 3.02 kg/m^3 and t_{eq} equals 4.8 years, then by straight-line interpolation the allowable equivalent equilibrium constant (C_{oeq}) is 0.29 kg/m^3.

$$C_{oeq} = C_{o-total}\,(t_{eq}/50) \tag{4}$$

$$C_{oeq} = (3.02)(4.8/50)$$

The allowable leakage factor ($LR_{allowable}$) is equal to allowable equivalent equilibrium constant (C_{oeq}) divided by the bridge field site environmental chloride equilibrium (C_o). For a moderate environment the worst-case condition (C_o = 4.8 kg/m^3) will be used. Thus , $LR_{allowable}$ is 6.0 percent.

$$LR_{allowable} = (C_{oeq}/C_o)\,100 \tag{5}$$

$$LR_{allowable} = (0.29/4.8)100$$

The laboratory LR from the 30-week test with sealed and untreated (control) chloride contents at a depth of 1.3 cm of 0.2 and 4.1 kg/m^3, respectively, is 4.9 percent.

$$LR = (C_{o-1s}/C_{o-1c})100 \tag{6}$$

$$LR = (0.2/4.1)100$$

The estimated service life (t_{sl}) for this sealer applied to the defined specific bridge conditions in a moderate environment with the specified effective diffusion constant is 5.9 years.

$$t_{sl} = (LR_{allowable}/LR)(t_{eq}) \qquad (7)$$

$$t_{sl} = (6.0/4.9)(4.8)$$

Tables 3 and 4 present the estimated service lives for horizontal and vertical bridge structure surfaces, respectively, for various field bridge site exposure conditions with an average cover depth of 5.1 cm and a standard deviation of 0.5 cm. To limit the percentage of reinforcing steel that would be above the corrosion threshold of 0.71 kg/m^3 to 2.5 percent, the depth X would be equal to 4.1 cm [5.1 − (1.96) (0.5)]. Thus, if the sealers presented in Tables 3 and 4 were applied to new horizontal and vertical surfaces and reapplied after each time period shown, in 50 years the chloride concentration at the depth of the shallowest 2.5 percent of the reinforcing steel will reach the corrosion threshold level.

In conclusion, the results of the study presented here provide a means of estimating the corrosion protection service lives of sealers based on the environmental exposure conditions of ultraviolet light damage, abrasion, and leakage of chloride through the sealed surface. Although the methodology was presented for bridge component exposures in the United States for new structures, the methodology is applicable to all reinforced concrete structure types in chloride-laden environments and existing chloride-contaminated structures. For chloride-contaminated structures the corrosion initiation concentration would have to be adjusted to account for the present chloride contamination level. Service life protection periods can also be determined for existing structures. The corrosion protection periods for existing structures will most likely be less than 50 years.

Publication of this paper sponsored by Committee on Corrosion.

Determination of End of Functional Service Life for Concrete Bridge Decks

MICHAEL G. FITCH, RICHARD E. WEYERS, AND STEVEN D. JOHNSON

The end of functional service life for concrete bridge decks was estimated by quantifying the terminal levels of physical damage that warrant deck overlay. The study focused specifically on decks in snowbelt states, which can suffer accelerated deterioration as a result of expansive reinforcing steel corrosion that is initiated by chloride deicing salts. The terminal damage levels were determined from an opinion survey of state department of transportation bridge engineers, who evaluated plan-view maps of existing decks showing areas affected by cracks, delaminations, spalls, asphalt patches, and concrete patches and recommended when each deck should have been or should be rehabilitated. Linear regression models were developed to relate the engineers' responses to the level of physical damage. The terminal damage levels determined from the recommended model define the end of functional service life as a range of percent damage in the worst traffic lane.

The transportation engineering community of the United States faces a tremendous problem: the gradual deterioration of the nation's bridges. Reinforced concrete bridge components that are exposed to chloride salt solutions, such as coastal seawater or water containing dissolved winter deicing salts, can suffer accelerated deterioration as a result of chloride-induced corrosion of the reinforcing steel. The progression of events resulting from the formation of expansive corrosion products (*1*) can include cracking, delamination, spalling, and patching of the surface concrete. Manning (*2*) stated in 1986 that "the unfunded liability to correct corrosion-induced distress in bridges is approximately $20 billion and the amount is increasing at almost $500 million annually."

Concrete bridge components that are commonly affected by corrosion-induced deterioration are decks, beams, piers, and abutments. In snowbelt states decks are generally more susceptible to corrosion-induced damage than are other bridge components, because winter deicing salts are applied directly to deck riding surfaces. A concrete bridge component reaches the end of its functional service life when the level of physical damage warrants not just repair but rehabilitation of the component. For example, a concrete bridge deck can be considered to have reached the end of its functional service life when the level of damage warrants overlay of the entire deck surface following the removal of unsound concrete and the patching of excavated areas. The level of physical damage that warrants rehabilitation can be called the terminal damage level.

This paper describes a research study that was conducted to determine the end of functional service life (EOFSL) for reinforced concrete bridge decks. The study focused specifically on bare concrete decks that deteriorate as a result of reinforcing steel corrosion that is initiated by chloride deicing salts (i.e., decks in snowbelt states). Consideration was given only to decks having an original bare concrete surface not overlaid with asphalt. The EOFSL was to be determined by quantifying the terminal damage level for decks as the percentage of the deck surface area affected by cracks, delaminations, spalls, and patches. It was expected that the terminal damage level would be a range of percent damage rather than a single percent damage value.

M. G. Fitch, CTL Engineering, Inc., 2860 Fisher Road, Columbus, Ohio 43204. R. E. Weyers, Department of Civil Engineering, Virginia Polytechnic Institute and State University, 200 Patton Hall, Blacksburg, Va. 24061. S. D. Johnson, School of Civil Engineering, Purdue University, 1284 Civil Engineering Building, West Lafayette, Ind. 47907.

SIGNIFICANCE OF EOFSL FOR DECKS

In 1984 Cady and Weyers (*3,4*) proposed a corrosion-deterioration model for concrete bridges (Figure 1). The model presents a qualitative relationship between the cumulative percentage of concrete surface area damaged and time and is believed to be applicable to any reinforced concrete bridge component exposed to chloride salt solutions. The model is defined by four critical points on the time axis:

1. Time at which chloride ion diffusion through the cover concrete begins.
2. Time at which corrosion of the reinforcing steel begins.
3. Time at which cracking of the concrete surrounding the reinforcing steel begins.
4. Time at which the bridge component reaches the end of functional service life because of an accumulation of physical damage.

Each of the four time points corresponds to a level of physical damage.

By 1990, the year that the present study was initiated, the diffusion, corrosion, and damage accumulation time periods of the model had been studied and estimated (*3,4*). However, the time point and damage level defining the end of functional service life had not been determined conclusively, and thus there was no consensus within the bridge engineering community regarding the level of physical damage that justifies rehabilitation. Since it is defined as the point at which rehabilitation is warranted, EOFSL is ultimately based on decisions that are made by bridge engineers who work for the various state departments of transportation (DOTs). Because bridge rehabilitation decisions are currently made by individuals or small groups within each state, the terminal damage level for bridge decks varies considerably from one locality to another. For example, the present study included examination of 18 existing bridge decks that had been designated for rehabilitation within the previous year (i.e., had been determined by local engineers to have reached the EOFSL). For these 18 decks from five different states, the terminal damage level was found to range from 1.0 to 29.8 percent of the deck surface area.

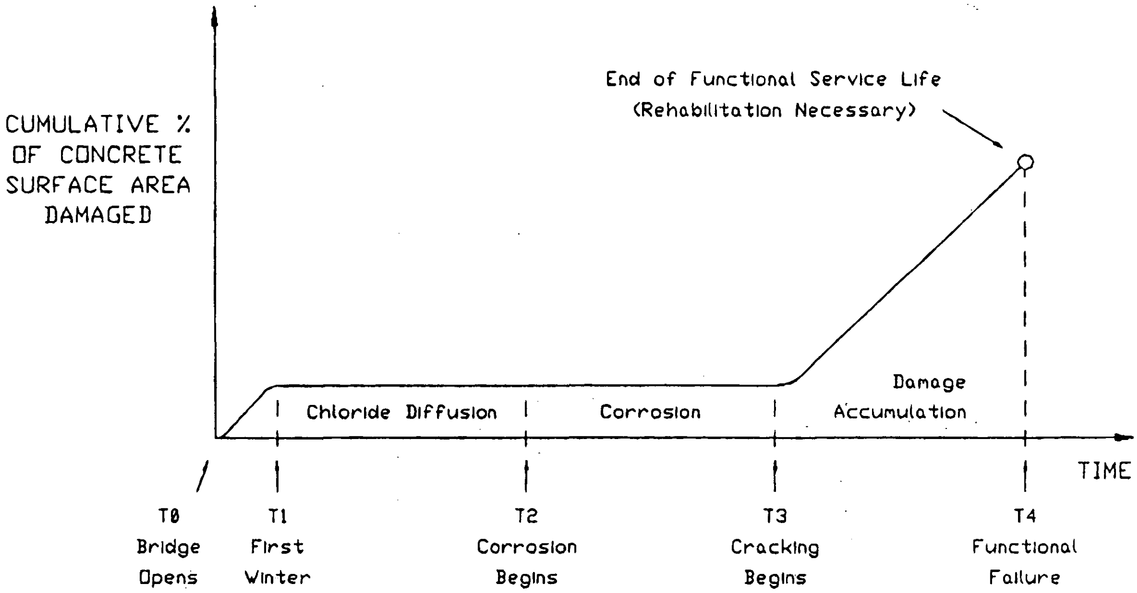

FIGURE 1 Corrosion-deterioration model for concrete bridges (*3,4*).

The lack of a quantitative definition of EOFSL is a problem for two reasons. First, it prevents any objective means of prioritizing bridge rehabilitation needs within each state and nationwide. Second, it hinders engineers' ability to evaluate bridge treatments based on life-cycle cost. The service life of a bridge component cannot be determined accurately unless the end of service life is clearly defined.

Several previous efforts to define bridge deck service life have been made. A draft report on Bridge Management Systems (*5*) summarizes five studies (*5–9*) that related bridge deck inspection condition ratings to deck age for large samples of existing bridge decks; however, no terminal damage levels were developed in those studies. In 1985 Chamberlin and colleagues (*10,11*) surveyed 30 bridge and materials engineers regarding maintenance treatments for decks. According to Weyers et al. (*11*) the survey responses "indicated that overlay of the entire surface is appropriate when spalling attains a level somewhere between 2.0 and 4.0 percent of the deck area"; however, this terminal damage level based on a single deterioration indicator (i.e., spalls) may have limited applicability, since additional deterioration indicators (i.e., cracks, delaminations, and patches) can be present on a deck. Mean age-at-overlay values that were estimated by Cady and Weyers for four sets of existing decks varied considerably, from 16 to 39 years. Mean damage-at-overlay values that were estimated by Cady and Weyers for two sets of existing decks varied considerably, from 22.0 to 38.1 percent. Although those studies provided preliminary data regarding deck service life, a need to further define the end of service life for concrete bridge decks was indicated.

RESEARCH APPROACH

In the present study terminal damage levels for concrete bridge decks were determined from an opinion survey of state DOT bridge engineers who make bridge rehabilitation decisions. A field study of 18 existing deteriorated concrete bridge decks that had been designated for rehabilitation within the past year was conducted to develop plan-view deck maps showing areas affected by cracks, delaminations, spalls, and patches. Survey kits based on the damage maps were distributed to bridge engineers in 25 states that use deicing salts. The engineers evaluated the damage maps and recommended when each deck should be or should have been rehabilitated. Based on the engineers' responses, linear regression models were developed to relate the recommended deck rehabilitation time point to the physical damage level. Ranges of percent damage were then determined from the models to define the terminal damage levels corresponding to the EOFSL for concrete bridge decks.

The 18 decks that were mapped for damage were selected from Michigan, Ohio, Pennsylvania, Virginia, and Wisconsin. To ensure that the resultant damage maps would represent a realistic sample of the deteriorated decks that exist in the United States, the decks were chosen to represent ranges of geographical location, snowfall exposure, and traffic volume (Figure 2). All 18 decks carried two lanes of traffic, were less than 91m (300 ft) long, and had total surface areas not greater than approximately 2,834m^2 (9300 ft^2).

Each deck was surveyed in two longitudinal halves by blocking one lane of traffic at a time. On each longitudinal deck half drag chains and hammers were used to locate delaminations of the surface concrete. Then, all cracks, delaminations, spalls, and patches were outlined on the deck surface with different colors of temporary water-based paint. The paint was applied with roller-type paint handles with 5-cm (2-in.) roller heads. Finally, photographs of the deck surface were taken at 6-m (20-ft) intervals along the length of the deck by using a 35-mm camera pointed toward the deck at a fixed oblique tilt angle (*12,13*) from a height of 4-m (12 ft). Later, the resultant oblique photographs were digitized to create computer coordinate files to represent the outlined areas of damage. The oblique damage area images were then rectified (FORTRAN rectification program by Steven D. Johnson; unpublished) to form plan-view damage area images, which were linked together by using ERDAS software and which were plotted by using a color ink-jet printer to produce a composite plan-view map of the deck showing the areas of damage.

Snowfall (In./Yr.)	0 - 8000	> 8000 - 16000	> 16000
> 50	PA-1 MI-3	OH-5 OH-6	OH-4
> 20 - 50	PA-2 WI-2 MI-2 WI-3 WI-1 WI-4	MI-1 OH-3	
0 - 20	VA-3	VA-1 OH-1 VA-2 OH-2	
	Average Annual Daily Traffic (Vehicles/Day)		

FIGURE 2 Field study matrix for 18 concrete bridges mapped for damage (*11*).

The plotted damage maps showed cracks, delaminations, spalls, asphalt patches, and concrete patches in different colors. The map colors were carefully selected to be distinguishable by brightness, to not confuse survey respondents with color-defective vision, and to minimize the use of certain overpowering colors that might bias the respondents' evaluations of the damage areas (*14,15*).

OPINION SURVEY OF BRIDGE ENGINEERS

A survey kit was developed on the basis of the deck damage maps. The purpose of the survey kit was to present the damage maps to bridge engineers so that the engineers could evaluate the maps and make responses that could be used to develop terminal damage levels for concrete bridge decks. Each kit contained three damage maps to be evaluated by the respondent.

Concept of Time to Rehabilitate

Since the Cady-Weyers deterioration model is based on physical damage as a function of time, the survey kit items were written such that the engineers' responses were based on a time continuum. For each deck damage map that they evaluated the respondents were asked to recommend the time to rehabilitate (TTR), which was defined in the survey kit as follows:

> Assume that every concrete bridge component exposed to deicing salts eventually deteriorates to a physical condition that justifies rehabilitation. Define this physical condition as the *rehabilitation condition*. The true rehabilitation condition is reached when the component has reached the end of its functional service life, and *significant correction* is necessary to return it to an acceptable level of service. The *time to rehabilitate* is the time when a concrete bridge component reaches its rehabilitation condition. It may be in the past, present, or future. For example, the time to rehabilitate was in the past if the component should have been rehabilitated about 5 years ago. The time to rehabilitate is in the present if the component should be rehabilitated now. The time to rehabilitate is in the future if the component should be rehabilitated in about 5 years. The rehabilitation condition (a measure of physical damage) is a point on the y-axis of the Cady-Weyers model, whereas the time to rehabilitate is a point on the x-axis.

The engineers were asked to recommend the TTR by choosing a response from a time scale; for example, two of the possible choices from this scale were the following: "this component should be rehabilitated in about 10 years" and "this component should have been rehabilitated about 10 years ago." The time scale ranged from 20 years before the rehabilitation condition to 20 years beyond the rehabilitation condition, in increments of 2 years.

The engineers were given the age of each deck that they evaluated so that they could estimate the rate of physical deterioration to assist in estimating the TTR. The traffic volume (expressed as the average annual daily traffic (AADT)) and the typical speed of traffic (expressed as greater than 72 kph (45 mph) or less than 72 kph (45 mph)) were also provided so that the respondents could estimate a deck usage factor.

Concepts of Local Standards and Snowbelt Standards

It was reasoned that since the rehabilitation condition is a subjective estimate it may vary considerably from one engineering district to another. Thus, it was considered unlikely that the engineers' TTR responses using local standards would form a strong consensus about the rehabilitation condition. Accordingly, the engineers were asked to estimate the rehabilitation condition using two hypothetical sets of criteria: local standards and snowbelt standards. The difference between local standards and snowbelt standards could be described as the difference between current practices and recommended practices, respectively.

Opinion Survey Results

A total of 90 survey kits were sent to bridge engineers in the following 25 states identified as using deicing salts (*11,16*):

Connecticut	Massachusetts	Ohio
Delaware	Michigan	Pennsylvania
Illinois	Minnesota	Rhode Island
Indiana	Missouri	Tennessee
Iowa	Nebraska	Vermont
Kansas	New Hampshire	Virginia
Kentucky	New Jersey	West Virginia
Maine	New York	Wisconsin
Maryland		

Sixty qualified respondents returned survey kits with responses, representing a 67 percent response rate. At least one survey kit with responses was received from every targeted state except Delaware and Massachusetts.

Four of the 60 qualified respondents were found to have made outlier TTR responses. Outlier responses were identified by internal inconsistencies within an engineer's responses and included mistakes such as recommending the time to repair for a deck rather than the time to rehabilitate. In total 6 of 162 deck TTR responses (3.7 percent) were discarded as outliers.

Linear regression techniques and Minitab statistical software were used to develop regression model equations relating the engineers' TTR responses to the level of damage on the deck. The regression equations were developed by using a data-splitting approach (*17*) for cross-validation purposes (*18*), in which half of the engineers' responses were used to develop the equation and the other half were used to cross-validate it. Twenty variables were identified as potential predictors of the engineers' TTR responses, including the following:

- Surface area of deck [m^2 (ft^2)];
- Percentage of whole deck spalled;
- Percentage of whole deck delaminated;
- Percentage of whole deck patched with asphalt;
- Percentage of whole deck patched with concrete;
- Lineal feet of cracks/surface area of deck [m/m^2 (ft/ft^2)];
- Age of deck;
- AADT;
- Typical speed of traffic on deck;
- Percentage of whole deck delaminated, spalled, patched with asphalt, and patched with concrete;
- Percentage of worst traffic lane delaminated, spalled, patched with asphalt, and patched with concrete; and
- Percentage of both traffic lanes delaminated, spalled, patched with asphalt, and patched with concrete.

The Minitab command BREGRESS was used in the evaluation of the variables and selection of the optimum models.

Local Standards TTR Model

The best model developed from the engineers' TTR responses based on local standards was as follows:

$$\hat{y} = -10.3 + 14.0x - 11.4\, x^{1.05} \quad (1)$$

where $\hat{y}$ is equal to the fitted time to rehabilitate for decks, based on local standards, and x is the percentage of the whole deck delaminated, spalled, and patched with asphalt. Minitab computed the following statistics that describe the model:

Predictor	*Coefficient*	*Standard Deviation*	*t-ratio*	*p*
Constant	−10.303	1.939	−5.31	0.000
x	14.014	5.795	2.42	0.017
$x^{1.05}$	−11.438	4.979	−2.30	0.023

$s = 6.906$ $R^2 = 22.0\%$ $R^2(\text{adj}) = 21.0\%$
Regression: F computed $= 21.59$, $p = .000$

The p-values are close to zero, which means the probability that the linear relationship indicated by the sample of TTR responses does not actually exist for the population of all TTR responses is sufficiently low. The cross-validation percentage for the model was determined to be 97.4 percent, indicating that the model works well for other data samples within the population of TTR responses.

The deficiency of the model is the low value of the coefficient of multiple determination, R^2, which indicates that the regression equation explains only 22.0 percent of the variability in the engineers' TTR responses. Since R^2 is low there is too much unexplained variability to conclude that the model equation is a good predictor of future individual TTR responses. However, since the model cross-validates well, 95 percent confidence intervals based on the model equation can be used to predict future mean TTR responses with 95 percent certainty (*19*).

The model equation line and 95 percent confidence interval (CI) lines are presented in Figure 3, which shows that the confidence interval lines intersect the horizontal line of TTR equal to zero at x values of 5.8 percent and 10.0 percent. For deck damage values of 5.8 percent or less there is at least 95 percent certainty that the mean TTR response will not be a TTR equal to zero. Similarly, for deck damage values of 10.0 percent or greater there is at least 95 percent certainty that the mean TTR response will not be a TTR equal to

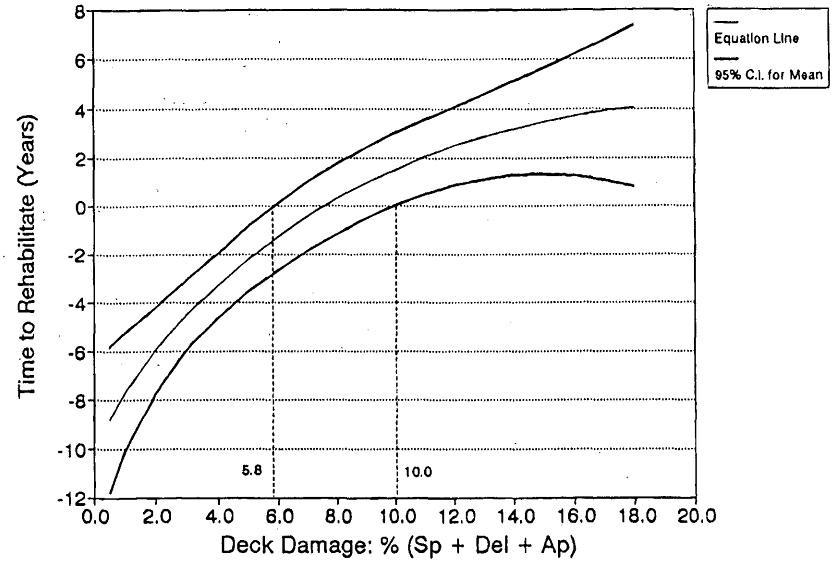

FIGURE 3 Local standards TTR model for concrete bridge decks.

zero. A mean recommendation by bridge engineers to rehabilitate the deck now is probable only for deck damage values between 5.8 and 10.0 percent. Thus, the indicated local standards terminal damage level for decks is 5.8 percent $< x <$ 10.0 percent.

Snowbelt Standards TTR Model

The best model developed from the engineers' TTR responses based on snowbelt standards was as follows:

$$\hat{y} = -11.2 + 5.34\,x - 3.41\,x^{1.1} \qquad (2)$$

where $\hat{y}$ is equal to the fitted time to rehabilitate for decks, based on snowbelt standards, and x is equal to the percentage of worst traffic lane delaminated, spalled, and patched with asphalt. Minitab computed the following statistics that describe the model:

Predictor	*Coefficient*	*Standard Deviation*	*t-ratio*	*p*
Constant	−11.229	1.586	−7.08	0.000
x	5.345	1.318	4.06	0.000
$x^{1.1}$	−3.4073	0.9123	−3.73	0.000

$s = 6.021$ $R^2 = 31.7\%$ $R^2\,(\text{adj}) = 30.9\%$
Regression: F computed $= 35.59$, $p = .000$

The p-values and cross-validation percentage (94.6 percent) for the model were considered to be acceptable. Figure 4 presents the model equation line and 95 percent confidence interval lines. The confidence interval lines intersect the horizontal line of TTR equal

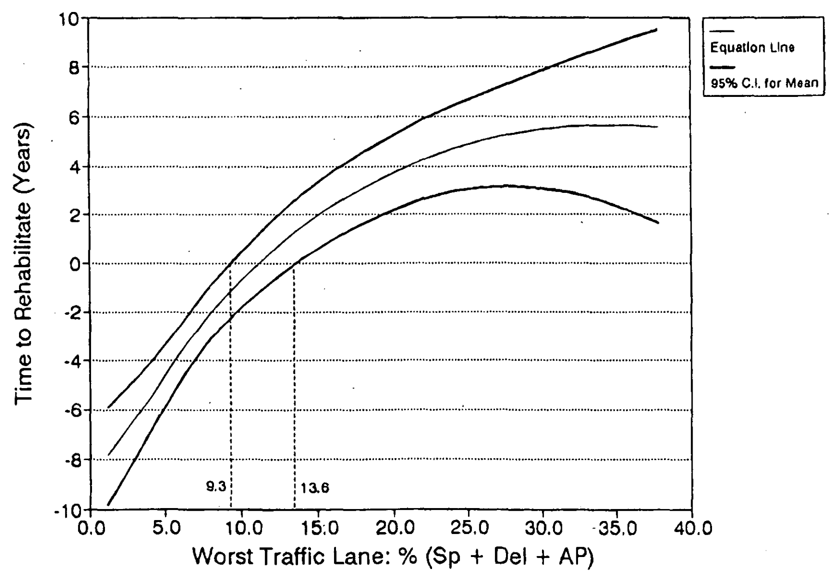

FIGURE 4 Snowbelt standards TTR model for concrete bridge decks.

to zero at x-values of 9.3 and 13.6 percent; thus, the indicated snowbelt standards terminal damage level for decks is 9.3 percent $< x < 13.6$ percent.

Comparison of TTR Models

For the snowbelt standards TTR model the independent variable is the percentage of the worst traffic lane area that is delaminated, spalled, and patched with asphalt. For the local standards TTR model the independent variable is the percentage of the whole deck area that is delaminated, spalled, and patched with asphalt. Essentially, the snowbelt standards TTR model shows a lower level of data variability and a more specific independent variable than the local standards TTR model.

Despite this difference the independent variables for both models are based on the same aggregate of damage, namely, delaminations, spalls, and asphalt patches. It is realistic for these models to indicate that cracks and concrete patches, which are generally less likely to affect the present or future riding quality of a deck than are delaminations, spalls, and asphalt patches, do not have a quantifiable impact on deck rehabilitation decisions relative to the other deterioration indicators.

Limitations of TTR Models

Both models are based on engineers' evaluations of damage maps for bridge decks that carry two lanes of traffic and that have surface areas not greater than approximately 2,835 m^2 (9,300 ft^2). The deck models may be less applicable to decks having other than two lanes of traffic or having surface areas greater than approximately 2,835 m^2 (9,300 ft^2). Rehabilitation of single-lane decks may require bridge closure and traffic detours, whereas rehabilitation of decks with more than two lanes may require additional lane changes. The rehabilitation labor and materials costs are likely to be greater for decks with surface areas exceeding the surface areas of the decks in the present study. Thus, for decks outside the scope of the study potentially greater rehabilitation costs may correspond to elevated terminal damage levels.

Findings from Other Survey Kit Items

The survey kits contained several items in addition to those that asked the respondent to recommend the time to rehabilitate for bridge decks. The findings from these other survey kit items are summarized as follows.

1. A majority of bridge engineers indicated that their ratings of the overall physical condition of a deteriorated concrete bridge deck are influenced more by the physical condition of traffic-lane areas than by the physical condition of shoulder areas.
2. The five deck rehabilitation decision factors most frequently selected by bridge engineers as being influential are as follows, listed in the order of selection frequency:

- Amount of physical deterioration,
- Availability of funds/labor,
- Condition of the superstructure,
- Volume of traffic (AADT), and
- Rate of physical deterioration.

3. A majority of bridge engineers indicated that their ratings of the overall physical condition of a concrete bridge are influenced more by the physical condition of the superstructure than by the physical condition of either the deck or the substructure.
4. A majority of bridge engineers indicated that their decisions to repair or rehabilitate concrete bridge substructure components are often significantly affected by whether a decision has been made to repair or rehabilitate the deck. Thus, it may be impractical to quantify terminal damage levels to define the end of functional service life for concrete bridge substructure components.

CONCLUSIONS

Because the survey respondents evaluated damage maps representing particular types of bridge decks, these conclusions are applicable only to two-lane bridge decks with surface areas not greater than approximately 2,835 m^2 (9,300 ft^2).

1. Based on snowbelt standards (i.e., recommended practices) it is likely that the end of functional service life for concrete bridge decks is reached when the percentage of the worst traffic lane surface area that is delaminated, spalled, and patched with asphalt ranges from 9.3 to 13.6 percent.
2. Based on local standards (i.e., current practices) it is likely that the end of functional service life for concrete bridge decks is reached when the percentage of the whole deck surface area that is delaminated, spalled, and patched with asphalt ranges from 5.8 to 10.0 percent.

It is the researchers' opinion that the snowbelt standards TTR model is more useful than the local standards TTR model, because it describes recommended practices rather than the highly variable current practices. The snowbelt standards TTR model is also considered to be more valid statistically, because the R^2 values indicate a greater consensus among the respondents for this model than for the local standards TTR model. In addition, the independent variable for the snowbelt standards TTR model, which is based on the damage level in the worst traffic lane, is consistent with the responses from the majority of bridge engineers who indicated that their ratings of the overall physical condition of a deteriorated concrete bridge deck are influenced more by the physical condition of the traffic-lane areas than by the physical condition of the shoulder areas.

Either model can be used as a tool for prioritizing bridge deck rehabilitation needs. For example, by using the snowbelt standards TTR model as shown in Figure 4, the recommended TTR ranges for decks at various damage levels in the worst traffic lane can be determined graphically from the upper and lower boundaries of the 95 percent confidence interval:

Damage Level (%) in Worst Lane	*Recommended TTR*
2.5	5.2 to 8.4 years from now
7.3	1.5 to 3.7 years from now
12.8	2.4 years ago to 0.4 years from now
17.4	4.4 to 1.5 years ago

Unlike the end of structural service life, which often can be objectively defined on the basis of a readily observable failure, the EDFSL is ultimately a matter of opinion. The findings from the present study indicate that the decision to rehabilitate a bridge deck may be based in part on factors other than the extent of physical deterioration, such as the availability of funds or labor, the condition of the superstructure, the volume of traffic (AADT), or the rate of physical deterioration. Nonetheless, the terminal damage levels that were determined in the study represent a general estimate of EDFSL for concrete bridge decks and may provide a basis for discussion within the bridge engineering community to further define EDFSL.

ACKNOWLEDGMENTS

The research described herein was supported by the Strategic Highway Research Program (SHRP). SHRP is a unit of the National Research Council that was authorized by section 128 of the Surface Transportation and Uniform Relocation Assistance Act of 1987. The authors are grateful to the SHRP coordinators and maintenance and materials engineers at the state and provincial transportation departments who graciously assisted us by providing service life performance information and traffic control during our field surveys of bridges. In particular, we wish to acknowledge the help of DOT personnel in the states of Michigan, Ohio, Pennsylvania, Virginia, and Wisconsin.

REFERENCES

1. Mehta, P. K. *Concrete: Structure, Properties, and Materials.* Prentice-Hall, Englewood Cliffs, N. J., 1986.
2. Manning, D. G. Technical Research Area 4: Detailed Planning for Research on Bridge Component Protection. *Strategic Highway Research Program Research Plans: Final Report.* TRB, National Research Council, Washington, D.C., May 1986, pp. 4-1-4-60.
3. Cady, P. D., and R. E. Weyers. Deterioration Rates of Concrete Bridge Decks. *Journal of Transportation Engineering,* Vol. 110, No. 1, Jan. 1984, pp. 34–44.
4. Cady, P. D., and R. E. Weyers. Predicting Service Life of Concrete Bridge Decks Subject to Reinforcement Corrosion. In *Corrosion Forms and Control for Infrastructure, ASTM STP 1137* (V. Chaker, ed.), ASTM, Philadelphia, 1992, pp. 328–338.
5. *Bridge Management Systems.* Draft. FHWA, U.S. Department of Transportation, 1987.
6. Hymon, W., D. Hughes, and T. Dobson. *The Least Cost Mix of Bridge Replacement and Repair Work on Wisconsin's State Highways Over Time—A Computer Simulation.* Draft technical report. Wisconsin Department of Transportation, Madison, April 1983.
7. Busa, G., M. Ben-Akiva, and O. Buyukozturk. *Modelling Concrete Deck Deterioration.* Department of Civil Engineering, Massachusetts Institute of Technology, Cambridge, Sept. 1985.
8. Busa, G., M. Cassella, W. Gazda, and R. Horn. *A National Bridge Deterioration Model.* Transportation Systems Center (SS-42-U5-26), U.S. Department of Transportation, Cambridge, Mass., Sept. 1985.
9. Fitzpatrick, M., D. Law, and W. Dixon. Deterioration of New York State Highway Structures. In *Transportation Research Record 800,* TRB, National Research Council, Washington, D.C., 1981, pp. 1–8.
10. Chamberlin, W. P. *Long-Term Evaluation of Unprotected Concrete Bridge Decks.* Research Report 128. Engineering Research and Development Bureau, New York State Department of Transportation, Nov. 1985.
11. Weyers, R. E., W. P. Chamberlin, P. Hoffman, and P. D. Cady. *SHRP C-103 Task 1 Interim Report.* Strategic Highway Research Program Contract SHRP-87-C-103. Concrete Bridge Protection and Rehabilitation: Chemical and Physical Techniques. The Charles E. Via, Jr., Department of Civil Engineering, Virginia Polytechnic Institute and State University, Blacksburg, Jan. 31, 1991.
12. Johnson, S. D. *Civil Engineering A359: Photogrammetry.* Department of Civil and Environmental Engineering, University of Wisconsin-Madison, 1976.
13. Wolf, P. R. *Elements of Photogrammetry,* 2nd ed. McGraw-Hill Book Company, Inc., New York, 1983.
14. Nickerson, D. Color. In *Encyclopedia Americana,* Vol. 7. Grolier, Inc., USA, 1991 ed., pp. 307–315.
15. Glass, R. A., G. L. Howett, K. Lister, and B. L. Collins. *Some Criteria for Colors and Signs in Workplaces.* NBSIR 83-2694. National Bureau of Standards, U.S. Department of Commerce, Washington, D.C., April 1993.
16. *Survey of Salt, Calcium Chloride and Abrasive Use in the United States and Canada for 1981–1982 and 1982–1983.* Salt Institute, Alexandria, Va. 1983.
17. Ott, L. *An Introduction to Statistical Methods and Data Analysis,* 3rd ed. PWS-Kent Publishing, Boston, 1988.
18. Walpole, R. E., and R. H. Myers. *Probability and Statistics for Engineers and Scientists,* 4th ed. Macmillan Publishing Co., New York, 1989.
19. Ryan, B. S., B. L. Joiner, and T. A. Ryan. *MINITAB Handbook,* 2nd ed. PWS-Kent Publishing Co., Boston, 1985.

Publication of this paper sponsored by Committee on Corrosion.

Service Life Evaluation of Concrete Surface Coatings

JERZY ŻEMAJTIS AND RICHARD E. WEYERS

The use of surface coatings for concrete bridge substructures is one of the methods used as corrosion protection. The results of a 1-year laboratory study on three generic coatings, epoxy, urethane, and methyl methacrylate (MMA), are presented. Specimens were built to simulate four exposure conditions typical for concrete bridges located in the coastal region or inland where deicing salts are used. The exposure conditions were horizontal surface, vertical surface, tidal zone, and immersion zone. The service life of each coating was estimated on the basis of chloride ion diffusion through the coating and concrete. The diffusion equation for the condition that the surface chloride concentration changes as a function of the square root of time was used to estimate the service lives of the coatings for various component exposure conditions and the range of environmental exposure conditions in the United States.

The number of bridges in the United States was estimated to be 578,218 in the late 1980s (*1*). According to the U.S. Department of Transportation about 40 percent of these bridges were either structurally deficient or functionally obsolete (*2*).

A major cause of the deterioration of concrete bridge structures is associated with corrosion of the reinforcing steel. During the 1960s most states introduced a "bare road policy," which resulted in a significant increase in deicer salt applications (*3*). Because of the salting as well as the exposure to the salt water in the coastal regions, a large number of concrete bridges are contaminated with chlorides, which initiate the corrosion of the reinforcing steel. The resulting presence of chlorides and the loss of the alkaline environment cause the embedded steel to loose its surface passivity. Corrosion follows as water and oxygen become available to the steel. Accumulated corrosion products, which occupy more volume than the reactants, cause cracking of the protective concrete cover. This allows for the intrusion of chlorides and oxygen at a much faster rate, thus accelerating the corrosion process. Deterioration caused by the corrosion of reinforcing steel is not limited to bridge decks only. It can also affect other bridge members such as piles, walls, diaphragms, girders, abutments, piers, and pier caps (*4*).

Application of coatings on surfaces of concrete elements is one of the methods used to delay the deterioration process. The term *coating* refers to such surface treatment that forms a film on the surface of concrete and that penetrates the concrete little or not at all (*5*). Coatings' surface thicknesses range from 25 μm to 1 mm (*6*). Although there are only several generic groups of coatings (epoxies, polyurethanes, acrylics, polyesters, etc.), the performances of two coatings from the same generic group may be very different; thus, the maintenance engineer needs to know how to evaluate the performances of particular products. Since coatings form a layer on the surface their application is limited to substructure components and other elements that are not exposed to traffic wear. Their performance will be influenced by geographical location (coastal region, inland), average annual daily traffic (splash zone), average annual snowfall (deicing salts), and surface preparation of the concrete before coating application.

This paper presents the results of a 1-year study of three generic coatings: epoxy, methyl methacrylate (MMA), and polyurethane (urethane). The methodology used for service life (reapplication period) determination is also presented.

The Charles E. Via Department of Civil Engineering, 200 Patton Hall, Virginia Polytechnic Institute and State University, Blacksburg, Va. 24061-0105.

EXPERIMENTAL DESIGN

For the present study three generic types of coatings were selected: epoxies, MMAs, and urethanes. The coatings were selected primarily on the basis of the coating's history (use of the product on concrete bridge substructures in the past), cost of materials (up to $11.0/m^2), and film thickness (from 375 μm to 1 mm). The selected coatings are presented in Table 1.

Two specimens were used to assess the performance of the coatings. Each specimen (Figure 1) was covered with two coatings (or one coating and a control that was not coated). Specimen dimensions were 107 by 107 cm for the slab and 107 by 91 cm for each of the walls. The thicknesses for both walls and the slab were 10 cm. Cover depth over temperature/shrinkage reinforcement was designed to be 4.6 cm.

The concrete mixture used for the two specimens had the following properties: coarse aggregate, no. 7 (maximum aggregate size, 19 mm); water-cement ratio, 0.45; slump, 9 cm, and air content, 6 percent. Each sample was reinforced against concrete shrinkage with a mesh of 10-mm bars. The 28-day compressive strength was 40 MPa.

Since surface preparation is very important special care was taken during construction of the specimens. The specimens were wet cured for 1 week; this was followed by air dry curing for 3 weeks. Surfaces were sand-blasted because of contamination with form release agent and laitance. Small voids that appeared on the surfaces were then filled with mortar.

All coatings were applied by brushing and according to the manufacturers' specifications. Urethane was applied as one coat, with the dry thickness being approximately 625 μm. Epoxy coating was applied in two, 200-μm-thick coats. The MMA coating system consisted of three layers: the primer (penetrating sealer) and two topcoats (each approximately 200 μm thick). The two specimens were then exposed to accelerated wet and dry cycles (ponding) with a 3 percent solution of sodium chloride. The specimens were designed

TABLE 1 Characteristics of Coatings

Coating type	Number of Coats:	Cost [$/m²]	Coverage [m²/l]
Epoxy	two coats	3.77	6.1-7.4/coat
MMA	primer (penetrating sealer) two topcoats	9.04	2.5 4.9-6.1/coat
Urethane	one base coat	10.76	1.5-1.6

to represent four exposure conditions, as will be described. Since coatings are used only on bridge substructures the simulation of surface wear, typical for bridge decks, was not necessary. Also, ultraviolet light reaches bridge substructure elements in an amount much lower than that for superstructure elements (bridge decks). Thus, the specimens were housed inside the laboratory, where ultraviolet light exposure was a minimum.

The horizontal section of the specimens (horizontal) simulated wetted surfaces such as the top surface of pier caps, diaphragms, and abutments. For this exposure condition an area of 0.57 m^2 (107 by 53 cm) was covered with each coating. The upper 53 cm of the specimens' legs (wall or vertical surface) simulated the vertical surfaces of abutments, pier caps, and piers. Each coating covered an area of 0.49 m^2 (53 by 91 cm). These two wall sections were exposed to 3 percent sodium chloride solution for 3 days and were allowed to air dry for 4 days during each 1-week ponding cycle. A vertical area between the 28th and the 38th cm from the bottom of specimens on the inner side of the specimens' legs (tide or tidal zone) simulated the tidal zones of concrete bridge substructures in coastal regions, with each tidal zone coating covering an area of 0.09 m^2. These sections of specimens were exposed to immersion in 3 percent sodium chloride solution for 4 days and were then allowed to air dry for 3 days during each 1-week ponding cycle. The very bottom section of the vertical sections (immersed zone) simulated concrete bridge substructures, piles, or piers in a coastal region immersed in seawater. Each immersion zone coating covered an area of 0.26 m^2, from the bottom of the specimen's legs to a height of 28 cm. During the 1-week ponding cycle these areas were immersed in 3 percent sodium chloride solution for the entire period. The four exposure conditions are presented in Figure 2.

DATA ANALYSIS

A coating's effectiveness was evaluated on the basis of chloride permeation through the concrete (and coatings). The chloride concentration was determined in accordance with the ASTM Standard Method [C-114, Section 19, Chloride (Reference Method)]. Measurements of chloride concentration were attained by collecting samples of pulverized concrete at three depths: 1.3, 2.5 and 3.8 cm. For each coating (and control) and for each exposure condition a set of three samples was taken at three locations. Each sample set consisted of samples from three depths, for a total of nine samples for each exposure condition at selected exposure times. Ten samples were taken to determine the background chloride concentration. Other samples for chloride content determination were collected after 7, 14, 21, 30, and 52 1-week ponding cycles. Each of these measurements included three samples for each coating (and control) at three depths for each exposure condition. The numbers of samples collected during the study are presented in Table 2.

The average background chloride content was 0.26 kg/m^3 of concrete. The average chloride concentration gain at a 1.3-cm depth for the control section varied from 5.69 kg/m^3 for the immersed zone exposure condition to 12.2 kg/m^3 for the wall exposure condition. The highest chloride concentration for coated surfaces was found

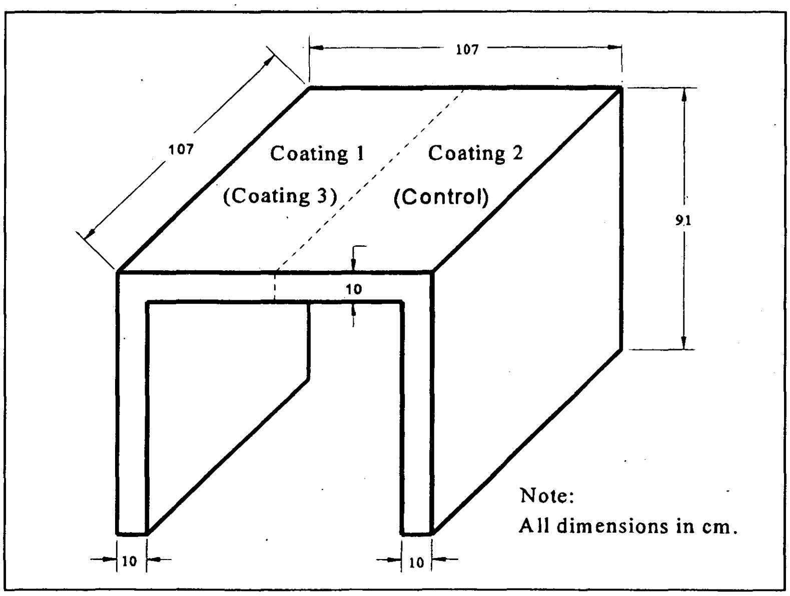

FIGURE 1 Typical specimen.

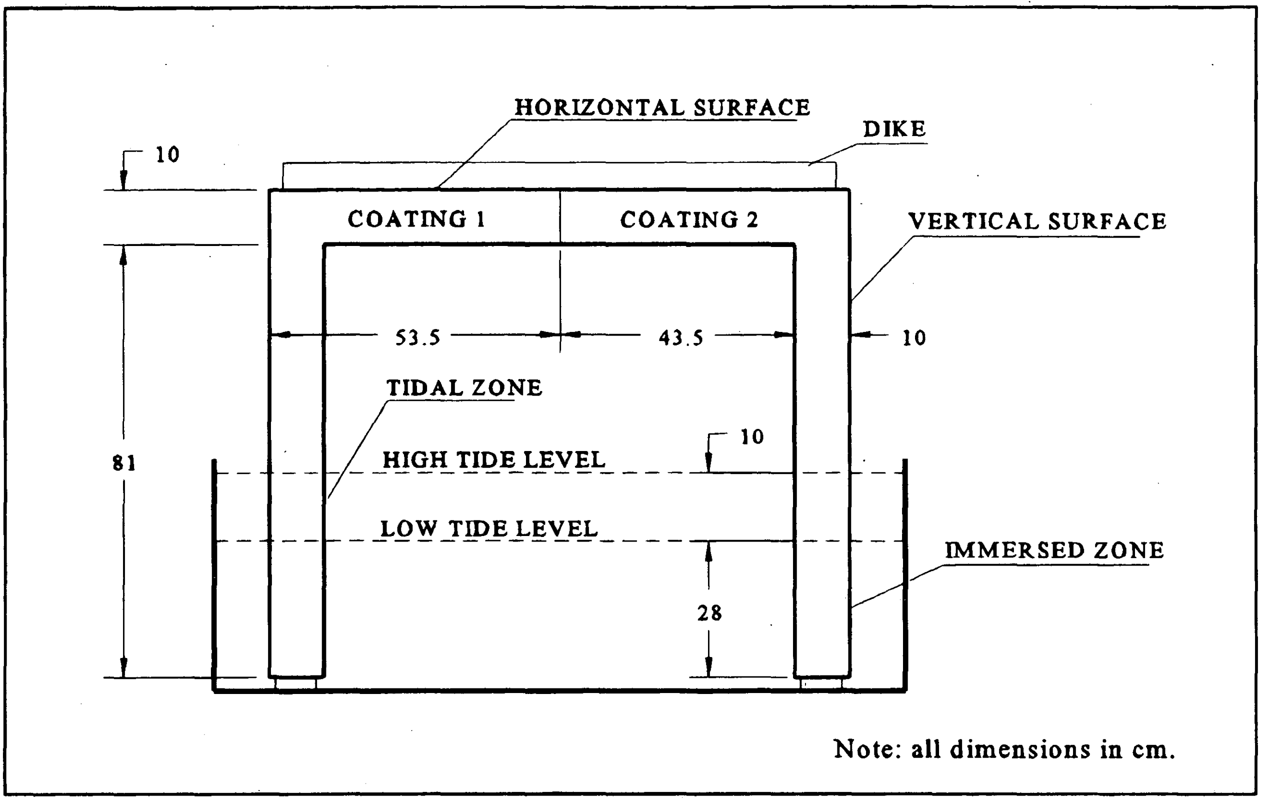

FIGURE 2 Exposure conditions.

with the epoxy coating in the tidal zone exposure condition (5.33 kg/m^3). All results of the chloride content measurements for horizontal surface, vertical surface, tidal zone, and immersion zone conditions for the three tested coatings and the control are presented in Tables 3 to 5. The average gains in acid-soluble chloride concentrations above the background value over time for each coating and control at a 1.3-cm depth are given in Figures 3 to 6.

Visual observations for discoloring, blistering, and peeling were made each week. Peeling was observed on the specimen half covered with the MMA coating after every sampling session. The peeling was caused by the impact from the drill during the collection of powdered chloride content samples. Some blisters were observed on the urethane coating after only a couple of days following the coating application. It is believed that the blistering was caused by entrapped air during coating application (the coating was applied as one thick coat in a very short time). After 1 year of testing the specimens were removed from the laboratory and were stored outdoors. After several freezing-thawing cycles (during the winter of 1994) the MMA coating had almost completely peeled off. The epoxy and urethane coatings remained intact during this outdoor exposure period.

TABLE 2 Number of Samples

Number of One-Week Ponding Cycles	Number of Samples
0 (background)	10
7	108
14	144
21	144
30	144
52	144
Total	694

ANALYSIS AND DISCUSSION OF RESULTS

A regression analysis for the gain in chloride concentration for the 1.3-cm depth was performed and was found to be a function of the square root of time. Coefficients (k) that represent the chloride ingress rate through the coated surfaces are presented in Table 6. The solution for the semi-infinite medium whose surface concentration varies with the function of time (square root) is obtained by the Laplace transform of the diffusion equation (*7*). The solution equation is as follows:

$$C_{(x,t)} = k\sqrt{t}\left[e^{-x^2/4D_c t} - \frac{x\sqrt{\pi}}{2\sqrt{D_c t}}\left(1-erf\frac{x}{2\sqrt{D_c t}}\right)\right] \quad (1)$$

where

C = chloride concentration,
D_c = diffusion constant,
t = time,
x = depth, and
k = coating characteristics constant.

TABLE 3 Chloride Content Measurements at 1.3-cm Depth

Depth = 1.3 cm		Average Gain in Chloride Concentration [kg/m³]					
		Number of One-Week Exposure Cycles					
Exposure	**Coating**	**0**	**7**	**14**	**21**	**30**	**52**
Immersed	Control	0.00	4.01	6.62	5.42	6.09	5.69
	Epoxy	0.00	1.34	1.75	1.78	0.88	1.39
	MMA	0.00	0.43	0.53	0.89	0.58	0.75
	Urethane	0.00	0.00	0.18	0.16	0.25	0.27
Tide	Control	0.00		6.05	8.52	9.10	9.83
	Epoxy	0.00		3.56	3.79	3.86	5.33
	MMA	0.00		0.33	0.45	0.37	1.03
	Urethane	0.00		1.58	2.12	1.70	3.66
Wall	Control	0.00	7.89	10.37	9.93	11.77	12.17
	Epoxy	0.00	3.75	1.60	1.73	1.73	1.85
	MMA	0.00	0.04	0.60	0.18	0.27	0.34
	Urethane	0.00	0.00	0.71	0.81	0.73	0.34
Horizontal	Control	0.00	7.52	9.10	8.99	9.34	11.43
	Epoxy	0.00	0.21	0.29	0.37	0.30	0.29
	MMA	0.00	0.05	0.03	0.09	0.12	0.21
	Urethane	0.00	0.00	0.04	0.15	0.14	0.21

TABLE 4 Chloride Content Measurements at 2.5-cm Depth

Depth = 2.5 cm		Average Gain in Chloride Concentration [kg/m³]					
		Number of One-Week Exposure Cycles					
Exposure	**Coating**	**0**	**7**	**14**	**21**	**30**	**52**
Immersed	Control	0.00	1.01	2.33	1.66	2.47	3.89
	Epoxy	0.00	0.43	0.64	0.48	0.33	0.63
	MMA	0.00	0.07	0.25	0.20	0.22	0.34
	Urethane	0.00	0.00	0.12	0.13	0.21	0.22
Tide	Control	0.00		1.73	3.40	3.77	6.16
	Epoxy	0.00		0.87	1.55	1.68	3.21
	MMA	0.00		0.02	0.17	0.22	0.55
	Urethane	0.00		0.10	0.39	0.38	1.56
Wall	Control	0.00	3.96	5.01	4.76	5.76	7.90
	Epoxy	0.00	0.94	0.53	0.52	0.62	0.77
	MMA	0.00	0.00	0.10	0.15	0.23	0.27
	Urethane	0.00	0.01	0.12	0.34	0.33	0.25
Horizontal	Control	0.00	1.62	4.06	3.65	4.08	6.87
	Epoxy	0.00	0.21	0.02	0.16	0.17	0.20
	MMA	0.00	0.12	0.01	0.07	0.08	0.20
	Urethane	0.00	0.00	0.04	0.08	0.13	0.19

TABLE 5 Chloride Content Measurements at 3.8-cm Depth

Depth = 3.8 cm		Average Gain in Chloride Concentration [kg/m^3]					
		Number of One-Week Exposure Cycles					
Exposure	**Coating**	**0**	**7**	**14**	**21**	**30**	**52**
Immersed	Control	0.00	0.06	0.58	0.24	0.82	1.57
	Epoxy	0.00	0.04	0.12	0.08	0.11	0.22
	MMA	0.00	0.02	0.12	0.07	0.05	0.14
	Urethane	0.00	0.00	0.06	0.08	0.12	0.19
Tide	Control	0.00		0.19	1.06	1.08	3.69
	Epoxy	0.00		0.10	0.35	0.36	1.19
	MMA	0.00		0.13	0.07	0.07	0.12
	Urethane	0.00		0.00	0.09	0.15	0.31
Wall	Control	0.00	1.38	1.75	1.64	1.44	4.60
	Epoxy	0.00	0.13	0.10	0.10	0.11	0.35
	MMA	0.00	0.02	0.14	0.00	0.10	0.26
	Urethane	0.00	0.00	0.09	0.10	0.17	0.26
Horizontal	Control	0.00	0.15	0.72	0.75	1.14	2.38
	Epoxy	0.00	0.05	0.06	0.07	0.11	0.19
	MMA	0.00	0.03	0.13	0.03	0.07	0.19
	Urethane	0.00	0.00	0.03	0.05	0.06	0.17

A 1-year testing period was chosen to achieve a nearly steady-state diffusion rate and an almost constant surface chloride concentration. This is important for a more accurate determination of the k constant and to allow chloride concentrations to increase at the 2.5- and 3.8-cm depths to achieve a more accurate gain in chloride concentrations at these depths.

The chloride exposure conditions in the United States have been categorized as low (with a surface concentration, $C_{surface}$, = 0 to 2.4 kg/m^3), moderate ($C_{surface}$ = 2.4 to 4.8 kg/m^3), high ($C_{surface}$ = 4.8 to 5.9 kg/m^3), and severe ($C_{surface}$ = 5.9 to 8.9 kg/m^3) (*8*). The effective D_c's within each of these four chloride exposure conditions are 0.32, 0.58, and 0.84 cm^2/year (*8*).

In the analysis, 50 years of corrosion protection was selected as the maximum corrosion protection service life. Also, the depth x was selected as 4.1 cm, which is the depth of 2.5 percent of the reinforcing steel, which is a function of the design cover of 5.1 cm with

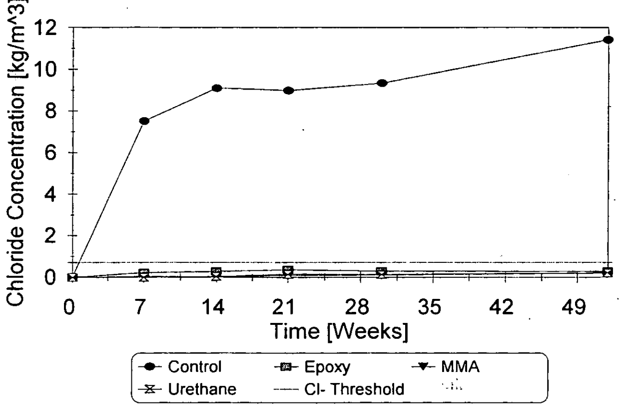

FIGURE 3 Average gain in chloride concentration, horizontal surface exposure.

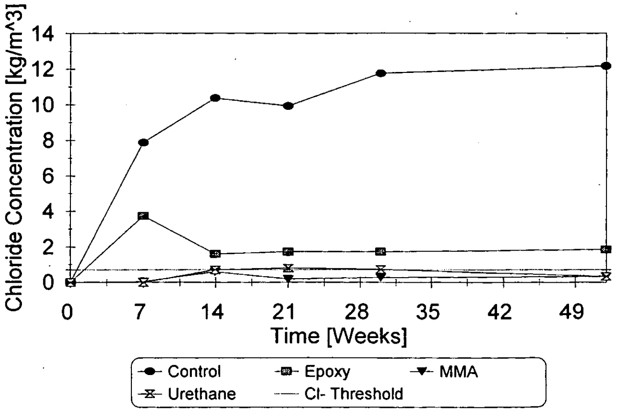

FIGURE 4 Average gain in chloride concentration, vertical surface exposure.

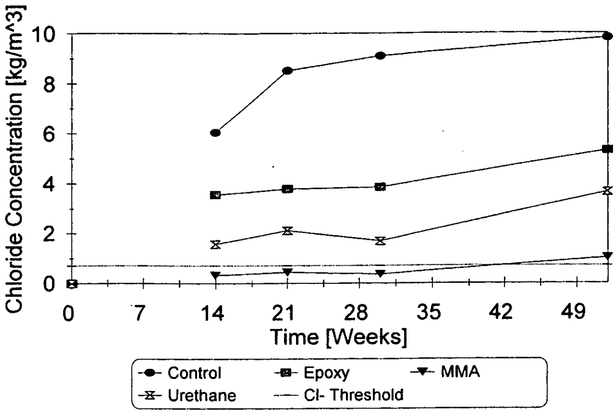

FIGURE 5 Average gain in chloride concentration, tidal zone surface exposure.

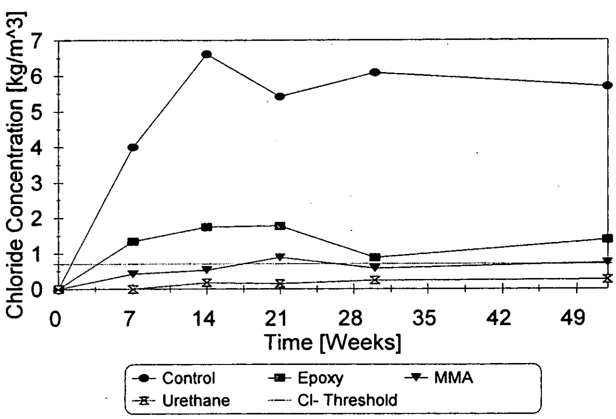

FIGURE 6 Average gain in chloride concentration, immersed zone surface exposure.

a standard deviation of 0.5 cm. The chloride threshold value for corrosion initiation for bare steel is $C_{(x,t)}$ of 0.71 kg/m^3. For the desired t of 50 years for corrosion protection and the field C_{surface} of 2.4 kg/m^3, for low chloride exposure condition, the corresponding k-value, k_{field}, is 0.339 kg/(m^3 · year$^{0.5}$), which was calculated from the following equation:

$$C_{\text{surface}} = k_{\text{field}} \sqrt{t} \tag{2}$$

$$2.4 = k_{\text{field}} \sqrt{50} \Rightarrow k_{\text{field}} = 0.339 \tag{3}$$

For low, moderate, high, and severe exposure conditions k_{field} values are 0.339, 0.679, 0.834, and 1.26 kg/(m^3 · year$^{0.5}$), respectively. To determine the field time equivalent t_{eq} for the tested coatings it is necessary to use field diffusion constant and chloride concentration at depth x and a modified k coefficient:

$$k_{\text{modified}} = (k_{\text{coating}}/k_{\text{control}}) \cdot k_{\text{field}}$$

For the severest exposure condition (D_c = 0.84 cm^2/year, C_0 = 8.9 kg/m^3, and the epoxy coating in the immersed zone exposure condition) the modified k coefficient is.

$$k_{\text{modified}} = (k_{\text{coating}}/k_{\text{control}}) \cdot k_{\text{field}} = (1.928/7.829) \cdot 1.26 = 0.31 \text{ kg/(m}^3 \cdot \text{year}^{0.5})$$

The corrosion protection time t_{eq} is determined by an interactive solution to Equation 1, as shown in Equation 4:

$$0.71 = 0.31\sqrt{t_{\text{eq}}}\left[e^{-4.1^2/(4 \cdot 0.84\, t_{\text{eq}})} - \frac{4.1\sqrt{\pi}}{2\sqrt{(0.84\, t_{\text{eq}})}}\left(1 - erf\frac{4.1}{2\sqrt{(0.84\, t_{\text{eq}})}}\right)\right] \tag{4}$$

The time equivalent for the epoxy coating in the immersed zone exposure condition is equal to 29 years. Tables 7, 8, and 9 present calculated equivalent times for the three coatings and the control that correspond to all exposure conditions occurring in the United States. Note that the protection times presented for the control section (no coating) agree with field observations and thus validate the presented methodology.

If the service life (equivalent time) exceeded 50 years then 50 years was recorded as the maximum service life. One must remember that these values are based on the diffusion properties of particular coatings. Other factors, such as resistance to ultraviolet light or mechanical or other characteristics may be contributing to a much faster rate of coating degradation.

The methodology presented here is a rational approach to estimating the corrosion protection service lives of various coatings based on chloride diffusion through the coating. It recognizes and accounts for the fact that coatings do not or will not exclude all chloride. However, field studies are needed to determine if and what exposure conditions other than chloride diffusion would limit the corrosion protection service lives of concrete coatings.

TABLE 6 Regression Analysis Results: k Coefficients [kg/(m^3 year$^{0.5}$)]

	Coating Type			
Exposure Condition	Control	Epoxy	MMA	Urethane
Horizontal	13.303	0.375	0.164	0.175
Vertical (Wall)	14.932	2.713	0.421	0.740
Immersed	7.829	1.928	0.944	0.273
Tide	11.241	5.564	0.772	3.153

TABLE 7 Time Equivalent for Field Conditions and Diffusion Constant of 0.32 cm^2/year

Field Surface Concentration [kg/m^3]	Exposure Condition	Time Equivalent [years] Control	Epoxy	MMA	Urethane
8.9	Horizontal	18	50	50	50
	Wall	18	50	50	50
	Immersed	18	47	50	50
	Tide	18	27	50	42
5.9	Horizontal	22	50	50	50
	Wall	22	50	50	50
	Immersed	22	50	50	50
	Tide	22	37	50	50
4.8	Horizontal	26	50	50	50
	Wall	26	50	50	50
	Immersed	26	50	50	50
	Tide	26	44	50	50
2.4	Horizontal	44	50	50	50
	Wall	44	50	50	50
	Immersed	44	50	50	50
	Tide	44	50	50	50

TABLE 8 Time Equivalent for Field Conditions and Diffusion Constant of 0.58 cm^2/year

Field Surface Concentration [kg/m^3]	Exposure Condition	Time Equivalent [years] Control	Epoxy	MMA	Urethane
8.9	Horizontal	12	50	50	50
	Wall	12	47	50	50
	Immersed	12	34	50	50
	Tide	12	19	50	30
5.9	Horizontal	15	50	50	50
	Wall	15	50	50	50
	Immersed	15	50	50	50
	Tide	15	26	50	46
4.8	Horizontal	18	50	50	50
	Wall	18	50	50	50
	Immersed	18	50	50	50
	Tide	18	32	50	50
2.4	Horizontal	32	50	50	50
	Wall	32	50	50	50
	Immersed	32	50	50	50
	Tide	32	50	50	50

TABLE 9 Time Equivalent for Field Conditions and Diffusion Constant of 0.84 cm²/year

Field Surface Concentration [kg/m³]	Exposure Condition	Time Equivalent [years]			
		Control	Epoxy	MMA	Urethane
8.9	Horizontal	9	50	50	50
	Wall	9	40	50	50
	Immersed	9	29	50	50
	Tide	9	15	50	25
5.9	Horizontal	12	50	50	50
	Wall	12	50	50	50
	Immersed	12	45	50	50
	Tide	12	22	50	39
4.8	Horizontal	14	50	50	50
	Wall	14	50	50	50
	Immersed	14	50	50	50
	Tide	14	26	50	49
2.4	Horizontal	26	50	50	50
	Wall	26	50	50	50
	Immersed	26	50	50	50
	Tide	26	50	50	50

REFERENCES

1. *Our Nation's Highways. Selected Facts and Figures.* Publication FHWA-PL-90-024. FHWA, U.S. Department of Transportation, undated, p. 11.
2. *A Federal Surface Transportation Program for the Future.* (American Road & Transportation Builders Association, undated, p. 8.
3. Bennett, J. Corrosion of Reinforcing Steel in Concrete and Its Prevention by Cathodic Protection. *Anti-Corrosion Methods and Materials,* Vol. 33, No. 11, Oct. 1986, pp. 12–15, 17.
4. Pfeifer, D. W., and M. J. Scali. *NCHRP Report 244: Concrete Sealers for Protection of Bridge Structures.* TRB, National Research Council, Washington, D.C., Dec. 1981.
5. Wohl, R. L., and R. W. LaFraugh. Criteria for the Selection of Penetrating Hydrophobic Sealers Used in the Repair of Concrete Parking Decks. In *Building Deck Waterproofing,* ASTM STP 1084 (L. E. Gish, ed.), American Society for Testing and Materials, Philadelphia, 1990, pp. 75–82.
6. Ashmore, W. F. Coating Concrete in Industrial Facilities. *Journal of Protective Coatings & Linings,* Nov. 1986, pp. 48–54.
7. Crank, J. *Mathematics of Diffusion.* The University Press, Oxford, U.K., 1970.
8. Weyers, R. E., B. D. Prowell, M. M. Sprinkel, and M. Vorster. *Concrete Bridge Protection, Repair, and Rehabilitation Relative to Reinforcement Corrosion: A Methods Application Manual.* Report SHRP-S-360. Strategic Highway Research Program, National Research Council, Washington, D.C., 1993.

Publication of this paper sponsored by Committee on Corrosion.

Mechanism of Action of Corrosion-Inhibited Highway Deicers

R. SCOTT KOEFOD

The corrosion rates of steel exposed to salt solutions inhibited with several phosphate or phosphonate salts together with salts of magnesium, calcium, or zinc were measured to determine their effectiveness as low-corrosion deicers. At levels present in commercially available deicers, ortho- and polyphosphates mixed with magnesium or zinc salts provided strong inhibition of chloride corrosion. Linear polarization resistance (LPR) was used to monitor the corrosion rate of an orthophosphate-inhibited deicer over time, showing that the corrosion rate remained very stable and low in the presence of the inhibited deicer. The overall decreases in the corrosion rate of the inhibited salt relative to those of plain salt determined by LPR and weight loss were 89 and 81 percent, respectively, indicating good agreement between the two methods. Electron microscopy and energy dispersive spectroscopy were used to analyze steel surfaces exposed to different deicer formulas. Surface studies indicate that the inhibitors become incorporated into the surface of the steel, causing the formation of a compact, uniform layer that may reduce the corrosion by forming a barrier between the metal and the corrosive environment.

Historically, salt has been the deicer of choice for roads, highways, and bridges and will probably continue to be so because of its high ice-melting capacity, efficient ice-melting characteristics, and low cost. However, the low cost of salt is mitigated by the fact that it results in corrosion damage to motor vehicles, bridges, and the highway infrastructure. Estimates of the cost of deicer corrosion damage to vehicles and infrastructure range from \$2 billion to \$4.5 billion per year (*1*). To address this problem there is currently a great deal of interest in the development of alternative, low-corrosion deicing products.

One approach to developing low-corrosion deicing products has been to use the salts of organic acids such as calcium magnesium acetate (*2*). Since these organic deicers do not contain the aggressive chloride ion they are relatively less corrosive than salt. However, in some cases these organic compounds do not have the high deicing effectiveness of salt, and they may be prohibitively expensive (*3*). Another approach to developing low-corrosion deicers has been to add small amounts of chemical corrosion inhibitors to deicing salt. The corrosion inhibitors are designed to dissolve in the deicing brine melt and limit the corrosion caused by exposure to the runoff. To choose the most appropriate inhibitor formulations for deicing mixtures it is necessary to understand the mechanism of action of inhibitors in the deicing brine environment. This paper presents the results of recent investigations of the mechanism of action of corrosion-inhibited deicers on exposed carbon steel surfaces.

Central Research Department, Cargill, Incorporated, P.O. Box 5699, Minneapolis, Minn. 55440-5699.

CORROSION RATE MEASUREMENT

Corrosion rates were measured on 3 percent deicer solutions. Concentrations of 3 percent were chosen to provide the most aggressive concentration for testing inhibitor effectiveness. Uhlig (*4*) points out that the corrosiveness of salt solutions to steel reaches a maximum at 3 percent and then begins to fall off because of decreasing oxygen solubility. The 3 percent concentration is also observed in deicing brine runoff concentrations measured in the field (*5*). Corrosion measurements were made on coupons of 1010 carbon steel because this is fairly representative of the steels in automobiles, highway fixtures, and bridge components.

Phosphorus-based inhibitors were chosen for the present study because these are used in a number of commercial anticorrosive deicing products. The formulas tested in the study were taken from commercially available corrosion-inhibited deicing products. All of the deicers tested were salt based, consisting of sodium chloride mixed with a phosphorus-containing inhibitor and a divalent metal salt. Formulas containing three different classes of phosphorus-based inhibitors were chosen: orthophosphates, polyphosphates, and organic phosphonates.

Orthophosphates, polyphosphates, and phosphonates are good candidates as deicer corrosion inhibitors. They are relatively inexpensive and nontoxic, and they are well known to be effective inhibitors in such industrial applications as cooling water treatment (*6*), potable water treatment (*7*), protection of steel in seawater (*8*), and protection of automobile cooling systems (*9*). Previous studies exploring the potential of polyphosphates as inhibitors for seawater indicate that the effectiveness of polyphosphates in salt solution can be increased by the addition of calcium, magnesium, or zinc salts (*8,10*). Thus, magnesium, calcium, and zinc salts may be present in the commercial phosphate-phosphonate-inhibited deicers to increase the inhibition effectiveness. The relative importance of the phosphate-phosphonate and divalent metal ion in inhibiting the corrosion of deicing salt remains to be determined. This information is necessary to determine the optimum amount of each inhibitor for an effective low-corrosion deicer.

Corrosion rates were measured on all test formulas by weight loss measurements consistent with the guidelines of ASTM G31 (*11*). One formula, the orthophosphate composition, was chosen for simultaneous measurement of the corrosion rate by weight loss and linear polarization resistance (LPR) to determine if LPR could be used to quickly and accurately monitor the corrosion rates of steel in deicing solutions. LPR is a commonly used electrochemical technique that measures instantaneous corrosion rates and that has been shown to correlate well with weight loss measurements for a wide variety of metals and corrosive media (*12*), including concrete-embedded rebar (*13*), although no measurements of the corrosion rate of concrete-encased rebar were made in the present study. The technique involves imposing a small potential change on a metal sample. The slope of the resulting potential-versus-current curve at the corrosion potential is termed the polarization resistance (R_p). The actual corrosion rate can be calculated from the polarization resistance by the Stern-Geary equation (*12*):

$$i_{corr} = (\beta_a \beta_c)/2.3(\beta_a + \beta_c) \cdot 1/R_p \qquad (1)$$

where i_{corr} is the corrosion current (corrosion rate), and β_a and β_c are the anodic and cathodic Tafel slopes, respectively. The Tafel slopes are determined by taking the slope of the log i-versus-E polarization curves in the Tafel region, that is, the region where the curve is linear. Polarization scans were run on independent samples to determine the Tafel constants, but acceptable Tafel regions were not obtained. Cathodic polarization curves began to slope steeply within 30 mV of the corrosion potential, possibly due to oxygen reduction or passive film breakdown, which distorts the Tafel behavior in this range. Similar behavior has been observed for steel exposed to solutions of calcium magnesium acetate (*14*). Consequently, values of β_a and β_c of 110 mV/decade were used to calculate corrosion rates. These values have been used by other investigators to calculate corrosion rates when the actual Tafel constants were not known (*14*).

SURFACE ANALYSIS

A variety of surface studies have been done on steel exposed to phosphate-type inhibitors in different environments. Electron diffraction studies indicate that steel exposed to solutions of dihydrogen phosphate form a surface film that is made up of γ-Fe_2O_3 and $FePO_4 \cdot 2H_2O$ (*15*). Steel inhibited by calcium and sodium hexametaphosphate in salt solution has been shown to form a viscous surface film with a composition corresponding to a complex hydrated compound of iron, calcium, sodium, and metaphosphate (*8*). Electron spectroscopy for chemical analysis (ESCA) studies on a mild steel tube from a pilot plant cooling tower of a stabilized phosphate corrosion inhibition program indicated the formation of a surface layer that contained carbon, phosphorous, calcium, iron, and oxygen (*16*).

To gain information about the mechanism by which the inhibited deicers work and determine if surface behavior similar to that seen in other environments can be observed, scanning electron microscopy (SEM) was used to obtain photographs of steel surfaces exposed to salt and various inhibited deicers. In addition to information on the changes in surface morphology caused by the inhibited deicers provided by electron microscopy, further information was gained by analyzing the elemental compositions of the surfaces by using energy dispersive spectroscopy (EDS). Examined together, the physical appearance of the film that forms on a metal surface, the elements detected in the surface film, and the corrosion rate of the metal provide basic information about the corrosion process of a metal exposed to a given deicer.

PROCEDURE AND MATERIALS

Weight Loss Measurement

Deicers containing phosphate and polyphosphate inhibitors were obtained directly from their commercial sources. Samples of the phosphonate-inhibited deicer were obtained from the stockpile of an end user. Four coupons of 1010 steel of 2.54 × 5.08 × 0.16 cm (1 × 2 × 0.0625 in.) were immersed in 3 kg of each deicer solution. All concentrations of the deicer solutions were 3 percent and were made with deionized water (18 MΩ). The coupons were totally immersed in the solutions except for two 1-hr drying periods a day, 5 days per week, when they were suspended in air. The solutions were replaced with freshly made 3 percent solutions of the same type once a week. After 4 weeks of exposure weight loss measurements were made according to ASTM G31. The percent protection was calculated by Equation 2 (weight loss measurements were also made on uncorroded coupons exposed to the same cleaning procedure as the test coupons; the average weight loss due to cleaning was subtracted from the weight loss of the test coupons before calculating percent protection):

$$\text{Percent protection} = 100 \cdot (W_s - W_d)/(W_s - W_w) \qquad (2)$$

where

W_s = weight loss of the salt control,
W_d = weight loss of the inhibited deicer sample, and
W_w = weight loss of the water control sample.

Thus, percent protection calculated in this manner provides a measurement of the inhibition of salt-induced corrosion since the calculation subtracts the amount of corrosion arising from pure water. A value of greater than 100 percent protection indicates a corrosion rate less than that observed in pure water, and a value of less than 0 percent indicates a corrosion rate greater than that observed with plain salt.

LPR Measurement

Simultaneous LPR and weight loss measurements were made by the same procedure described above except that the coupons were prepared in the manner described for electrode specimens in SHRP Standard H-205.7 (*17*). After preweighing a 22-gauge stainless steel wire, the wire was attached to each coupon with a brass screw and nut through a hole drilled in the top. The top portions of the coupons were coated with liquid electrical tape, including the connection to the steel wire, so that 3.0 cm (1.18 in.) of the coupon was left exposed on the bottom. Four sets of four coupons each were exposed to solutions of salt and inhibited salt. Polarization resistance measurements were made consistent with the method outlined in ASTM G59 (*18*) by using a Schlumberger SI 1286 electrochemical interface with software written by Capcis March Ltd. A graphite rod obtained from the Carbide/Graphite Group, Inc., was used as the counter electrode. The reference electrode was a saturated calomel electrode (SCE) coupled to the solution via a Luggin probe. Four sets of four coupons each were tested for salt and the inhibited deicer. Each set of coupons was immersed in 3 kg of solution and was given one 1-hr drying period per day, 5 days per week. (Coupons in the LPR experiment were given only one drying period per day for increased measurement convenience. Upon completing the LPR measurements on a given day, the coupons were given their 1-hr drying period and were then allowed to remain in solution overnight to ensure that the corrosion potential and rate had restabilized before taking readings on the following morning.) Trapezoidal integration of the corrosion currents measured over 4 weeks was done to calculate the average corrosion currents for the salt and inhibited deicer solutions, i_s and i_d, respectively. At the end of the 4 weeks of exposure, the coupons were cleaned and weight loss mea-

TABLE 1 Corrosion rates of 1010 Steel in 3 Percent Deicer Solutions

Deicer / Inhibitor	MPY[a]	% Protection
Salt / No Inhibitor	13.3 (1.5)	0
Water control	3.2 (0.4)	100
Salt / Phosphonate + $CaCl_2$	15.0 (0.8)	-17
Salt / Hexametaphosphate + $ZnSO_4$	-1.6 (0.02)	115
Salt / Tripolyphosphate + $MgCl_2{\cdot}6H_2O$	0.3 (0.04)	128
Salt / Orthophosphate + $MgSO_4$	0.6 (0.1)	125

[a] Standard deviations are listed parenthetically.

surements were made in the same manner described earlier. Because of the difficulties in measuring electrochemical corrosion rates in the absence of electrolyte, a water control was not run in this experiment, and percent protections could not be calculated as described earlier to permit comparison of the electrochemical and weight loss measurements. Therefore, comparison of the two methods was made by calculating the percent inhibition simply by using salt as the standard by the equation

$$\text{Percent inhibition} = 100 \cdot (i_s - i_d)/i_s \text{ or } (W_s - W_d)/W_s \qquad (3)$$

where w refers to weight loss values and i refers to corrosion currents as defined earlier.

SEM and Energy Dispersive Surface Analysis

Coupons of 1010 steel [2.54 × 5.08 × 0.16 cm (1 × 2 × 0.0625 in.)] were exposed to 3 percent solutions of inhibited deicer and salt in the same manner that was used to make the weight loss corrosion measurements. Coupons were exposed for both 1 and 4 weeks. After exposure was complete the coupons were rinsed with deionized water, rinsed with methanol, and allowed to air dry. The coupons were subsequently vapor deposited with carbon, and the measurements were made by SEM and EDS. Electron microscopy was performed with a JEOL 840II scanning electron microscope, EDS was performed with a Tracor Northern TN-5500. All samples were photographed at a magnification of ×250.

RESULTS AND DISCUSSION OF RESULTS

Corrosion Rate Measurements

The data in Table 1 show the results of weight loss corrosion rate measurements on the test deicer formulas. The data indicate that orthophosphate and polyphosphate formulas all gave corrosion rates lower than those observed in deionized water. The amount of inhibitor in the phosphonate-containing deicer was fairly low (less than 0.1 percent). The corrosion rate observed for this product probably indicates that higher levels of the phosphonate inhibitor are required to achieve a high level of corrosion inhibition.

LPR was used to monitor the corrosion rate of coupons exposed to the orthophosphate deicer formula and a salt control as a function of time. Figure 1 shows the changes in corrosion potential and

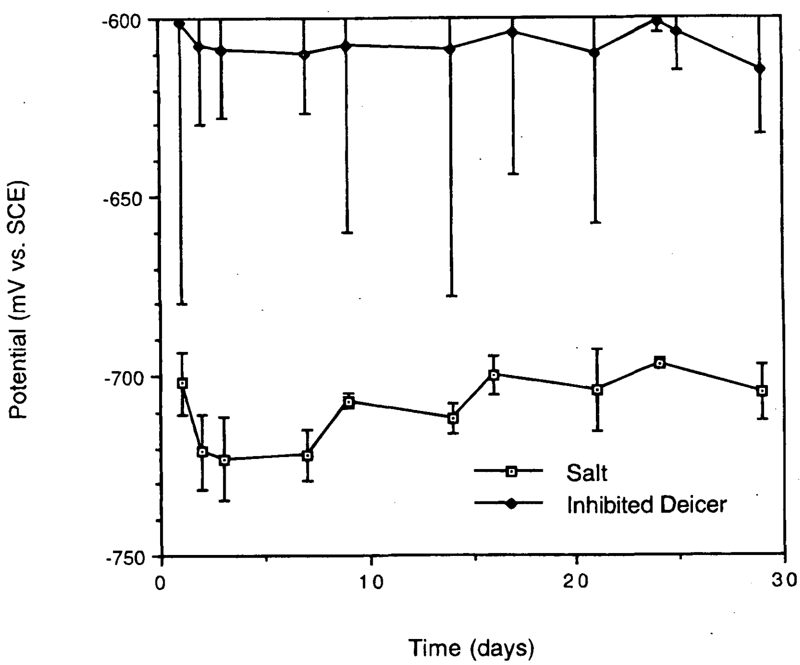

FIGURE 1 Corrosion potential of 1010 steel coupons exposed to 3 percent deicer solutions (error bars indicate 95 percent confidence intervals).

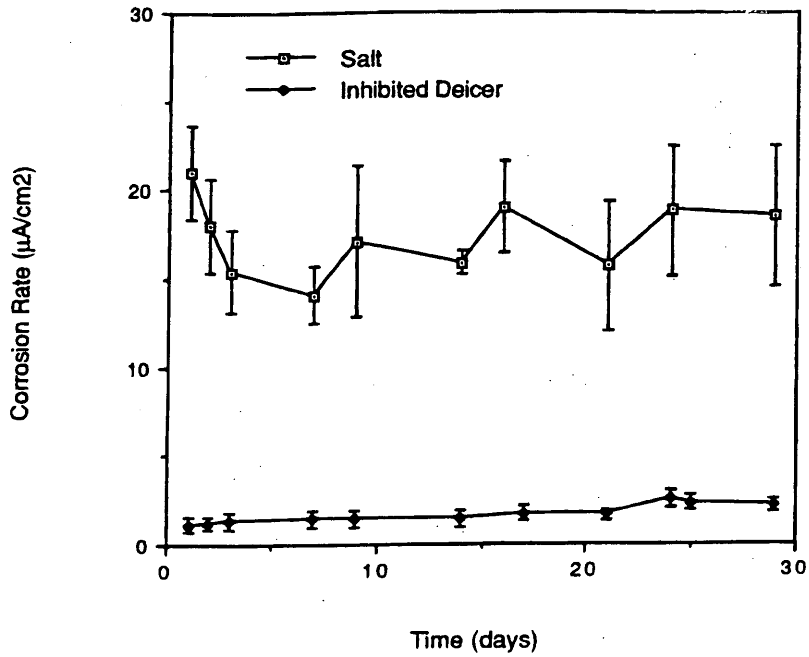

FIGURE 2 Corrosion rate of 1010 steel coupons exposed to 3 percent deicer solutions (error bars indicate 95 percent confidence intervals).

Figure 2 shows the corresponding instantaneous corrosion rates of these steel samples. The data given in Figures 1 and 2 are only for the salt solutions with and without inhibitor; electrochemical measurements in deionized water were not made because of the difficulty of making electrochemical measurements in the absence of electrolyte. The corrosion potential provides an indication of the relative degree of passivation of a metal surface. Shifts to more negative corrosion potential are a qualitative indication of active corrosion (*19*). Figure 1 shows that the inhibited deicer causes the steel potential to shift by more than 100 mV to less corrosion active potentials. The potential of steel exposed to inhibited deicer is much more variable than that of steel exposed to the salt solution (indicated by the much larger error bars in Figure 1), but even within experimental error there is a consistent, significant shift to more positive potentials, suggesting that the inhibited deicer helps preserve passivation in the presence of the aggressive chloride ion.

The corrosion potential only provides a qualitative indication of whether the steel is likely to corrode or not. For an unambiguous determination of corrosion it is necessary to measure actual corrosion rates. This can be seen for salt and the inhibited deicer in Figure 2, which provides quantitative confirmation of the effect suggested by Figure 1. It can be seen that within 1 day the corrosion rate in the inhibited solution has already reached a minimum, and the corrosion rate does not change significantly over 30 days of exposure.

To determine the accuracy of the LPR technique in monitoring deicer corrosion over time the average corrosion rate of the samples was measured by weight loss at the end of the experiment and was compared with that calculated by a trapezoidal integration of the instantaneous corrosion rates depicted in Figure 2. Since electrochemical corrosion rate measurements were not attempted for the water control, the percent protection could not be calculated in the same manner as that used to calculate the values in Table 1. However, it is possible to compare the percent decrease in the corrosion

TABLE 2 Corrosion Rates of 1010 Steel Measured by LPR and Weight Loss

	Plain Salt	Salt + Orthophosphate/$MgSO_4$
Weight Loss Corrosion Rate (MPY)	5.3	0.99
LPR Corrosion Current (µA/cm2)	473	51
Weight Loss % Inhibition	-	81%
LPR % Inhibition	-	89%

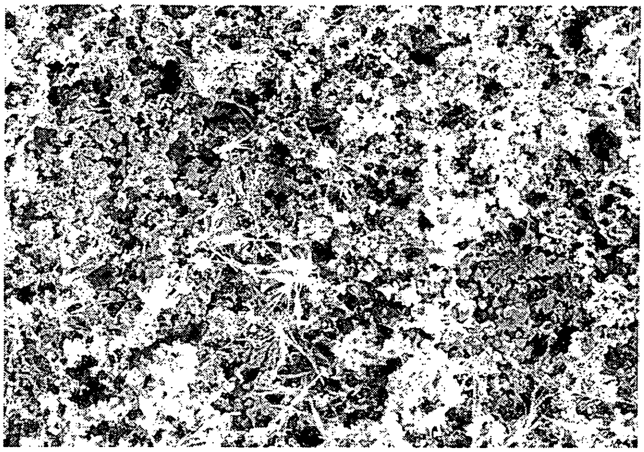

FIGURE 3 Scanning electron micrograph of steel exposed to 3 percent salt solution for 1 week.

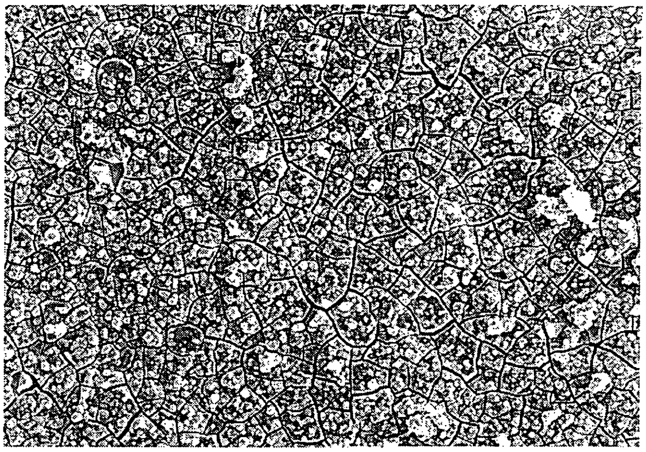

FIGURE 4 Scanning electron micrograph of steel exposed for 1 week to a 3 percent solution of salt inhibited with zinc and hexametaphosphate.

rate of the inhibited salt relative to that of the plain salt control from the weight loss and electrochemical measurements. The corrosion rates and percent inhibition calculated by weight loss and LPR are given in Table 2. The relative corrosion rates measured by the two techniques agree very well. Weight loss measurements indicate an 81 percent reduction of the corrosion rate of the inhibited deicer relative to that of salt, whereas corrosion rates measured by LPR indicate an 89 percent reduction in the corrosion rate relative to that of salt. Thus, LPR provides an accurate, rapid means of measuring deicer corrosion rates and permits observation of changes in the corrosiveness of the deicer over time.

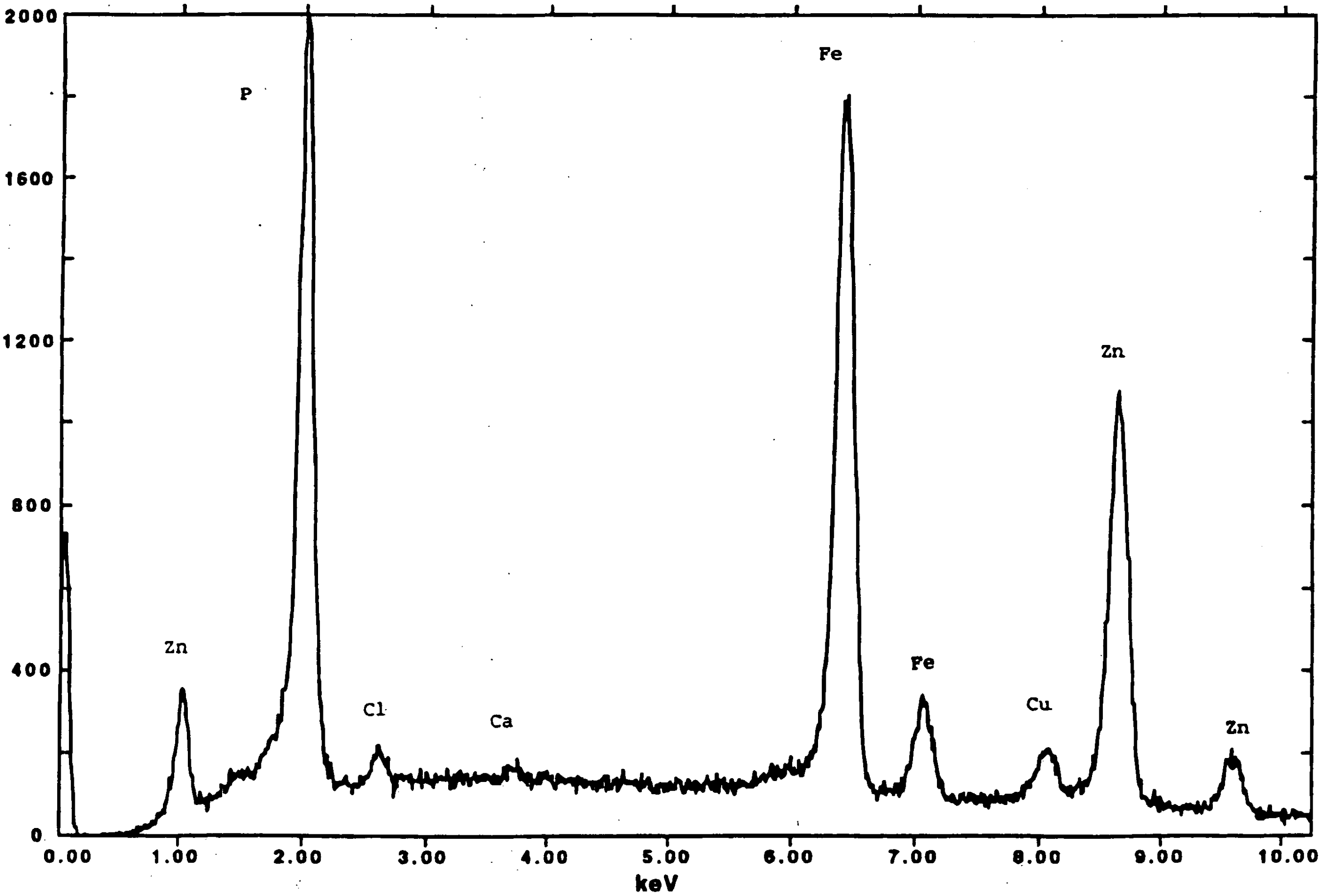

FIGURE 5 EDS elemental analysis of steel surface exposed to a 3 percent solution of salt inhibited with zinc and hexametaphosphate.

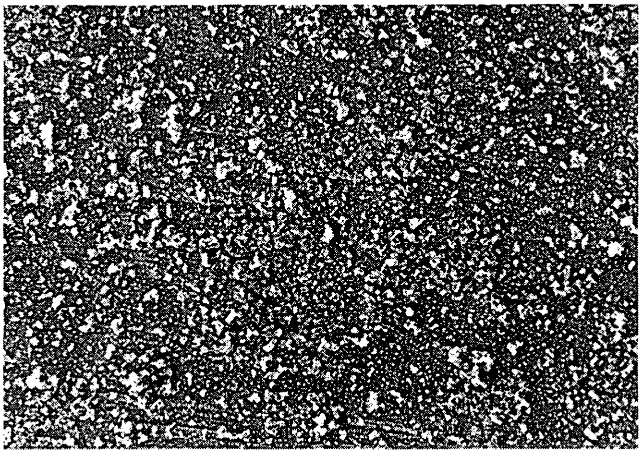

FIGURE 6 Scanning electron micrograph of steel exposed for 1 week to a 3 percent solution of salt inhibited with magnesium and orthophosphate.

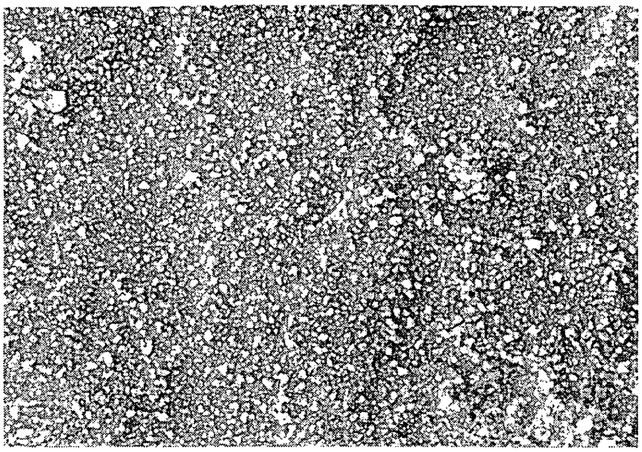

FIGURE 7 Scanning electron micrograph of steel exposed for 4 weeks to a 3 percent solution of salt inhibited with magnesium and orthophosphate.

Surface Analysis

Figure 3 shows the surface of steel exposed to salt solution for 1 week. The electron micrograph shows that as the steel corrodes in salt solution a very porous, flocculent, and mossy-looking layer grows on the salt surface. The EDS elemental analysis of this surface shows only iron and chloride and is consistent with the formation of a surface layer of iron oxide rust (oxygen does not show up in the elemental analysis because the EDS probe was not sensitive to elements with an atomic number lower than that of sodium) together with some iron chloride. The porous nature of this layer visible in the scanning

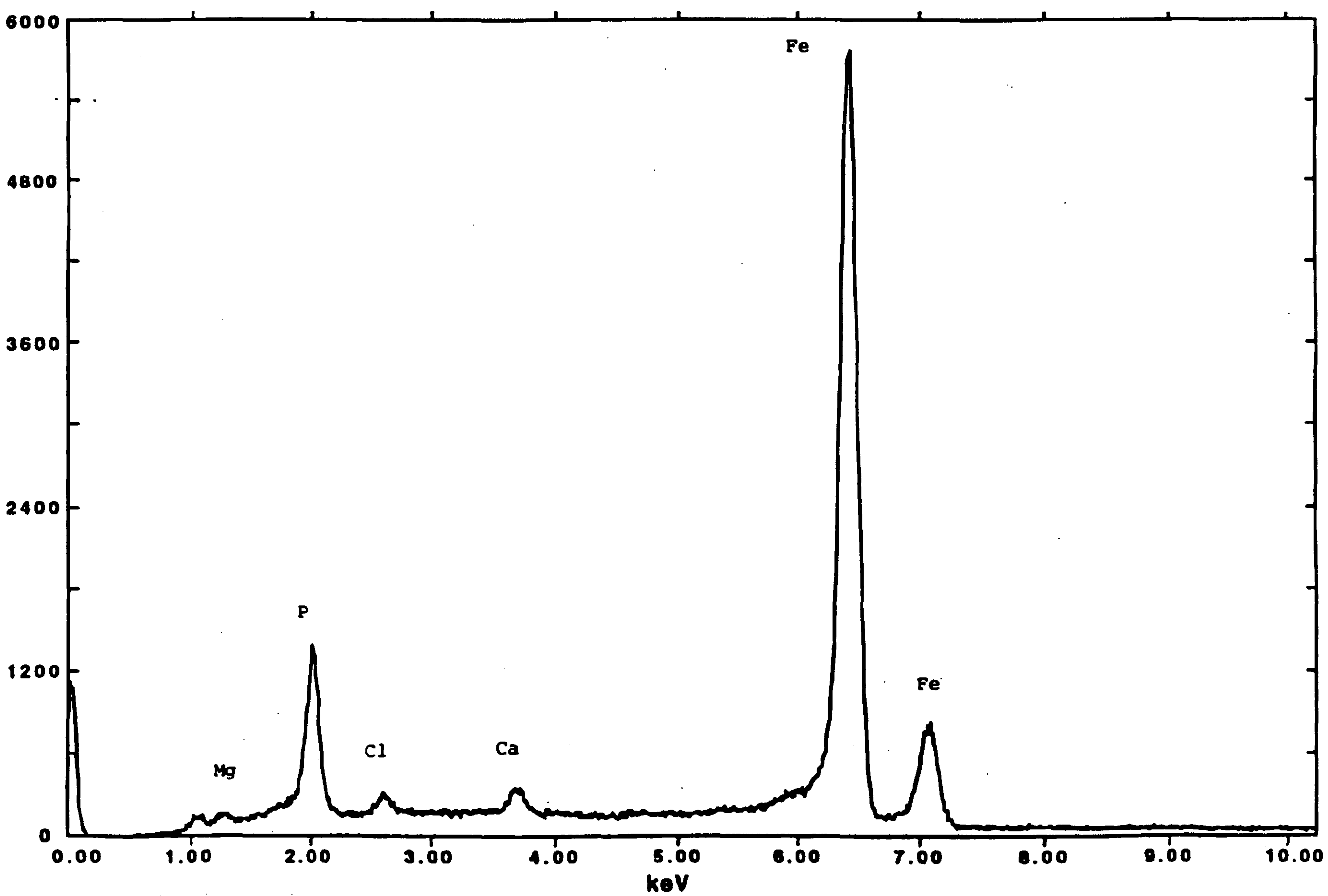

FIGURE 8 EDS elemental analysis of steel surface exposed to a 3 percent solution of salt inhibited with magnesium and orthophosphate.

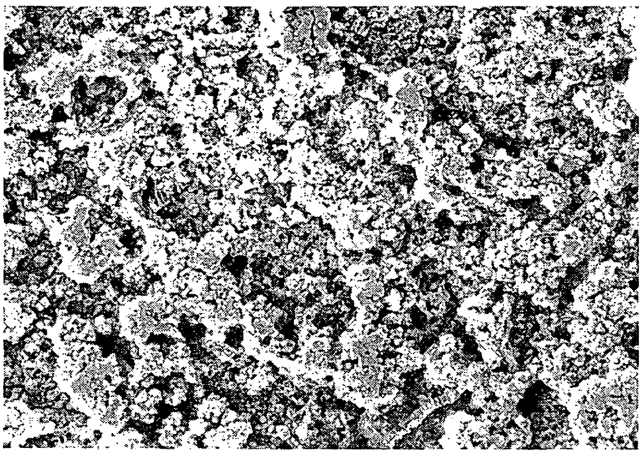

FIGURE 9 Scanning electron micrograph of steel exposed for 1 week to a 3 percent solution of salt inhibited with calcium and phosphonate.

electron micrograph probably permits the easy ingress of oxygen and water to the steel surface, allowing the corrosion reaction to proceed freely.

Figure 4 shows the surface of steel exposed to the zinc-hexametaphosphate-inhibited deicer for 1 week, and it is immediately apparent that a very different kind of surface layer forms. Rather than the voluminous, mossy-looking layer seen in the salt sample, the steel surface in the presence of the inhibitors forms a very compact, flat, uniform layer. The EDS elemental analysis of this surface (Figure 5) shows peaks characteristic of phosphorus and zinc, indicating that the inhibitor molecules become incorporated into the surface layer, presumably causing it to form a dense, compact protective layer. It is reasonable to assume that this flat, compact layer forms a barrier on the steel surface that both prevents the easy ingress of oxygen and water to the underlying metal and interferes with the diffusion of corrosion products away from the metal surface, resulting in the low corrosion rate indicated in Table 1.

The formation of compact, uniform surface layers into which the inhibitor molecules were incorporated was characteristic of steel surfaces exposed to the orthophosphate- and polyphosphate-inhibited deicers tested in the present study. Another example of this can be seen in Figures 6 and 7, which show the steel surface exposed to the orthophosphate-inhibited deicer for 1 and 4 weeks, respectively. After 1 week so little corrosion has occurred that there is only spotty accumulation of corrosion products on the surface visible on the surface in Figure 6, but Figure 7 shows that after 4 weeks of exposure a compact, uniform sheet has formed over the entire steel surface. The EDS elemental analysis in Figure 8 confirms that the magnesium and phosphorus from the inhibitor are present in the surface layer.

Figure 9 shows the surface of steel exposed to the inhibited deicer containing the low level of phosphonate. It is interesting to note that in this case SEM reveals a surface that looks very similar to that in Figure 3 for plain salt. In both this case and the case of noninhibited salt, the porous, mossy-looking surface layer is associated with high corrosion rates, as shown in Table 1. The EDS elemental analysis of the sample exposed to the phosphonate formula can be seen in Figure 10 and shows only iron, a trace of calcium, but no phosphorus. The lack of inhibitor on the steel surface is consistent with the surface remaining essentially the same as that exposed to plain salt and further suggests that the compact, uniform film formed by the higher levels of orthophosphate and polyphosphate inhibitors is responsible for the low corrosiveness of those deicers.

CONCLUSIONS

Weight loss measurements of the corrosion rate of carbon steel subjected to alternate drying and immersion in 3 per-

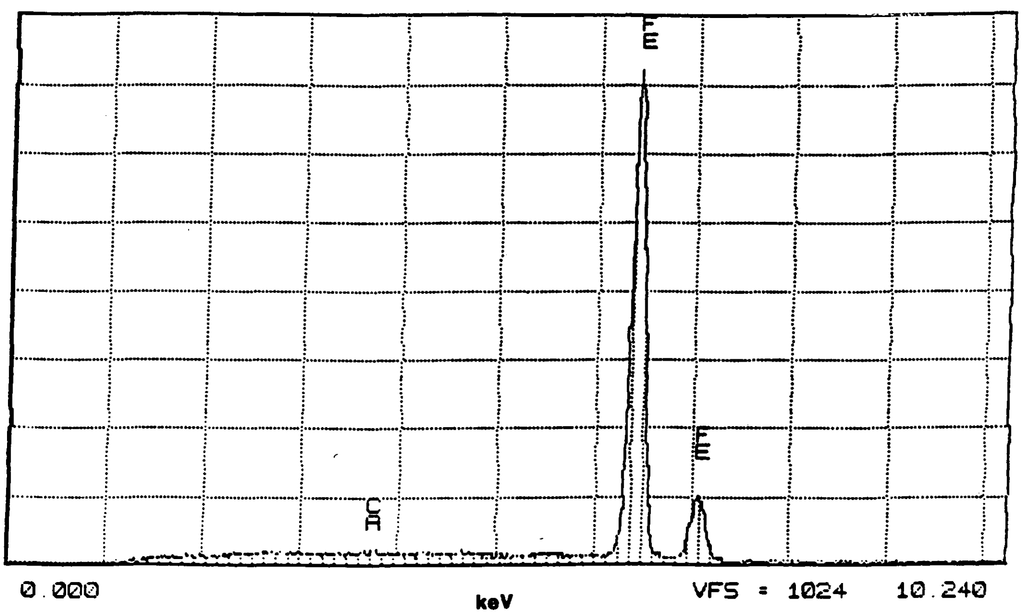

FIGURE 10 EDS elemental analysis of steel surface exposed to a 3 percent solution of salt inhibited with calcium and phosphonate.

cent deicer solutions indicated that the addition of three different phosphates in combination with zinc or magnesium salts effectively reduces the corrosive effects of the chloride ion. The low corrosion rate of salt inhibited with orthophosphate and a magnesium salt was independently verified by linear polarization resistance measurement. The accuracy of the linear polarization resistance measurement in measuring corrosion rate suggests that it can be a useful tool for rapidly determining the corrosiveness of deicers under different concentration, temperature, or length-of-exposure conditions. Phosphate and zinc or magnesium added to deicing salts in amounts of a few percent appear to inhibit the corrosion caused by chloride by becoming incorporated into the surface film that forms on the metal surface. Incorporation of the inhibitor into the surface layer is consistently observed to result in a compact, uniform film rather than the voluminous, mossy-looking oxide deposits seen in the absence of inhibitor or in the presence of a level of inhibitor too low to provide inhibition. This suggests that a primary mechanism for inhibition in these mixtures is through the formation of a protective barrier that insulates the steel from the corrosive environment.

REFERENCES

1. Committee on the Comparative Costs of Rock Salt and Calcium Magnesium Acetate (CMA) for Highway Deicing. In *Special Report 235: Highway Deicing. Comparing Salt and Calcium Magnesium Acetate,* TRB, National Research Council, Washington, D.C., 1991, Ch. 3.
2. Buscemi, C. D., K. A. Hoenke, and K. L. Eklund. Recent Research on Alternative Deicers at Chevron. In *Transportation Research Record 1347,* TRB, National Research Council, Washington, D.C., 1992.
3. Committee on the Comparative Costs of Rock Salt and Calcium Magnesium Acetate (CMA) for Highway Deicing. *Special Report 235: Highway Deicing. Comparing Salt and Calcium Magnesium Acetate,* TRB, National Research Council, Washington, D.C., 1991, pp. 1–12.
4. Uhlig, H. H. *Corrosion and Corrosion Control.* John Wiley and Sons, Inc., New York, 1963.
5. Burggraf, F., H. P. Orland, and E. W. Jackson. Effect of an Inhibitor on the Corrosion of Autobody Steel by De-Icing Salt. *HRB Proc.,* Vol. 41, 1962, pp. 221–254.
6. Boffardi, B. P. Corrosion Control of Industrial Cooling Water Systems. In *Reviews on Corrosion Inhibitor Science and Technology* (A. Raman and P. Labine, eds.), National Association of Corrosion Engineers, Houston, 1993, pp. II-6-1–II-6-13.
7. Hatch, G. B. Polyphosphate Inhibitors in Potable Water. *Materials Protection,* Nov. 1969, pp. 31–35.
8. Rozenfeld, I. L. *Corrosion Inhibitors.* McGraw-Hill, New York, 1981, Ch. 5.
9. Ibid., Ch. 8.
10. Lahodny-Sarc, O., and L. Kastelan. Inhibition of Mild Steel by Polyphosphates. *Corrosion Science,* Vol. 16, 1976, pp. 25–34.
11. Standard Practice for Laboratory Immersion Corrosion Testing of Metals. *1989 Annual Book of ASTM Standards,* Vol. 03.02. ASTM, Philadelphia, 1989, pp. 108–115.
12. Callow, L. M., J. A. Richardson, and J. L. Dawson. Corrosion Monitoring Using Polarisation Resistance Measurements. I. Techniques and Correlations. *British Corrosion Journal,* Vol. 11, No. 3, 1976, pp. 123–131.
13. Andrade, C., C. Alonso, M. Acha, and B. Malric. Preliminary Testing of Na_2PO_3F as a Curative Corrosion Inhibitor for Steel Reinforcement in Concrete. *Cement and Concrete Research,* Vol. 22, 1992, pp. 869–881.
14. Locke, C. E., and K. J. Kennelley. *Corrosion of Highway and Bridge Structural Metals by CMA.* Report FHWA-RD-86-064. FHWA, U.S. Department of Transportation, June 1986.
15. Rozenfeld, I. L. *Corrosion Inhibitors.* McGraw-Hill, New York, 1981, Ch. 2.
16. Moriarty, B. E. Surface Studies of Corrosion Inhibitors in Cooling Water Systems. *Materials Performance,* Vol. 29, 1990, pp. 45–48.
17. Chappelow, C. C., R. R. Blackburn, D. Darwin, and C. E. Locke. Test Method for Evaluation of Corrosive Effects of Deicing Chemicals on Metals. *SHRP-H-332 Handbook of Test Methods for Evaluating Chemical Deicers.* Strategic Highway Research Program, National Research Council, Washington, D.C., 1992, pp. 185–197.
18. Standard Practice for Conducting Potentiodynamic Polarization Resistance Measurements. *1989 Annual Book of ASTM Standards,* Vol. 03.02. American Society for Testing and Materials, Philadelphia, 1989, pp. 221–223.
19. Shoesmith, D. W. Kinetics of Aqueous Corrosion. *Metals Handbook,* 9th ed., Vol. 13. *Corrosion.* ASM International, Metals Park, Ohio, 1987, pp. 29–36.

Publication of this paper sponsored by Committee on Corrosion.

Use of Hydrodemolition To Remove Deteriorated Concrete from Bridge Decks

ERIC C. LOHREY

Hydrodemolition is a relatively new method of removing select portions of a hardened concrete structure. By using the erosive power of high-velocity water streams, hydrodemolition equipment breaks up concrete by disintegrating the cement matrix between aggregates. The demolishing effect can be tightly controlled to a desired level of removal, ranging from light scarification of the surface to deep penetration of the structural element. The use of the hydrodemolition process has several advantages over conventional concrete removal methods, such as jackhammering. These advantages include a reduction in new damage caused by the removal process; automation, which produces a very consistent level of removal energy over large areas; the ability to seek out and remove weak or deteriorated locations at various depths; and a rough, high-quality bonding surface for repair materials. These characteristics are favorable for construction projects that involve rehabilitation of corrosion-damaged reinforced concrete structures, particularly bridge decks. Details of the hydrodemolition process, equipment operating parameters, and incidental requirements are provided. In addition, appropriate structural conditions that favor the use of hydrodemolition and various methods of specifying work items related to bridge deck rehabilitation are described. The need for comprehensive field evaluations of concrete structures before rehabilitation strategies are developed was found during the course of the work.

An increasing amount of infrastructure construction involves the renewal of existing facilities. Over time the structures within these facilities become inadequate either because of obsolescence or because of degradation caused by continued use and exposure to their environment. At some point in time it becomes necessary or desirable to renovate the structures to restore the functional quality of the facility. In many instances it is beneficial to repair and use selected portions of an existing structure rather than to completely rebuild it. This is often the case with steel-reinforced concrete structures, which are extremely durable by nature but which can be prone to deterioration in isolated areas. Differential deterioration is usually caused by corrosion of reinforcing steel, which creates internal forces sufficient to crack the concrete in locations where tensile stresses are concentrated. As more cracks develop, the process is accelerated and various levels of deterioration occur at different locations throughout the structure. When this situation exists it is desirable to remove the deterioration and place new concrete, which bonds to become part of the structure. The new concrete may be a simple replacement for the deterioration or it may be formed to increase the size of the structural element.

Hydrodemolition is one method used to partially remove selected areas of a concrete element. First developed in Europe in the late 1970s, this method has become a widely used and significant part of concrete rehabilitation. By using the erosive power of high-velocity water streams, hydrodemolition equipment breaks up concrete by disintegrating the cement matrix between aggregates. The disintegration is achieved by the following mechanisms, which occur simultaneously: cavitation, in which rapidly changing pressures in flowing water produce shock waves with magnitudes sufficient to break up the cement matrix; pressurization of cracks and pores, which breaks the concrete in tension; and direct impact of the water jet, which dislodges loosened fragments (*1*). During these processes the aggregates themselves are not fractured. The demolishing effect can be tightly controlled to a desired level of concrete removal, ranging from light scarification of the surface to deep penetration of the structural element.

Office of Research and Materials, Connecticut Department of Transportation, 280 West Street, Rocky Hill, Conn. 06067.

ADVANTAGES OF HYDRODEMOLITION

The use of hydrodemolition has several advantages over conventional removal methods, such as jackhammering and rotomilling. A primary advantage of hydrodemolition is its ability to remove concrete around and in between reinforcing bars without inducing additional damage to the surrounding concrete. This advantage is very important because a majority of concrete deterioration occurs adjacent to corroding reinforcing steel. Rotomilling is an effective method, but it is only capable of removing concrete above reinforcing steel. Conventional impact methods, such as jackhammering, are versatile, but they are also slow and labor-intensive for large areas. In addition, jackhammers have been shown to cause new microcracks in concrete because of the intense vibrations in the immediate vicinity of the impact tool (*2,3*). When these tools come into contact with reinforcement and large aggregates, the destructive vibrations are further transferred to sound areas of the concrete that are intended to remain in place.

Selective Removal

Another advantage of hydrodemolition is its consistent execution of the removal operation because of the automated nature of the equipment. Once operating parameters have been established for a particular structure they are held constant to deliver a uniform level of removal energy throughout the process. This consistency produces the unique advantage of selective removal. Areas of a structure that contain weaker or more deteriorated concrete will break up faster, allowing time for the demolition to penetrate deeper, where it is needed. By maintaining stable control of the water stream's dispersion characteristics, hydrodemolition equipment has the ability to remove only low-strength or deteriorated concrete, whereas it leaves sound concrete intact. The penetration depth of the removal process varies to match the depth to which the lower strength or

FIGURE 1 Hydrodemolished bridge deck surface.

deterioration has progressed (*1*). Figure 1 shows a hydrodemolished bridge deck surface with various penetration depths.

Bonding Surface Quality

Additional advantages of hydrodemolition are related to the quality of the surface left behind after the removal operation. Of the many factors that affect the bond quality between new and old concrete, the condition of the scarified surface is among the most important. To provide long-term repairs through the use of concrete patching or overlays, the bonding surface of the original concrete must be clean, rough, and free of microcracks. It has been demonstrated that the concrete remaining after partial removal with impact hammers contains microcracking in approximately the upper 9 mm (0.35 in.) of the exposed surface (*2*). Depending on their sizes and densities, these cracks have been shown to dramatically reduce bond strengths and are very likely to contribute to the premature delamination of patch materials. Conversely, the surfaces remaining after the use of hydrodemolition contain significantly fewer microcracks. Tests have shown that the magnitude of surface roughness after hydrodemolition is approximately 50 percent higher than that after scarification with impact hammers. This rougher profile provides a greater bonding surface area, inhibits the formation of local shear planes, and can result in a doubling of the tensile bond strength of the overlay material (*2,3*).

Lastly, the hydrodemolition operation simultaneously blast cleans any exposed reinforcing steel as the removal is taking place. This promotes a good bond of the new concrete to the reinforcement and reduces the need for additional blast cleaning of the steel. However, precautions should be taken to inhibit new corrosion of the reinforcing steel, both while it is exposed to the atmosphere and after new concrete is placed.

DESCRIPTION OF EQUIPMENT

A typical hydrodemolition apparatus is composed of two distinct parts: a power unit that filters, pressurizes, and delivers the water supply and a demolishing unit that directs the flow of water to the concrete surface in a precisely controlled manner. The power unit, usually housed in a semitrailer, is versatile for many applications of the hydrodemolition method. The demolishing unit is designed for particular uses, such as on horizontal, vertical, or overhead surfaces. The majority of hydrodemolition work is performed on flat, essentially horizontal concrete elements such as bridge and parking garage decks. For this application the demolishing unit is usually mounted on the rear of a tractor-like vehicle, which travels over the deck's surface in a controlled manner.

The demolishing unit consists of a screedlike housing in which the high-pressure water jet is directed toward the concrete surface from a moving nozzle. The movement is produced by mounting the nozzle in a rotating head, off center of the axis of rotation. The head is attached to a cross-feed carriage that moves laterally in both directions across the full width of the demolishing unit. The combined motion of the rotating head and the cross-feed carriage produces a spiral path of the water jet. As the water jet passes over the concrete surface the removal is accomplished by the mechanisms described earlier. After a programmed number of lateral carriage passes the entire tractor advances forward a set distance and the cycle is repeated. All of these preprogrammed movements create an automated progression of the demolishing jet over the work area, allowing the removal to be performed in a consistent manner. Figure 2 shows a typical demolishing unit for horizontal applications.

Equipment Operating Parameters

Several operating parameters of the hydrodemolition equipment are adjusted to strike a balance between obtaining top-quality results for the specific project and maximizing production and efficiency. The basic equipment operating parameters are as follows: water pressure, flow rate, nozzle rotation rate, transverse carriage speed, and the tractor advance rate. Variations in any of these parameters affect the amount of energy delivered by the system per unit area of concrete traversed. Generally, the water pressure and flow rate are variables set by the operating contractor on the basis of the capabilities of the system. The water pressure and flow rate are inversely proportional for a fixed amount of removal energy. Some equipment models can develop water pressure as high as 241 MPa (35,000 lb/in.^{2}), allowing a relatively low flow rate of about 120 L/min (32 gal/min) for typical bridge deck removal. Equipment models that develop a lower maximum pressure will require a greater flow rate

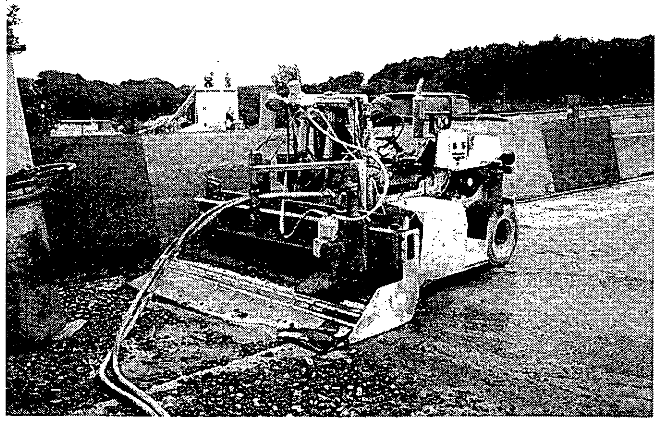

FIGURE 2 Hydrodemolishing unit.

to deliver the equivalent removal energy. In addition to these parameters, the optimum nozzle rotation rate is established by the hydrodemolition contractor on the basis of experience and is not routinely changed on a project-by-project basis.

The two main parameters that are routinely adjusted for each individual project or structure are the transverse carriage speed and the tractor advance rate. These adjustments work on the principle that the longer a fixed-energy water jet stays in one place the deeper it will penetrate. Therefore, the slower the nozzle traverses the concrete surface the more removal energy will be delivered per unit area. A typical bridge deck demolishing unit has a carriage width of approximately 2150 mm (7 ft). Depending on numerous structure-specific variables described later, the carriage speed is set and quantified by the amount of time that it takes to make one pass across the width of the screed. A typical setting is on the order of 400 mm/sec (1.31 ft/sec), or 5.4 sec/pass. Then, the entire tractor is programmed to advance forward after a set number of carriage passes, typically one to four passes per advance increment. The distance that the tractor advances each time [usually about 30 mm (1.18 in.)] can also be adjusted and must be monitored to ensure that the removal depth and production rate remain consistent.

For example, the desired removal on a typical bridge deck is achieved when the carriage speed is 5.0 sec-pass, and the tractor advances 30 mm after three passes. This means that an area of 2150 mm by 30 mm (7 ft by 0.1 ft) or 64,500 mm^2 (0.7 ft^2) is removed every 15 sec. This gives a production rate of 15.6 m^2/hr (168 ft^2/hr). This example shows that small changes in these equipment settings can greatly affect the amount of time that it takes to demolish a fixed-size bridge deck. Also, actual production rates can be significantly influenced by unforeseen problems such as downtime because of equipment failure and poor coordination of project activities. Maintaining a profitable production rate is primarily a concern of the hydrodemolition contractor. However, it is beneficial for bridge engineers to understand these relationships when they are involved in a hydrodemolition project.

Equipment Calibration Procedure

Because every structure and application is unique it is necessary to calibrate the hydrodemolition equipment before each use. The objective of the calibration is to balance the removal energy such that all deteriorated concrete will be removed without excess penetration of the sound areas. The procedure used to strike this balance involves adjusting the operating parameters mentioned earlier to produce the desired results.

Usually, an extensive evaluation of project goals and structure-specific variables is used to specify a minimum mean depth of removal for the entire demolition area. Since deeper removal will occur in weak and deteriorated areas, verification of the depth is performed at locations known to be sound and with strength characteristics typical of those of the original structure. For a bridge deck it is desirable to locate a sound area that is at least 2 m^2 (21.5 ft^2) for the calibration. Then, using past experience, the hydrodemolition equipment operator sets initial adjustments that are anticipated to achieve the minimum removal depth in the sound area. After several advances of the demolishing unit the operation is stopped and a depth measurement is taken. Depending on whether the penetration is too deep or too shallow, the transverse carriage speed is changed appropriately until the proper removal depth is accomplished. As stated, these adjustments may reduce the production rate of the unit, but achieving the proper removal depth is essential for high-quality results.

Once the equipment settings are established on a sound area of the deck, it is beneficial to check the level of removal on a weak or delaminated section. This secondary calibration is not performed for further adjustment of the machine settings but rather to ensure that the equipment will seek out and selectively remove all deterioration with the current settings. Chain dragging or other sounding methods are generally used to determine whether or not all deterioration has been removed. It is the responsibility of the project engineer to determine if additional adjustments are necessary. Once the calibration is complete the equipment settings should not be modified during the production removal.

PROJECT-SPECIFIC VARIABLES

Each hydrodemolition project contains an array of unique circumstances that make it necessary to assess goals and plan operations accordingly. Before the start of any construction work it is assumed that an extensive structure evaluation survey that led to a design calling for partial removal of the concrete structure and subsequent repair was performed. The condition surveys should include a delamination survey of all exposed surfaces; concrete strength tests by various methods; chloride ion concentration tests at various depths within the structure; half-cell potential survey at as many locations as possible; depth of cover over reinforcement survey; and an assessment of cracking, airvoids, and related characteristics of the hardened concrete (*4*). Additional test methods, now available for more detailed evaluations, have been developed as follows: measurement of reinforcing steel corrosion rates, automated flaw detection equipment that operates on both bare and asphalt-covered bridge decks, and various methods of evaluating the condition of existing corrosion-reducing techniques (*5*). The completeness and accuracy of the preconstruction condition survey of a concrete structure is fundamental to the success of the hydrodemolition and the overall rehabilitation strategy.

Structure Variables

If the results of the condition survey support the use of hydrodemolition for partial removal and repair, additional factors must be addressed. One factor is the amount of removal area that is accessible to the hydrodemolition equipment. Hydrodemolition is the preferred removal method and should be used wherever possible on a bridge deck. Certain areas around parapets, expansion joints, and other obstacles will require the use of impact hammers. It must also be determined whether the entire surface or only specific delineated areas showing deterioration will be subjected to removal. This type of spot removal and patching can be effective and economical, provided that all deterioration is found and removed.

Mean Depth of Removal

Depending on the findings of the condition survey the desired mean depth of removal must be specified such that all deteriorated and weak concrete is completely removed but that excessive concrete from sound areas is not removed. The automated, consistent energy characteristics of hydrodemolition increase the need for comprehensive and accurate data related to the existing condition of the concrete. Specifically, the total area and average depth of deterioration (delamination, microcracks, etc.) will greatly affect the volume of concrete removed by the hydrodemolisher. It has been estimated that when the anticipated amount of full-depth deck removal approaches 25 to 30 percent of the total area it is not cost-effective to pursue partial removal and repair. In these cases complete replacement of the bridge deck is probably warranted. If a high percentage of the deck's area is delaminated but it is predominantly limited to the top mat of reinforcement, partial removal down to a sound level is still a viable strategy. It is only large areas of full-depth deterioration that escalate the cost of rehabilitation, rendering it less economical to salvage any of the old deck. When the condition survey accurately quantifies the amount of full-depth deterioration, strategy decisions are more easily justified. Another consideration is the possibility that the length of time between the condition survey and the actual demolition may be long enough for additional corrosion and loading to significantly increase the amount of deterioration, and hence the quantity of removal.

Uniformity

Another structural variable unique for each bridge deck is the uniformity of the concrete slab. Decks that have not been altered since their original construction generally have uniform concrete strength or hardness with various levels of deterioration. When this is the case the hydrodemolisher will selectively remove deteriorated areas as described earlier. However, many times a bridge deck has undergone minor patching and repairs over its life. These patches usually have different strength characteristics than the original surrounding concrete because of the use of different materials, such as fast-setting or high-early-strength cements. When the hydrodemolisher reaches a patch significant changes in the depth of removal may occur. Usually, less removal takes place on the patch itself, and deeper removal occurs around the perimeter of the patch. The causes of this phenomenon include differential chloride ion concentrations that tend to passivate reinforcement corrosion within the patch material and accelerate corrosion in the older concrete and the possibility that jackhammering for the patches induced microcracking. Both of these situations promote further deterioration around the perimeter of the patch. When the presence of past patching is encountered while designing a rehabilitation strategy, special provisions for dealing with variable removal depths may require consideration. Figure 3 shows the presence of past patching on a hydrodemolished bridge deck.

Aggregate and Reinforcement Characteristics

Lastly, the size and density of the deck materials are structure-specific variables that affect the mean depth of removal and production rate of the hydrodemolition operation. The composition of the original concrete mix determines such variables as the gradation and maximum size of the aggregates and, hence, the ratio of large aggregate volume to cement matrix volume. Since the demolishing water jet erodes only the cement matrix of the concrete, the aggregates remain essentially intact. More energy and time may be required to demolish with the water jet concrete mixes that have more large aggregate by volume, indicating a lower volume of cement matrix. This condition exists under the assumption that the

FIGURE 3 Existing patches on a hydrodemolished bridge deck.

volume of cement matrix is not so low that the overall compressive strength is lower than a normal level. The vast number of combinations of aggregate sizes and mortar characteristics are interrelated variables that determine the strength and hardness of the concrete. Coring or other sampling techniques are good ways to identify the composition of the deck to better estimate removal quantities and production rates.

The size, spacing, and vertical placement of the reinforcement also vary from structure to structure, affecting the removal operation. The predominant variable regarding reinforcement is its depth of cover. Many bridge decks do not have the same top mat reinforcement cover as shown in the original design plans. Shallow cover is one of the primary reasons for premature delaminations and spalling. Sometimes, the amount of cover varies considerably over a deck's area. Although not often performed, an accurate depth-of-cover survey is valuable in developing rehabilitation strategies. For example, if a deck has at least 60 mm (2.36 in.) of cover over its entire area, it may be beneficial to rotomill down to the top mat before hydrodemolition. If they are done under the right conditions, this combination of removal methods can be more economical than hydrodemolition alone (*6*). However, if hydrodemolition is chosen and unanticipated areas of lower cover are encountered, the quality and cost-effectiveness of the job may be reduced. Consideration of these variables shows that a comprehensive and accurate evaluation of a structure before the design and construction of a rehabilitation strategy is extremely important for obtaining high-quality and cost-effective results.

Other Project-Specific Requirements

In addition to a detailed assessment of the physical condition of the bridge deck to be hydrodemolished, other aspects of the removal operation should be assessed before work begins. One requirement is a method of controlling the runoff water. As stated, water is dispensed during removal at a rate of approximately 120 L/min/nozzle (32 gal/min/nozzle). Once out on the deck this water must be routed, filtered, and disposed of in a manner compliant with environmental regulations. Usually, this is accomplished by either vacuuming the water immediately after its release or routing it to a sedimentation basin. Each structure has an unique geometry that will affect the water drainage and collection setup.

Also to be considered is the cleanup of the debris generated during hydrodemolition. As the unit progresses over the deck it leaves behind a wet mixture of concrete slurry and solid fragments. It is extremely important that this debris be washed off and removed from the scarified surface before it has a chance to dry up and rehydrate. If it is allowed to occur, rehydration will cause the slurry and rubble to rebond to the surface, making a poor bonding surface for repair materials. Pressure washing of the surface along with vacuuming of the rubble behind the hydrodemolition unit is effective in removing the debris in a timely manner. If the slurry is allowed to bond to the surface or the surface is contaminated because of prolonged exposure, sandblasting may be necessary to restore the high-quality bonding surface.

Lastly, safety precautions are very important aspects of the hydrodemolition operation. There is always a possibility that a weak area of the deck will blow out, causing pieces of concrete to fall below. This can be extremely dangerous because it usually occurs unexpectedly. Appropriate precautionary measures must be used to avoid blowout accidents. Also, flying debris can be expected near the demolishing unit. These units are equipped with protective shrouds around the nozzle area, but flying fragments still find their way out and can cause injury or property damage. This is of special concern at locations where traffic is present near the demolition area. In some cases it is necessary to set up plywood shields around the immediate work area. Safety glasses and face shields should also be worn by all personnel in the vicinity of the demolition unit.

CONTRACTING PRACTICES

When it is determined that hydrodemolition will be used a contract to complete the work must be developed such that quality is achieved at the lowest possible cost. When considering the content and format of a contract, it is important to identify all project tasks that are related to or affected by the removal operation. The relationships of these tasks can then be analyzed to determine the most cost-effective method of specifying contract items to complete the work. The quantities of some work items will be fixed, whereas the quantities of others may vary as construction progresses. If the design engineer has a good understanding of the variables mentioned earlier contract terms can be adjusted accordingly to obtain the best possible results.

Interrelated Work Items and Contractor Relationships

The facility owner awards most construction contracts to a single corporation, identified as the prime or general contractor. Often, when some of the construction items are highly specialized, requiring unique equipment and procedures, the general contractor will hire a specialty subcontractor to do those tasks. Usually, the general contractor is ultimately responsible for meeting all of the terms of the contract, regardless of who performs the work. Because of the expense of the equipment hydrodemolition is almost always subcontracted to a specialty firm. The responsibilities of the hydrodemolition subcontractor are usually limited to two basic tasks: mobilizing to the site in a timely manner and performing the removal operation on a fixed-size deck area to the specified minimum depth. Although very closely related to hydrodemolition, tasks such as cleanup of debris, runoff control, and final surface preparation are routinely done by the general contractor. The costs associated with the subcontractor's tasks are almost purely time dependent. Once the equipment is calibrated, which dictates the time required to cover the entire deck surface, variations in the volume of material removed do not affect the cost of the pure removal operation. The primary variable for the hydrodemolition subcontractor is the speed at which the equipment can achieve the minimum depth of removal in the sound areas of the deck. Because of the size of the equipment and its capital-intensive nature, hydrodemolition is most economical when large, continuous areas are accessible for removal with few mobilizations. When the removal area is approximately 500 m^2 (5,400 ft^2) or greater, the cost of the pure removal, excluding all incidentals, is about \$65/m^2 (\$6/ft^2) (*6*). Although higher costs may occur for a variety of reasons, this is a good initial estimate for typical circumstances.

In contrast, the general contractor is usually responsible for a multitude of removal-related tasks that are dependent on many variables. Before the hydrodemolition subcontractor mobilizes to the site the general contractor must do some preparation work, such as clear space and optimize accessibility for the equipment; set up traffic control systems; set up the water routing, filtration, and disposal system; and make safety precautions for flying debris and blowout areas. During the removal operation the general contractor is usually responsible for the cleanup and removal of the debris, which are dependent on the speed of the machine and the volume of material removed. Also, the general contractor is responsible for the ultimate quality of the prepared surface, which may require extra work such as power washing, sandblasting, and replacing damaged bars. In addition, placement of the new concrete in the form of patches and overlays is usually performed by the general contractor. These items are all related to or affected by the hydrodemolition operation, and the efforts required to perform most of them are affected by the volume of material removed. Because of these relationships it is beneficial to manipulate contract items on the basis of project-specific variables to obtain high-quality repairs at the lowest possible cost.

Methods of Specification

When developing special provisions for a bridge deck rehabilitation contract, all of the equipment operating characteristics, project goals, and structure condition information need to be considered. The detailed tasks required to complete the repair can be grouped into three major activities, as follows: the removal operation, including mobilization, preparation work, and efforts to provide the final surface quality; the cleanup and disposal of demolition debris; and the supply and placement of new material. These activities can be quantified together or separately to establish the work items that will be put out to bid. These bid items provide the basis for payment when the construction contract is awarded and the work is completed.

Items Combined

One specification strategy is to combine the three activities listed earlier into one contract item and to quantify it by volume. The volume is usually measured by the amount of new concrete placed, and the hydrodemolition is included in the work item as a surface preparation activity. This method is based on the premise that the volume of concrete placed will equal the volume of concrete removed, provided that there are to be no changes in the deck's geometry. Therefore, if the removal and replacement volumes are equal, they can be combined into a single item, resulting in fewer items to be measured. The disadvantages of this strategy become apparent when the quantity of concrete removed by the hydrodemolisher is greater than that originally estimated. When this occurs the costs of non-volume-dependent work activities, such as the pure removal operation, increase. The converse situation reduces costs: however, quantity overruns are more likely to occur. The practice of combining these activities into a single bid item can be beneficial if deterioration assessments, and hence, quantity estimates, are presented with a high level of confidence. Also, the single-item method may be appropriate for spot removal and patching situations, in which case the removal volumes are more easily estimated.

Items Separated

An alternate specification strategy is to present multiple contract items for the activities related to hydrodemolition. The two major items are the removal of the old concrete and the supply and placement of the new material. It is appropriate to quantify the removal item on the basis of the surface area of the deck, which is fixed and known for each structure. The costs associated with the supply and placement of new concrete vary with its volume, which is estimated before construction but which is not known exactly. Because of possible variations the placement item should be measured by volume, with subprovisions for full and partial depth placement. The activity that is difficult to clearly place in either of these two major items is the cleanup and disposal of demolition debris. This work is removal related but is also volume dependent. Since it is undesir-

TABLE 1 Theoretical Cost Analysis of Specification Methods

Bridge Deck Area: 2000 m^2 (21,528 ft^2)
Minimum Depth of Removal: 60 mm (2.4 in)
Estimated Removal and Replacement Volume: 150 m^3 (196 yd^3)
(including identified deterioration)

	Contract Pay Items			
	Combined		Separated	
Description	SI Units	US Customary Units	SI Units	US Customary Units
Unit price for hydro removal and placement of new concrete	$1500/$m^3$	$1148/$yd^3$	-	-
Unit price for hydro removal, only	-	-	$85.00/$m^2$	$7.90/$ft^2$
Unit price for placement of new concrete, only	-	-	$367/$m^3$	$281/$yd^3$
0% Removal overrun				
Total price for hydro removal	-	-	$170,000	$170,000
Total price for new concrete	-	-	$ 55,000	$ 55,000
Total price for hydro removal and placement of new concrete	$225,000	$225,000	$225,000	$225,000
20% Removal overrun				
Actual removal and replacement quantity	180 m^3	235 yd^3	180 m^3	235 yd^3
Total price for hydro removal	-	-	$170,000	$170,000
Total price for new concrete	-	-	$ 66,000	$ 66,000
Total price for hydro removal and placement of new concrete	$270,000	$270,000	$236,000	$236,000
Total cost overrun	$ 45,000 (20%)	$ 45,000 (20%)	$ 11,000 (4.9%)	$ 11,000 (4.9%)

- Indicates data not applicable.

able to create too many pay items the debris work should be considered part of the hydrodemolition operation and should be included with the removal item.

The advantages of separating the items are most established when more concrete is removed than was originally estimated. With the two-item setup, the cost of hydrodemolition remains constant, whereas the volume of replacement concrete varies with the volume removed. In addition, owners are better able to keep track of which deck repair items are the most costly. This information can then be used for future decisions regarding rehabilitation strategies. Although single-item specification can be appropriate when deterioration assessments are very accurate, it may significantly raise the cost of the hydrodemolition operation when overruns in the volume of concrete placed are incurred. Table 1 provides a simple example.

CONCLUSIONS

Several conclusions can be drawn from the analysis of the use of hydrodemolition to remove deteriorated concrete from bridge decks. First, it is important to identify the advantages associated with using hydrodemolition over using conventional impact removal methods. A top-quality bonding surface free of cracking is essential to the long-term success of any concrete repair effort. Second, it can be concluded that knowledge of the hydrodemolition operating parameters is beneficial for obtaining the best possible results. The equipment calibration procedure is key to the process of ensuring the removal of all deteriorated concrete at the most efficient operating speed. In addition, a comprehensive and accurate evaluation of an existing bridge deck's condition is essential for developing an appropriate rehabilitation strategy. Many project- and structure-specific variables must be considered during the design process to provide an appropriate solution to the needs of the particular situation. When the design is complete it is beneficial to analyze all related activities so that contract items can then be quantified and manipulated to maximize the quality and cost-effectiveness of the whole effort.

ACKNOWLEDGMENTS

The author acknowledges the support and cooperation of FHWA during the course of this work.

REFERENCES

1. Medeot, R. History, Theory and Practice of Hydrodemolition. *F.I.P. Industriale,* No. NT 722/86, Dec. 1986.
2. Hindo, K. R. In-Place Bond Testing and Surface Preparation of Concrete. *Concrete International.* American Concrete Institute, April 1990, p. 46–48.
3. Silfwerbrand, J. *Effects of Differential Shrinkage, Creep, and Properties of the Contact Surface on the Strength of Composite Concrete Slabs of Old and New Concrete.* Bulletin No. 147. Department of Structural Mechanics and Engineering, Royal Institute of Technology, Stockholm, Sweden, 1987.
4. Gannon, E. J., and P. D. Cady. *Condition Evaluation of Concrete Bridges Relative to Reinforcement Corrosion,* Vol. 1. *State of the Art of Existing Methods.* Strategic Highway Research Program, National Research Council, Washington, D.C., Sept. 1992.
5. Cady, P. D., and E. J. Gannon. *Condition Evaluation of Concrete Bridges Relative to Reinforcement Corrosion,* Vol. 8. *Procedure Manual.* Strategic Highway Research Program, National Research Council, Washington, D.C. Sept. 1992.
6. Vorster, M. C., J. P. Merrigan, R. W. Lewis, and R. E. Weyers. *Techniques for Concrete Removal and Bar Cleaning on Bridge Rehabilitation Projects.* Strategic Highway Research Program, National Research Council, Washington, D.C., Dec. 1992.

Publication of this paper sponsored by Committee on Structures Maintenance and Management.